Since January 2020 Elsevier has created a COVID-19 resource centre with free information in English and Mandarin on the novel coronavirus COVID-19. The COVID-19 resource centre is hosted on Elsevier Connect, the company's public news and information website.

Journal of Infection 86 (2023) 66–117

Contents lists available at ScienceDirect

Journal of Infection

journal homepage: www.elsevier.com/locate/jinf

Letters to the Editor

Pre-admission RT-qPCR based RSV screening reduces nosocomial RSV infections during epidemic outbreaks

Dear Editor,

We read with interest the manuscript "Sensitivity and specificity of surveillance case definitions in detection of influenza and respiratory syncytial virus among hospitalized patients, New Zealand, 2012–2016″ by Davis et al.,[1] on the importance of the surveillance of respiratory infections in children. In our experience, a similar method proved effective in preventing respiratory syncytial virus (RSV) nosocomial infections.

RSV is the most common respiratory agent to cause acute lower respiratory infections (ALRI) in infants and young children.[2,3] RSV is a nosocomial hazard for patients of any age and is the most frequent cause of nosocomial infection in pediatric wards during the autumn and winter seasons.[4] The reported rate of nosocomial RSV infection during epidemics is highly variable, ranging from 2.6% to 13.8%, depending on the entity of the seasonal outbreak and on the efficacy of the prevention measures.[5,6] Nosocomial RSV infections can cause significant morbidity in fragile and very young children, but they also impact the length of hospitalization and the total cost of treatment,[6,7] making preventing strategies a primary concern.

During an early and unexpected RSV epidemic occurring in the autumn of 2021, we introduced a widespread pre-admission quantitative Reverse Transcription Polymerase Chain Reaction (RT-qPCR) based RSV screening program at our tertiary hospital. Before the 24th of November 2021, the RSV testing was performed at any time during the hospital stay, whenever the patient developed symptoms consistent with ALRI. After the 23rd of November 2021, the pre-admission SARS-CoV-2 testing was combined with the RSV testing. As in the pre-screening period, patients with symptoms consistent with ALRI and a negative RSV and SARS-CoV-2 test were screened for other respiratory pathogens, using a PCR panel. Also, a combined SARS-CoV-2 and RSV test was performed every 4th day in long-term hospitalized patients.

RSV season was defined as the period between the first diagnosis of RSV infection (September 20th, 2021) and the last case diagnosed (February 28th, 2022). Within the RSV season, the epidemic period was defined as the period in which the weekly incidence of RSV cases/total patients-days/week was higher than 0.5×10^2 (from the 13th of October 2021 to the 18th of January 2022) (Fig. 1). RSV infection was considered nosocomial if the patient tested negative for RSV on a first nasal swab collected pre-admission or within 96 h from admission and positive thereafter. Although nosocomial infection usually is defined as an infection that occurs after at least 48 h from hospital admission,[8] we choose a wider cut-off (96 h) to be more conservative on the incubation period of RSV infection.[9] In patients admitted before November 24th in which the diagnosis of RSV infection was made after 96 h from hospital admission, the swab performed before admission for SARS-CoV-2 infection screening was retested by RT-qPCR for RSV to confirm or exclude a nosocomial infection (*Supplementary Figure 1*). Details on the laboratory methods are reported in the *Supplementary Methods*.

One hundred and sixty patients tested positive for RSV between the 20th of September 2021 and the 23rd of November 2021. Of them, eight were excluded because they were hospitalized for less than 48 h, and one because the SARS-CoV-2 swab had not been performed at our center and therefore it was not available for retesting to exclude a nosocomial infection. Therefore, 151 patients were included in the pre-screening study group, while 227 patients were enrolled in the screening group. No significant differences were found in terms of sex, median age, and ICU admission between the two groups, but we found a significantly higher number of patients older than six years ($p = 0.002$, Chi-square test) and a slightly lower duration of hospital stay in the screening group ($p = 0.001$, Mann Whitney test) (Table 1). In 80 out of 310 RSV-infected patients evaluated with an RT-qPCR for ALRI (25.8%) the nasal swab tested positive for other respiratory viruses. Among them, the most frequent coinfections consisted of Bocavirus in 38 (12.3%), Rhinovirus in 13 (4.2%), SARS-CoV-2 in 10 (3.2%), and Adenovirus in nine (2.9%) (Table 1).

In the pre-screening group, 137 patients tested positive for RSV within 96 h from admission and were therefore considered community infected. The pre-admission nasal swab of the remaining 14 patients was retested and resulted positive in three, while 11 were confirmed negative. Therefore, in the pre-screening group, 140/151 (92.7%) were considered as community-acquired infections while 11/151 (7.3%) were defined as nosocomial RSV infections. In the screening group, 222 out of 227 patients (97.8%) were found positive for RSV at admission ($n = 183$) or within 96 h ($n = 39$) from admission and were considered community infected, while five patients (2.2%) tested positive during hospitalization but had a negative RSV test performed before admission and were therefore considered nosocomial infected (*Supplementary Figure 1*).

The rate of nosocomial RSV infections significantly dropped from 7.3% (11/151) to 2.2% (5/227) after the introduction of the screening protocol ($p = 0.016$; OR 3.49, 95% CL 1.19–10.25, Chi-square test) (*Supplementary Figure 1*). When comparing the two periods including only symptomatic patients ($n = 334$), the rate of nosocomial infections in the screening group remained significantly lower (1.6%, 3/189), compared to the pre-screening group (7.3%, 11/151; $p = 0.009$; OR 4.87, 95% CL 1.33–17.79, Chi-square test). During the epidemic phase (Fig. 1), the incidence of nosocomial RSV infection dropped from 0.17×10^2/total patients-days (11/6490) in the pre-screening period to 0.05×10^2/total patients-days (4/7740) in the screening group ($p = 0.038$, Fisher's exact test).

https://doi.org/10.1016/j.jinf.2022.11.002

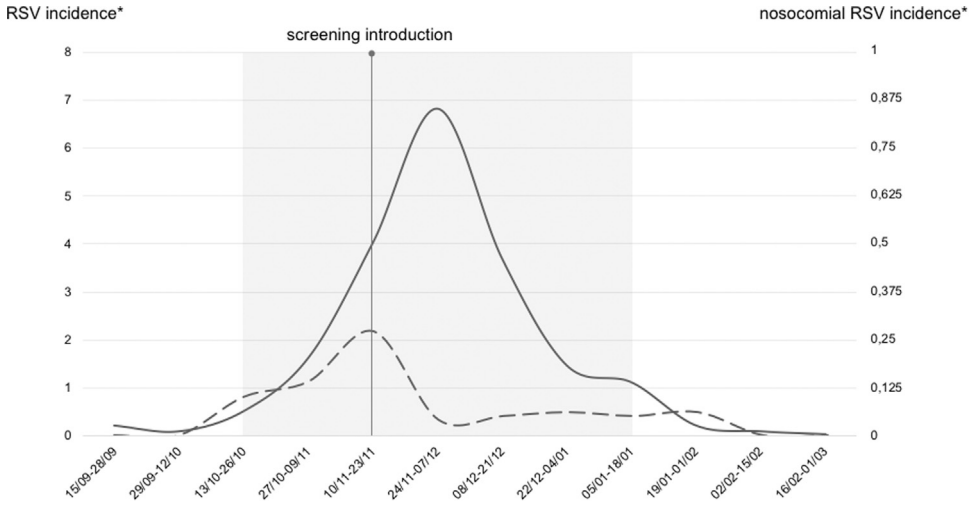

Fig. 1. Incidence of RSV infections during the 2021–2022 RSV season. The overall incidence of RSV infections is represented by the continuous line, while the dotted line represents the incidence of nosocomial RSV infections. * incidence is calculated as $x10^2$/total patients-days. RSV: respiratory syncytial virus.

Table 1
Patients' characteristics.

	Total $n = 378$	Pre-screening $n = 151$	Screening $n = 227$	*p*-value
Female sex, n (%)	171 (45.2)	71 (47.0)	100 (44.1)	0.599
Age at diagnosis, median (IQR) – *months*	9 (2–28)	9.5 (2–23)	8.5 (2–30)	0.659
Age groups, n (%)				
0–3 months	151 (39.9)	55 (36.4)	96 (42.3)	0.284
4–12 months	65 (17.2)	30 (19.8)	35 (15.4)	0.268
1–6 years	141 (37.3)	64 (42.3)	77 (33.9)	0.104
>7 years	22 (5.8)	2 (1.3)	20 (8.8)	0.002
Coinfections, n/n tested (%)	80/310 (25.8)	36/150 (24.0)	44/160 (27.5)	0.517
Rhinovirus	13 (4.2)	7 (4.6)	6 (3.8)	0.780
Bocavirus	38 (12.3)	16 (10.6)	22 (13.8)	0.489
Adenovirus	9 (2.9)	7 (4.6)	2 (1.3)	0.095
PIV3	8 (2.6)	5 (3.3)	3 (1.9)	0.489
SARS-CoV-2	10 (3.2)	1 (0.7)	9 (5.6)	0.020
Hospital stay, median (IQR) – *days*	6 (3–9)	6 (4–11)	5 (3–8)	0.001
ICU admission, n (%)	68 (18.0)	29 (19.2)	39 (17.2)	0.682

IQR: interquartile range; ICU: intensive care unit; PIV3: parainfluenza virus 3; SARS-CoV-2: severe acute respiratory syndrome coronavirus.

In our experience, the early identification of RSV before admission allowed the isolation of patients and the optimization of prevention measures for nosocomial infections during an unexpected RSV epidemic. Indeed, the combined, RT-qPCR-based pre-admission screening for SARS-CoV-2 and RSV resulted in a significant decrease in nosocomial RSV infections. The COVID-19 pandemic radically changed our approach to preventive measures for the diffusion of viral infections in hospital settings. The screening of SARS-CoV-2 has proven to be an effective measure to prevent nosocomial diffusion.[10] The same approach has been successfully used to face an unexpected RSV outbreak but is likely to be extended to other pathogens in the future.

Funding

This work was supported in the context of NETVAC project funded by "Bando Ricerca Salute 2018″ (Tuscany Region)

Declarations of Competing Interest

None.

Supplementary materials

Supplementary material associated with this article can be found, in the online version, at doi:10.1016/j.jinf.2022.11.002.

References

1. Davis W., Duque J., Huang Q.S., Olson N., Grant C.C., Newbern E.C., et al. Sensitivity and specificity of surveillance case definitions in detection of influenza and respiratory syncytial virus among hospitalized patients, New Zealand, 2012-2016. *J Infect* 2022;**84**:216–26 PMID: 34953903. doi:10.1016/j.jinf.2021.12.012.
2. Nolan T., Borja-Tabora C., Lopez P., Weckx L., Ulloa-Gutierrez R., Lazcano-Ponce E., et al. Prevalence and incidence of respiratory syncytial virus and other respiratory viral infections in children aged 6 months to 10 years with influenza-like illness enrolled in a randomized trial. *Clin Infect Dis* 2015;**60**:e80–9 PMID: 25673560. doi:10.1093/cid/civ065.
3. Barbati F., Moriondo M., Pisano L., Calistri E., Lodi L., Ricci S., et al. Epidemiology of respiratory syncytial virus-related hospitalization over a 5-year period in Italy: evaluation of seasonality and age distribution before vaccine introduction. *Vaccines (Basel)* 2020;**8**:15 PMID: 31947976. doi:10.3390/vaccines8010015.
4. Weinstein R.A., Hall C.B.. Nosocomial respiratory syncytial virus infections: the "cold war" has not ended. *Clin Infect Dis* 2000;**31**:590–6 PMID: 10987726. doi:10.1086/313960.
5. Wrotek A., Czajkowska M., Jackowska T.. Nosocomial infections in patients hospitalized with respiratory syncytial virus: a practice review. *Adv Exp Med Biol* 2020;**1271**:1–10 PMID: 32078148. doi:10.1007/5584_2020_483.
6. Simon A., Khurana K., Wilkesmann A., Muller A., Engelhart S., Exner M., et al. Nosocomial respiratory syncytial virus infection: impact of prospective surveillance and targeted infection control. *Int J Hyg Environ Health* 2006;**209**:317–24 PMID: 16697255. doi:10.1016/j.ijheh.2006.02.003.
7. Comas-Garciá A., Aguilera-Martiñez J.I., Escalante-Padron F.J., Lima-Rogel V., Gutierrez-Mendoza L.M., Noyola D.E.. Clinical impact and direct costs of nosocomial respiratory syncytial virus infections in the neonatal intensive care unit. *Am J Infect Contr* 2020;**48**:982–6 PMID: 32305431. doi:10.1016/j.ajic.2020.04.009.
8. World Health Organization Department of communicable disease, surveillance and response. *Prevention of Hospital-Acquired Infections: A Practical Guide*. 2nd

Ed; 2022. Available from: https://apps.who.int/iris/handle/10665/67350 Accessed 16 January.
9. Marcdante K.J., Kliegman R.M., Schuh A.M.. *Nelson Essentials of Pediatrics*, Edition Philadelphia, PA: Elsevier; 2020. (chapter 119, page 419).
10. Shen J., Sun J., Zhao D., Li S., Xiao W., Cai X., et al. Characteristics of nosocomial infections in children screened for SARS-CoV-2 infection in China. *Med Sci Monit* 2020;**26**:e928835 PMID: 33335084. doi:10.12659/MSM.928835.

Francesco Pegoraro[1]
Department of Health Science, University of Florence, Florence, Italy

Federica Barbati*[1]
Department of Health Science, University of Florence, Florence, Italy
Immunology Unit, Meyer Children's University Hospital, Florence, Italy

Laura Pisano, Maria Moriondo, Caterina Pelosi
Immunology Laboratory, Meyer Children's University Hospital, Florence, Italy

Lorenzo Lodi, Silvia Ricci
Department of Health Science, University of Florence, Florence, Italy
Immunology Unit, Meyer Children's University Hospital, Florence, Italy

Giuseppe Indolfi
Pediatric Unit, Meyer Children's University Hospital, Florence, Italy

Chiara Azzari
Department of Health Science, University of Florence, Florence, Italy
Immunology Unit, Meyer Children's University Hospital, Florence, Italy
Immunology Laboratory, Meyer Children's University Hospital, Florence, Italy

*Corresponding author at: Via G. Pieraccini 24, 50139.
E-mail address: federica.barbati@unifi.it (F. Barbati)

[1] These first authors contributed equally to this article.
Accepted 2 November 2022
Available online 5 November 2022

https://doi.org/10.1016/j.jinf.2022.11.002

Clinical experience with use of oral Tecovirimat or Intravenous Cidofovir for the treatment of Monkeypox in an Italian reference hospital

Dear Editor,

We read with interest the manuscript by Li D. and colleagues, recently published in this Journal, in which the authors revealed the potential binding mode for tecovirimat with a poxvirus phospholipase from monkeypox (MPX) virus [1].

Tecovirimat and cidofovir are potential options for severe cases of MPX, but limited data on their efficacy and safety are available [2–6].

Here we retrospectively describe clinical presentation, evolution, management and viral kinetics of the first 19 MPX cases treated with antivirals at the INMI Lazzaro Spallanzani IRCCS in Rome, Italy. The decision regarding treatments was based on international medical consensus and availability of drugs.

Viral DNA was extracted by the automatic extractor QIAsymphony (Qiagen, Hilden, Germany), and amplified using the real-time PCR method targeting the tumor necrosis factor receptor gene, G2R. Monkeypox virus (MPXV) DNA concentration was measured using threshold cycles (Ct) values of the MPXV-specific PCR. To obtain an absolute quantification of MPXV DNA in the clinical samples, the PCR assay was adapted to run in digital droplet PCR (ddPCR). The nucleic acid extracted from each sample was loaded into specific nanoplate and distributed, amplified and read in each one of the 26,000 partitions of each well, with a detection limit of the assay of 5 copies/µL.

The study was conducted as a part of biological studies on emerging infections approved by the Ethical Committee of the Lazzaro Spallanzani Institute (approval number 14/2015 and amendments). Patients provided written informed consent.

As of September 19, 2022, 19/128 (15%) diagnosed cases of MPXV infection at INMI L. Spallanzani received antiviral treatment. All patients were males aged between 27 and 50 years, all but one patients self-identified as men who have sex with men or bisexual and seven patients (37%) were HIV-positive. Systemic symptoms were reported in all but one patient. Muco-cutaneous lesions were observed in all patients (skin lesions in 89% and mucosal lesions in 95%) and in half of them preceded systemic symptoms.

The majority (79%) of patients complained of a painful lymphadenopathy. Patients were admitted to hospital within a median of 8 days (IQR 5-10) from date of symptoms onset (OD), mainly for mucosal inflammation caused by MPXV and/or superinfection of the lesions and/or management of severe pain due to the lesions. Specifically, proctitis was diagnosed in four patients (21%) and severe pharyngo-tonsillitis in six patients (32%). One patient presented ocular localization complicated by periorbital edema and conjunctival hyperemia. Nine patients (47%) presented with superinfection of the soft tissues, one of which was complicated by abscess of a finger. Finally, one patient was admitted and treated for worsening of genital lesions.

Antiviral treatment was started with a median time of 11 days (IQR 8-12) from OD with oral tecovirimat in 15 (79%) patients and intravenous (IV) cidofovir in 4 (21%) patients All patients treated with oral tecovirimat completed a 14-day course of therapy. Similarly, IV cidofovir was well tolerated. Symptoms improvement and no new lesion appearance were observed 72 hours after the start of treatment in all but one patient treated with cidofovir.

No significative alterations of blood tests were observed, apart from a transient increase of alanine aminotransferase after cidofovir. Complete recovery was observed in all patients with a median of 15 days (IQR 11-19) from treatment start. Three patients had still persistence of signs of MPX-mucosal involvement after the resolution of lesions (Table 1).

Finally, viral kinetics have been evaluated in 12 patients (Fig. 1). In all of them, MPXV-DNA was detected in at least one sample from at least one compartment. Particularly, during the follow-up, MPXV-DNA was detected by real-time PCR in: 10/12 patients on oropharyngeal swab (OPS), including 9 at the start of antiviral treatment, with a median Ct of 36 (IQR 33-41); 8/9 patients on blood samples with a median Ct of 41 (IQR 37-41); 6/6 patients on feces with a median Ct of 41 (IQR 36-41); 3/3 patients on saliva with a median Ct of 38 (IQR 32-40); 3/3 patients on seminal fluids with a median Ct of 39 (IQR 37-41). In almost all patients, a progressive decline in viral load was observed over the course of treatment. Most biological samples were negative at the last available observation. DdPCR results approximately mirrored the viral shedding expressed with real-time PCR. It is worth noting that, given the low threshold used for the ddPCR, several samples with high Ct values in real-timePCR, resulted negative in ddPCR.

Table 1
Patients' characteristics and clinical course.

	PT1	PT2	PT3	PT4	PT5	PT6	PT7	PT8	PT9	PT10	PT 11	PT 12	PT 13	PT 14	PT 15	PT 16	PT 17	PT 18	PT 19
Gender/Age/ Ethnicity	M/28 y/ Caucasian	M/33 y/ Caucasian	M/35 y/ Caucasian	M/46 y/ Caucasian	M/33 y/ Caucasian	M/33 y/Hispanic	M/42y/ Asian	M/40y/ Caucasian	M/47y/ Caucasian	M/27y/ Caucasian	M/36 y/ Caucasian	M/38y/ Hispanic	M/48y/ Caucasian	M/45y/ Caucasian	M/35y/ Caucasian	M/50y/ African	M/36y/ Hispanic	M/38y/ Caucasian	M/47y/ Caucasian
Sexual orientation	Bisexual	MSM	MSM	MSM	MSM	MSM	MSM	MSM	MSM	MSM	MSM	MSM	MSM	MSM	MSM	Hetero-sexual	MSM	MSM	MSM
HIV status (ART; last CD4 (cell/ mm3)/VL)	Neg	Neg	Neg	Pos(BIC/ TAF/FTC; 1622/ND)	Pos (3TC/DT; 872 /ND)	Pos* (TDF/FTC +DTG;526/ 26 cp/mL)	Neg	Neg	Pos (3TC/DTG; 828 /ND)	Pos**(BIC/ TAF/FTC;140/ <30cp/mL)	Neg	Neg	Neg	Neg	Neg	Neg	Pos(TAF/ FTC/DRV/ c+DTG; 253/22 cp/mL)***	Pos(TDF/ FTC/EFV; 1323; ND)	Neg
HbsAg/ HCVAb	Neg/Neg	Neg/Neg	Neg/Neg	Neg/Neg	Neg/Neg	NA/Neg	Neg/Neg	Neg/Neg	Neg/Neg	Neg/Neg	Neg/Neg	Neg/Neg	Neg/NA	Pos/Neg	NA/NA	Neg/Neg	Neg/Neg	NA/Neg	Neg/Neg
PREP	No	Yes	Yes	No	No	No	No	Yes	No	No	No	Yes	No	No	No	No	No	No	No
Smallpox vaccination	No	No	No	No	No	No	No	No	No	Yes	No	No	Yes	No	No	No	No	No	No
Systemic symptoms	Fever, headache	Fever, sore throat, myalgias, diarrhoea	Fever	Fever, myalgias, rectal pain with discharg, bleeding	Fever, headache, sore throat	Fever	Fever, sore throat, odynopha-gia	Fever, sore throat, odynopha-gia, myalgias, headache	Fever, sore throat, odynopha-gia, diarrhoea	No	Fever, headache	Fever, rectal pain, discharge and bleeding	Fever, sore throat; odynopha-gia	Fever	Fever	Fever, myalgias	fever, sore throat myalgias, headache, rectal pain, diarrhoea	fever, headache, rectal pain	fever, sore throat, headache
Cutaneous lesion	Head, trunk, right leg, suprapu-bic and perineal	Trunk, limbs including hands	Head, trunk, limbs	Trunk, legs	Head, trunk, limbs	Head, trunk, limbs	Head, trunk, limbs, including palms and soles	Head, trunk, limbs	No	Head including eyelids, trunk, limbs including palms and soles	Head, trunk, limbs	Head, trunk, limbs	No	Trunk	Upper lip	Head including scalp, trunk, arms including hands	Head, trunk, legs	Feet, trunk	Head including upper lip and scalp, limbs, trunk
Mucosal lesion	Eyelids	Penis	Penis, scrotum, perianal	Perianal and oropharyn-geal	Oropha-ryngeal	Penis, oropharyn-geal	Oropha-ryngeal penis and perianal	Oropharyngeal	Oropha-ryngeal	Penis, scrotum, perianal	Penis	Penis, scrotum, perianal	Penis; oropha-ryngeal	Penis	No	Penis	Perianal, scrotum	Perianal	Penis, oropha-ryngeal

(*continued on next page*)

Table 1 (*continued*)

	PT1	PT2	PT3	PT4	PT5	PT6	PT7	PT8	PT9	PT10	PT 11	PT 12	PT 13	PT 14	PT 15	PT 16	PT 17	PT 18	PT 19
Number of lesions	11-20	11-20	11-20	<5	<5	11-20	≥20	11-20	<5	≥20	5-10	≥20	<5	5-10	<5	≥20	≥20	<5	5-10
Systemic symptoms onset after lesions	Yes	Yes	Yes	No	No	Yes	Yes	Yes	No	-	No	Yes	Yes	Yes	No	No	Yes	No	Yes
Lymphad-enopathy	Inguinal	Inguinal	Inguinal	No	Neck	Inguinal	Inguinal	Neck	Neck	Inguinal	Inguinal	No	Neck	Axillary	No	Yes	Inguinal, neck	Inguinal	Neck
Localized disease	Ocular	No	No	Proctitis	Pharyngoton-sillitis	No	Pharyngoton-sillitis	Pharyngoton-sillitis	Pharyngoton-sillitis	No	No	Proctitis	Pharyngoton-sillitis	No	No	No	Proctitis	Proctitis	Pharyngoton-sillitis
Type of treatment	Cidofovir	Teco-virimat	Teco-virimat	Teco-virimat	Teco-virimat	Teco-virimat	Cidofovir	Cidofovir	Teco-virimat	Cidofovir	Teco-virimat	Teco-virimat	Teco-virimat	Teco-virimat	Teco-virimat	Teco-virimat	Teco-virimat	Teco-virimat	Teco-virimat
Reason for treatment	Ocular involve-ment	Super-infection of cutaneous lesion	Soft-tissue superin-fection	Proctitis	Pharyngotons-illitis	Soft-tissue superinfec-tion	Pharyngotons-illitis, pain manage-ment	Compli-cated pharyn-goton-sillitis (right peri-tonsillar abscess)	Pharyngoton-sillitis	Super-infection of cutaneous lesions, pain management	Pain man-agement	Compli-cated proctitis	Pharyngoton-sillitis	Super-infection of cut-aneous lesions	Soft-tissue superin-fection (upper lip)	Super-infection of cut-aneous lesions	Super-infection of cut-aneous lesions/ Proctitis	Proctitis	Soft-tissue superin-fection (upper lip)
Days from OD to admission/ treatment	5/12	10/18	7/10	9/11	11/13	6/7	3/6	9/12	4/11	8/11	11/12	10/11	9/10	7/9	5/6	9/9	10/12	7/8	5/7
Days from treatment to recovery	13	10	21	9	12	11	14	4	7	18	6	21	14	20	7	18	17	27	15

* HIV diagnosis 2 months before MPX; ** AIDS presenters with HIV/AIDS diagnosis six months before MPX (multidrug resistant disseminated tuberculosis on treatment); *** recent virological failure. Abbreviations: M, male; y, years, MSM men who have sex with men; Neg, negative; Pos, positive; Unk, unknown; ART, antiretroviral therapy; VL, viral load; ND, not detectable, PREP, pre-exposure prophylaxis; BIC, bictegravir; TAF, tenofovir alafenamide fumarate; FTC, emtricitabine; 3TC, lamivudine; DTF dolutegravir, TDF, tenofovir disoproxil fumarate; DRV/c, darunavir/cobicistat; EFV, efavirenz; NA, not available; STD, sexual transmitted disease; CT computed tomography; OD, onset date.

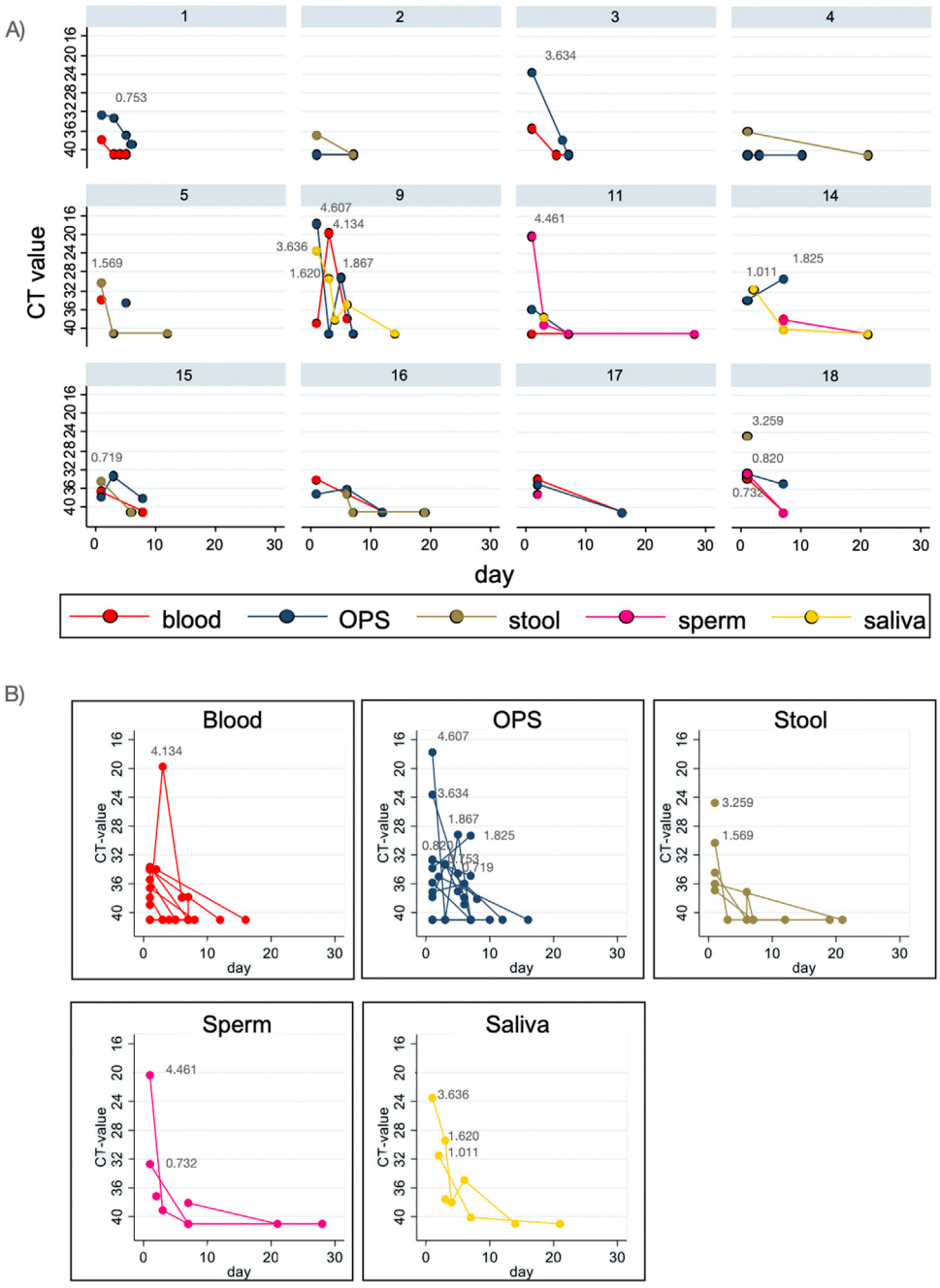

Fig. 1. Kinetics of MPXV DNA shedding in different biological samples from starting of the antiviral therapy. **A)** MPXV DNA levels detected in different longitudinal samples are shown for the 12 MPX patients followed up during infection. **B)** MPXV DNA levels detected in the different type of samples: blood, oropharyngeal swabs (OPS), stool, sperm and saliva. MPXV DNA levels are expressed as cycle threshold (Ct) values. In grey are shown digital droplet PCR (ddPCR) results express as Log_{10} copies/µL with a detection limit of the assay of 5 copies/µL.

Limited data on clinical effectiveness of tecovirimat are available, however, several recent reports on its use has shown good tolerability and no evolution versus severe disease in treated subjects [2–4,7]. Additionally, preliminary results from the first 549 MPX-positive patients treated with tecovirimat in United States (US), showed median time to subjective improvement of 3 days [7]. To the best of our knowledge, this is the first report of the use of antivirals for MPX with both clinical and virological results in this current outbreak. One case series of patients treated in 2018-2021 reported viral decay in one patient during tecovirimat treatment showing a shorter duration of viral shedding compared to the other patients [2]. Additionally, in a pre-print publication, outcomes, including viral kinetics, of 14 patients treated before February 2022 with tecovirimat were reported [8]. In contrast to that report, where rate of appearance of lesions decreased during treatment with a median of 5 days from treatment start [8], in our patients clinical improvement and no new lesions were reported in almost all patients 72 hours after tecovirimat initiation. The longer time elapsed from symptoms onset to treatment start (21 days) compared to our study (12 days) might partially explain this differ-

ent result. Of note, in our case series, 15% of MPX cases diagnosed received antiviral treatment, consistently with US data [9].

Concerning viral kinetics, it should be noted that low viral loads were observed. Additionally, some patients had all available samples negative in ddPCR since antiviral starting, in line with previous evidence showing that viral shedding occurs mainly during the first two weeks of the disease [10]. Due to the median time of 12 days from symptoms onset to starting treatment in this series, we cannot exclude a reduced impact of antiviral therapy on viral shedding or clinical resolution.

The main limitations of this study was the lack of control group, so that any conclusions on the effectiveness of antiviral therapy cannot be drawn, the small number of patients included, the heterogeneity of samples and the impossibility to collect samples for all the patients at each timepoint.

Data collected on observational studies such as this can help improve our knowledge of the use of antivirals for MPXV, waiting more robust results from the placebo-controlled randomized trial of tecovirimat for MPX.

Funding

This study was supported by Ricerca Corrente Linea 1 and 2, funded by the Italian Ministry of Health.

Conflicts of interests

The authors declare no conflict of interest for the present study.

Acknowledgments

INMI Monkeypox Study Group: Isabella Abbate, Alessandro Agresta, Camilla Aguglia, Alessandra Amendola, Andrea Antinori, Francesco Baldini, Tommaso Ascoli Bartoli, Alessia Beccacece, Rita Bellagamba, Giulia Berno, Aurora Bettini, Nazario Bevilacqua, Licia Bordi, Marta Camici, Priscilla Caputi, Fabrizio Carletti, Angela Corpolongo, Stefania Cicalini, Francesca Colavita, Alessandra D'Abramo, Angela D'Urso, Gabriella De Carli, Patrizia De Marco, Federico De Zottis, Silvia Di Bari, Lavinia Fabeni, Francesca Faraglia, Valeria Ferraioli, Carla Fontana, Federica Forbici, Concetta Maria Fusco, Marisa Fusto, Roberta Gagliardini, Anna Rosa Garbuglia, Saba Gebremeskel Teklé, Maria Letizia Giancola, Giuseppina Giannico, Emanuela Giombini, Enrico Girardi, Giulia Gramigna, Elisabetta Grilli, Susanna Grisetti, Cesare Ernesto Maria Gruber, Eleonora Lalle, Simone Lanini, Daniele Lapa, Gaetano Maffongelli, Fabrizio Maggi, Alessandra Marani, Andrea Mariano, Ilaria Mastrorosa, Giulia Matusali, Silvia Meschi, Valentina Mazzotta, Sabrina Minicucci, Claudia Minosse, Klizia Mizzoni, Martina Moccione, Annalisa Mondi, Vanessa Mondillo, Giorgia Natalini, Nicoletta Orchi, Sandrine Ottou, Jessica Paulicelli, Elisabetta Petrivelli, Maria Maddalena Plazzi; Carmela Pinnetti, Silvia Pittalis, Gianluca Prota, Vincenzo Puro, Silvia Rosati, Alberto Rossi, Gabriella Rozera, Martina Rueca, Laura Scorzolini, Eliana Specchiarello, Maria Virginia Tomassi, Massimo Tempestilli, Francesco Vaia, Francesco Vairo, Beatrice Valli, Alessandra Vergori, Serena Vita.

Supplementary materials

Supplementary material associated with this article can be found, in the online version, at doi:doi:10.1016/j.jinf.2022.11.001.

References

1. Li D, Liu Y, Li K, Zhang L.. Targeting F13 from monkeypox virus and variola virus by tecovirimat: Molecular simulation analysis. *J Infect* 2022;**85**:e99–e101.
2. Adler H, Gould S, Hine P, et al. Clinical features and management of human monkeypox : a retrospective observational study in the UK. *Lancet Infect Dis* 2022;**3099**:1–10.
3. Desai A, George T, Neumeister S, Arutyunova A, Stuart C.. Compassionate Use of Tecovirimat for the Treatment of Monkeypox Infection. *JAMA* 2022:1–3.
4. Matias WR, Koshy JM, Nagami EH, et al. Tecovirimat for the Treatment of Human Monkeypox: An Initial Series From Massachusetts, United States. *Open forum Infect Dis* 2022;**9**:ofac377.
5. Tarín-Vicente EJ, Alemany A, Agud-Dios M, et al. Clinical presentation and virological assessment of confirmed human monkeypox virus cases in Spain: a prospective observational cohort study. *Lancet* 2022;**400**:661–9.
6. Mailhe M, Beaumont A-L, Thy M, et al. Clinical characteristics of ambulatory and hospitalised patients with monkeypox virus infection: an observational cohort study. *Clin Microbiol Infect* 2022 Available at. doi:10.1016/j.cmi.2022.08.012.
7. O'Laughlin K, Tobolowsky FA, Elmor R, et al. Clinical Use of Tecovirimat (Tpoxx) for Treatment of Monkeypox Under an Investigational New Drug Protocol — United States. *MMWR Morb Mortal Wkly Rep* May-August 2022. ePub: 9 September 2022. DOI: http://dx.doi .
8. Festus Mbrenga, Emmanuel Nakouné, Christian Malaka, Josephine Bourner, J ake Dunning, Guy Vernet, Peter Horby PO. Monkeypox treatment with tecovirimat in the Central African Republic under an Expanded Access Programme Author. medRxiv Prepr doi:10.1101/2022.08.24.22279177.
9. Https://www.cdc.gov/poxvirus/monkeypox/response/2022/demographics-TPOXX.html accessed 26 September 2022.
10. Peiro-Mestres A, Fuertes I, Camprubi-Ferrer D, et al. Frequent detection of monkeypox virus DNA in saliva, semen, and other clinical samples from 12 patients, Barcelona, Spain, May to June 2022. *Eurosurveillance* 2022;**27**. Available at http://dx.doi.org/10.2807/1560-7917.ES.2022.27.28.2200503 .

Annalisa Mondi*, Roberta Gagliardini*, Valentina Mazzotta, Serena Vita
Clinical and Research Infectious Diseases Department, National Institute for Infectious Diseases Lazzaro Spallanzani IRCCS, Rome, Italy;

Fabrizio Carletti
Laboratory of Virology, National Institute for Infectious Diseases Lazzaro Spallanzani IRCCS, Rome, Italy;

Carmela Pinnetti, Maria Letizia Giancola
Clinical and Research Infectious Diseases Department, National Institute for Infectious Diseases Lazzaro Spallanzani IRCCS, Rome, Italy;

Eliana Specchiarello
Laboratory of Virology, National Institute for Infectious Diseases Lazzaro Spallanzani IRCCS, Rome, Italy;

Simone Lanini, Francesca Faraglia
Clinical and Research Infectious Diseases Department, National Institute for Infectious Diseases Lazzaro Spallanzani IRCCS, Rome, Italy;

Claudia Minosse
Laboratory of Virology, National Institute for Infectious Diseases Lazzaro Spallanzani IRCCS, Rome, Italy;

Jessica Paulicelli, Andrea Mariano
Clinical and Research Infectious Diseases Department, National Institute for Infectious Diseases Lazzaro Spallanzani IRCCS, Rome, Italy;

Gabriella Rozera
Laboratory of Virology, National Institute for Infectious Diseases Lazzaro Spallanzani IRCCS, Rome, Italy;

Carla Fontana
Laboratory of Microbiology and Biological Bank, National Institute for Infectious Diseases Lazzaro Spallanzani IRCCS, Rome, Italy;

Paolo Faccendini
Pharmacy Unit, National Institute for Infectious Diseases Lazzaro Spallanzani IRCCS, Rome, Italy;

Fabrizio Maggi
Laboratory of Virology, National Institute for Infectious Diseases Lazzaro Spallanzani IRCCS, Rome, Italy;

Enrico Girardi
Scientific Direction, National Institute for Infectious Diseases Lazzaro Spallanzani IRCCS, Rome, Italy

Francesco Vaia
General Direction, National Institute for Infectious Diseases Lazzaro Spallanzani IRCCS, Rome, Italy.

Emanuele Nicastri, Andrea Antinori
Clinical and Research Infectious Diseases Department, National Institute for Infectious Diseases Lazzaro Spallanzani IRCCS, Rome, Italy;

#Corresponding author: Dr. Roberta Gagliardini, Clinical and Research Infectious Diseases Department, National Institute for Infectious Diseases Lazzaro Spallanzani IRCCS, Via Portuense 292, 00149 Rome, Italy, 0039 3331045103, 0039 0655170368
E-mail address: roberta.gagliardini@inmi.it (R. Gagliardini)

* A.M. and RG. contributed equally to the manuscript.
Accepted 2 November 2022
Available online 5 November 2022

https://doi.org/10.1016/j.jinf.2022.11.001

Multidrug-resistant infection in COVID-19 patients: A meta-analysis

Dear Editor,

Yeonju La et al. reported the most problematic multidrug-resistant microorganisms (MDROs) increased after the Coronavirus disease 2019 (COVID-19) pandemic in South Korea, suggesting active and continuous monitoring of the increase in infections with MDROs.[1] We had a valuable opportunity to carefully read this interesting manuscript and additional published studies to further explore the infection rate of multidrug-resistant (MDR) in patients with COVID-19.

COVID-19 is a newly emerging disease in the human population. The World Health Organization classified COVID-19 as a pandemic on March 11, 2020. The disease is caused by severe acute respiratory syndrome coronavirus 2 (SARS-CoV-2). Some affected patients need hospitalization in the intensive care unit (ICU) for critical care and mechanical ventilation, increasing the risk of secondary infection. The cause of this secondary infection may be MDR bacterial infection.

MDROs are defined as those resistant to one or more classes of antimicrobial drugs, including methicillin-resistant *Staphylococcus aureus*, vancomycin-resistant enterococci, and certain Gram-negative Enterobacteriaceae, which produce ultra-broad-spectrum beta-lactamase or carbapenemase resistance. Antimicrobial resistance is recognized as a public threat of increasing urgency. By 2050, an estimated 10 million people will die annually from MDR infections (resistant to three or more antimicrobial drugs). Decreased effectiveness of antibiotics may exponentially increase the risk of medical and surgical procedures and immunosuppressive treatments such as cancer chemotherapy.

In the post-pandemic era, antibiotic resistance might become a bigger challenge. In view of the great danger posed by MDR bacteria, we tried to explore the prevalence of MDR bacteria in patients with COVID-19 to provide timely and effective prevention programs.

We found that some published studies explored the situation of patients with COVID-19 who acquired MDR bacteria during hospitalization. Fernández[2] et al. compared the colonization of MDROs in patients infected and uninfected with COVID-19 admitted to the ICU during the COVID-19 epidemic. It was concluded that the non-COVID-19 group in the ICU had a lower rate of MDR bacterial infections after admission than the COVID-19 group. Not only in the ICU, the use of mechanical ventilation also aggravated the secondary respiratory tract infection of patients with COVID-19. Patients with COVID-19 admitted to the ICU and requiring mechanical ventilation had a high rate of secondary infections during their hospital stay.[3] Moreover, within late secondary infections, one third of the isolated bacteria were MDR.

For this reason, PubMed, Web of Science, Embase, and Cochrane Library databases were extensively searched for all compliant studies published from January 1, 2020, to October 10, 2022. The inclusion criteria were as follows: (1) adult patients with COVID-19 confirmed by reverse transcriptase–polymerase chain reaction; (2) peer-reviewed original studies in English; (3) MDR-infected strains measured by the number of strains; and (4) the infection statistics of MDR based on the number of people. In total, 8 studies with 1423 patients were identified. Eight studies reported MDR bacterial infections in patients with COVID-19 pneumonia. General information about the included studies is summarized (Table 1).[2-9] We focused on collecting some of the most common strains, such as *Enterobacter, S. aureus*, and *Klebsiella pneumoniae*. The results of eight studies were showed that 42% of the patients with COVID-19 were infected with MDR (95% confidence interval (CI), 0.23–0.61; $P < 0.01$) (Fig. 1). Also, the heterogeneity (I^2) was 97.9% and the Egger value was 0.174, indicating no publication bias. We also collected data on common strains for collation to further investigate the specific strain distribution of MDR bacteria. Among the MDR strains, the *K. pneumoniae* rate in five studies was 21% (95% CI, 0.09–0.32; $P < 0.01$), the *Enterobacter* spp. rate in another five was 8% (95% CI, 0.04–0.12), and the *S. aureus* rate in five studies was

Table 1
The basic information of the included literature.

Author	Year	Country	Total	MDR	MDR strains	K. pneumoniae	Enterobacter spp.	S. aureus
María	2022	Chile	71	22	71	4(5.6%)	5(7%)	4(5.6%)
Junya L	2022	Brazil	43	28	38	11(28.9%)	2(5.3%)	6(15.8%)
Marie	2022	Europe	840	598	N	N	N	N
Ashish	2021	America	39	16	16	N	2(12.5%)	11(68.8%)
Prayudi	2022	Indonesia	182	74	74	14(18.9%)	N	1(1.4%)
Elisa	2020	Belgium	72	24	31	8(25.8%)	3(9.7%)	N
Fernández	2021	Spain	24	9	13	5(38.5%)	3(23.1%)	2(15.4%)
Priya	2020	America	152	24	N	N	N	N

Total: number of COVID-19 patient included in the study.
MDR: Number of people infected with MDR.
N: no data.

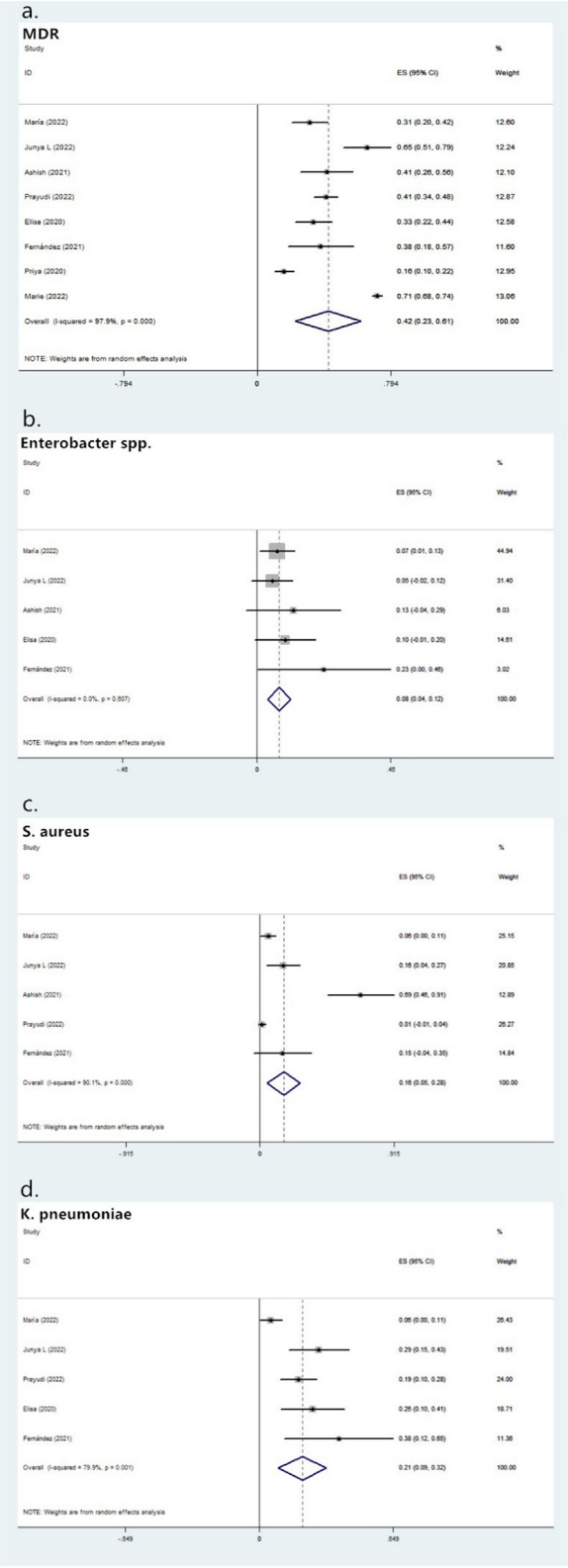

Fig. 1. a. Forest plot of MDR infection rate in COVID-19 patients.
b. Forest plot of the enterobacter spp. rate among multidrug-resistant strains.
c. Forest plot of the s. aureus rate among multidrug-resistant strains.
d. Forest plot of the k. pneumoniae rate among multidrug-resistant strains.

16% (95% CI, 0.05–0.28; $P < 0.01$). These are the main bacteria isolated from endotracheal aspirate and blood.

During the COVID-19 pandemic, medical care systems worldwide became overwhelmed, and the shortage of beds and personal protective equipment (PPE) in ICU also contributed to the rapid growth of MDR bacteria. Also, the reasons for the high infection rate of MDR bacteria in patients with COVID-19 might be as follows[10]: (i) Cough, sore throat, and fever, which were the most common symptoms of COVID-19, were independent factors associated with overuse of antibiotics in hospitals and communities. (ii) Antimicrobial drug use was common in patients with COVID-19, and more than 70% of the patients with COVID-19 received antimicrobial treatment despite less than 10% having bacterial or fungal coinfections. (iii) At the beginning of the pandemic, some broad-spectrum antimicrobial agents were suggested as treatments against COVID-19 and were tested for a possible efficacy against SARS-CoV-2, for example, teicoplanin, azithromycin, and tetracycline.

In a word, this study draws attention to the necessity of monitoring drug resistance/multidrug resistance and proper use of antibiotics, especially for patients with COVID-19 hospitalized for a long time. Nonpharmacological behavioral changes implemented during the COVID-19 pandemic to drop the spread of SARS-CoV2 may also reduce the prevalence of MDR infection in patients with COVID-19. For example, hospital hygiene habits, the improvement of PPE, and the use of antibacterial soap and disinfectant were adopted to a great extent. These practices may reduce the spread of MDR. In addition, restrictions on the number of hospital visits, the availability of nucleic acid testing, and distance policies implemented for inpatients may lead to future reductions in bacterial circulation.

Availability of data and materials

The authors confirm that the data supporting the findings of this study are available within the article.

Declaration of Competing Interest

No potential conflict of interest was reported by the author(s).

Acknowledgement

The presented study was Medical and Technology Project of Zhejiang Province (No.2021KY890); Hangzhou science and Technology Bureau fund (No.20191203B96; No.20191203B105); Clinical Research Fund of Zhejiang Medical Association(No.2020ZYC-A13); Zhejiang Kangenbei Hospital Management Soft Science Research Project (No2022ZHA-KEB316); Zhejiang Traditional Chinese Medicine Scientific Research Fund Project(No. 2022ZB280). The work was supported by the Key medical disciplines of Hangzhou.

References

1. La Y., et al. Increase of multidrug-resistant bacteria after the COVID-19 pandemic in South Korea: time-series analyses of a long-term multicenter cohort. *J. Infect.* 2022 Sep 30:S0163-4453(22)00556-4.
2. Fernández P., et al. Colonization by multidrug-resistant microorganisms in ICU patients during the COVID-19 pandemic. Medicina. Intensiva. 2021;**45**:313–15.
3. Ceballos M.E., et al. Secondary respiratory early and late infections in mechanically ventilated patients with COVID-19. *BMC. Infect. Dis.* 2022;**22**:760.
4. Bhargava A., et al. High rate of multidrug-resistant organisms (MDROs) among COVID-19 patients presenting with bacteremia upon hospital admission. *Am. J. Infect. Control.* 2021;**49**:1441–2.
5. Bogossian E.G., et al. The acquisition of multidrug-resistant bacteria in patients admitted to COVID-19 intensive care units: a monocentric retrospective case control study. *Microorganisms* 2020;**8**:1821.
6. de Hesselle M.L., et al. Invasiveness of ventilation therapy is associated to prevalence of secondary bacterial and fungal infections in critically ill COVID-19 patients. *J. Clin. Med.* 2022;**11**:5239.

7. Nori P., et al. Bacterial and fungal coinfections in COVID-19 patients hospitalized during the New York City pandemic surge. *Infect. Control. Hospital. Epidemiol.* 2021;**42**:84–8.
8. Santoso P., et al. MDR pathogens organisms as risk factor of mortality in secondary pulmonary bacterial infections among COVID-19 patients: observational studies in two referral hospitals in West Java, Indonesia. Int. J. General. Med. 2022;**15**:4741–51.
9. Singulani J.L., et al. The impact of COVID-19 on antimicrobial prescription and drug resistance in fungi and bacteria. *Brazil. J. Microbiol.* 2022:1–11 Sep 10.
10. Gasperini B., et al. Multidrug-resistant bacterial infections in geriatric hospitalized patients before and after the COVID-19 outbreak: results from a retrospective observational study in two geriatric wards. *Antibiotics. (Basel, Switzerland)* 2021;**10**:95.

Siqi Hu[1], Yao You[1], Shenghui Zhang[1], Jiake Tang, Chen Chen, Wen Wen, Chunyi Wang
Hangzhou Institute of Cardiovascular Diseases, Affiliated Hospital of Hangzhou Normal University, Hangzhou Normal University,Hangzhou, 310015, China

Yongran Cheng
School of Public Health, Hangzhou Medical College, Hangzhou, 311300, China

Mengyun Zhou
Department of Molecular & Cellular Physiology, Shinshu University School of Medicine, 3900803, Japan

Zhanhui Feng
Department of Neurology, Affiliated Hospital of Guizhou Medical University, Guiyang, 550000, China

Tao Tan
Faculty of Applied Science, Macao Polytechnic University, Macao SAR, 999078, China

Guanming Qi*
Division of Pulmonary, Critical Care and Sleep, Tufts Medical Center, Boston, MA, 02111, USA

Mingwei Wang*, Xiaoyan Liu*
Hangzhou Institute of Cardiovascular Diseases, Affiliated Hospital of Hangzhou Normal University, Hangzhou Normal University,Hangzhou, 310015, China

*Corresponding authors.
E-mail addresses: gqi@tuftsmedicalcenter.org (G. Qi), wmw990556@hznu.edu.cn (M. Wang), 772855717@qq.com (X. Liu)

[1] Siqi Hu, Yao You and Shenghui Zhang contributed equally to this work.

Accepted 23 October 2022
Available online 5 November 2022

https://doi.org/10.1016/j.jinf.2022.10.043

In vitro activity of imipenem/relebactam, meropenem/vaborbactam and comparators against *Pseudomonas aeruginosa* in Taiwan: Results from the Study for Monitoring Antimicrobial Resistance Trends (SMART) in 2020

Dear Editor,

We read with great interest the article by La et al. in which it was reported that bacteremia due to difficult-to-treat *Pseudomonas aeruginosa*, in which the isolates are not susceptible to carbapenems, antipseudomonal β-lactams, or fluoroquinolones, increased after the COVID-19 pandemic in Korea.[1] A similar trend has been observed in Taiwan.

Pseudomonas aeruginosa characteristically causes nosocomial infections but has also been found in serious community-acquired infections.[2,3] *P. aeruginosa* were reported to make up 5–15% of gram-negative pathogens isolated from intraabdominal infections (IAIs) and urinary tract infections (UTIs).[2] As a result of increased expression of β-lactamases (including carbapenemases), the presence of multiple efflux pumps, decreased expression of porin proteins, and changes in penicillin-binding proteins, treatment of resistant *P. aeruginosa* infections has become clinically challenging.[4,5] Imipenem-relebactam and meropenem-vaborbactam, both of which were recently approved by the U.S. FDA, contain novel β-lactamase inhibitors and carbapenems. However, data on the susceptibility of *P. aeruginosa* to these two new agents are lacking in Taiwan.

The Study for Monitoring Antimicrobial Resistance Trends (SMART) is a network of surveillance systems that track the in vitro antimicrobial susceptibility of clinically significant gram-negative bacteria nationwide.[6] Eight participating hospitals in Taiwan provided susceptibility data for *P. aeruginosa* isolated from IAIs and UTIs in 2020. Matrix-assisted laser desorption ionization-time of flight mass spectrometry was used to determine the presence of *P. aeruginosa*. At International Health Management Associates (IHMA, Schaumburg, IL, USA), antimicrobial susceptibility was determined by a broth microdilution method using frozen panels. Except in the case of meropenem-vaborbactam, MICs were interpreted according to the Clinical and Laboratory Standards Institute (CLSI) guidelines (M100-S31). The EUCAST 2021 standard was used to determine the susceptibility to meropenem-vaborbactam due to a lack of CLSI standards. The Institutional Review Board of National Taiwan University Hospital approved the study (NTUH 9561709108).

A total of 111 *P aeruginosa* isolates from 8 hospitals in Taiwan were gathered in 2020. The part of the body from which the bacteria were isolated and the time of collection are shown in Table S1. Fifty-eight (52.3%) of the isolates were obtained from UTIs, and 53 (47.7%) of the isolates were obtained from IAIs. Most of the *P. aeruginosa* were isolated from patients who had been admitted for 48 h or more. Seventy-four (66.7%) of the *P. aeruginosa* infections in the current report were nosocomial infections in which specimens were obtained $\geq$ 48 h after admission, and 37 (33.3%) infections were community-acquired infections. The incidence of nosocomial infection was 60.3% among UTIs and 73.6% among IAIs. Most of the isolates obtained from IAIs were from peritoneal fluid or from the gall bladder.

The antimicrobial susceptibility patterns of *P. aeruginosa* are summarized in Table 1. The two carbapenem-β-lactamase inhibitor combinations imipenem/relebactam and meropenem/vaborbactam were highly effective against *P. aeruginosa*. The susceptibilities were 97.3% and 96.4% for imipenem/relebactam and meropenem/vaborbactam, respectively. However, the susceptibilities to imipenem and meropenem alone were lower at 62.2% and 82.1%, respectively. Amikacin susceptibility (98.2%) was excellent, and *P. aeruginosa* exhibited fair susceptibility (85.6%) to cefepime. A small percentage of the isolates displayed colistin resistance (0.9%). In contrast, the susceptibility of the isolates to other traditional anti-*P. aeruginosa* agents, including aztreonam, cefepime, ceftazidime, levofloxacin, and piperacillin/tazobactam, was inferior, ranging from 72.1% to 78.4%. The incidence of antimicrobial resistance was higher in people with nosocomial infections caused by *P. aeruginosa* compared with that associated with community-acquired infections (Fig. 1A). There was a statistically significant reduction in susceptibility to imipenem, lev-

Table 1
Antimicrobial susceptibility patterns of 111 *Pseudomonas aeruginosa* isolates collected from patients in the Study for Monitoring Antimicrobial Resistance Trends (SMART) in 2020.

Agent	MIC (mg/L)			% of isolates in each susceptibility category		
	Range	MIC_{50}	MIC_{90}	S	I	R
Imipenem/relebactam	0.12–4	0.5	1	97.3	1.8	0.9
Meropenem/vaborbactam	0.25–16	0.5	4	96.4	0	3.6
Imipenem	0.25–32	2	16	62.2	17.1	20.7
Meropenem	0.25–16	0.5	4	80.1	8.1	9.9
Amikacin	4–32	4	8	98.2	0	1.8
Aztreonam	1–16	8	16	72.1	27.9	0
Cefepime	1–32	2	16	85.6	9.9	4.5
Ceftazidime	1–32	4	32	78.4	7.2	14.4
Colistin	1–4	1	1	–	99.1	0.9
Levofloxacin	0.5–4	0.5	4	74.8	9.1	16.2
Piperacillin/tazobactam	4–64	8	64	76.6	23.4	0

S, susceptible; I, intermediate; R, resistant.

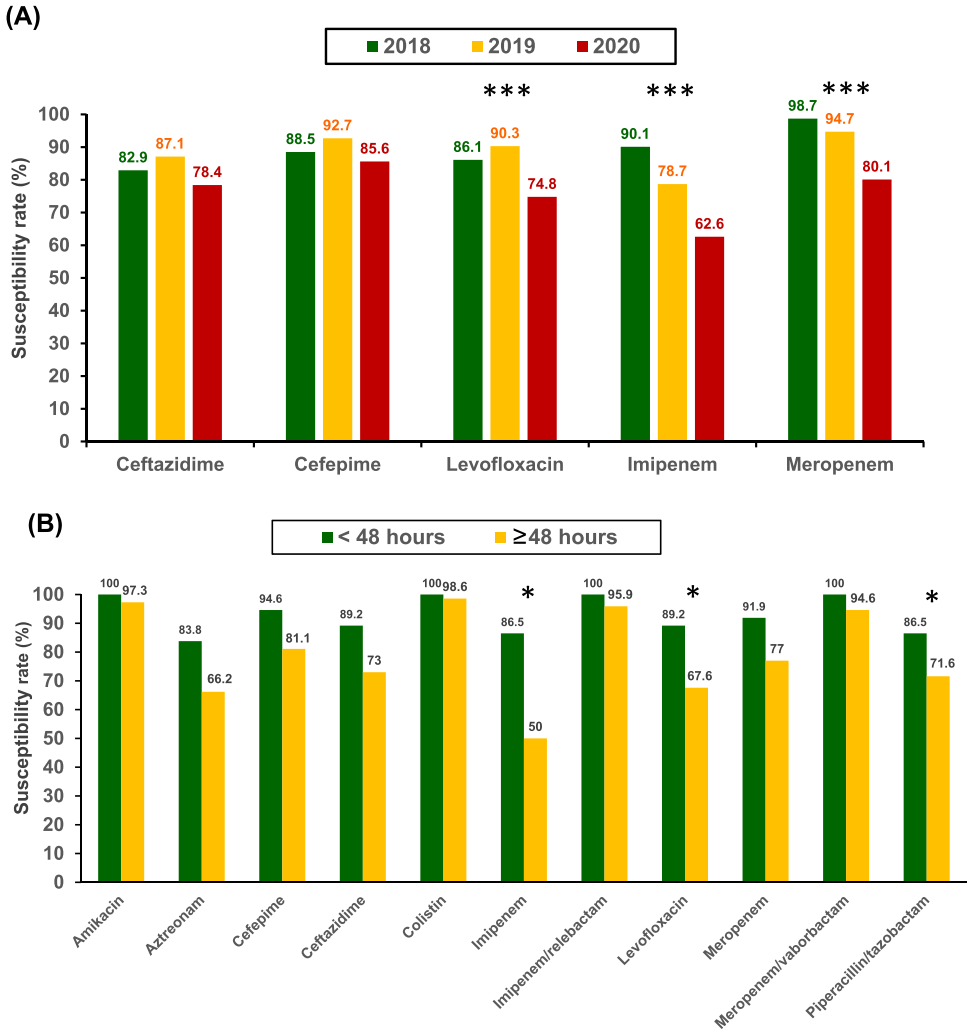

Fig. 1. Rates of in vitro susceptibility to antimicrobial agents of (A) *Pseudomonas aeruginosa* collected from patients in Taiwan during the period 2018–2020 and (B) *Pseudomonas aeruginosa* isolates collected from patients hospitalized for <48 or ≥48 h in 2020. Two-sided chi-square tests were conducted. Asterisks indicate that the differences in susceptibility rates in different years are significant. $^{*}p < 0.05$; *** $p < 0.001$.

ofloxacin, and piperacillin/tazobactam. Only imipenem/relebactam, meropenem/vaborbactam, amikacin, and colistin were effective against more than 90% of nosocomial *P. aeruginosa* infections (Fig. 1A).

The antimicrobial susceptibility profiles of *P. aeruginosa* isolated from patients with IAIs and UTIs were similar, except in the case of levofloxacin (Fig. S1). Compared to the surveillance studies conducted in 2018 and 2019 in Taiwan, current study in 2020 in Taiwan revealed lower susceptibility rates of *P. aeruginosa* to multiple agents (Fig. 1B).[7,8] Its susceptibility to levofloxacin, imipenem, and meropenem decreased significantly (Fig. 1B).[7,8]

A total of 45 *P aeruginosa* isolates were found to be nonsusceptible to meropenem or imipenem (MIC ≥ 4 mg/L). The susceptibility patterns of these carbapenem-nonsusceptible *P. aeruginosa* (CNPA) isolates are shown in Fig. S2. These CNPA were highly susceptible to amikacin (95.6%), imipenem/relebactam (93.3%), and meropenem/vaborbactam (91.1%). Only one CNPA isolate (2.2%) was resistant to colistin. CNPA displayed moderate susceptibility (71.1%) to cefepime. The susceptibility to aztreonam, ceftazidime, levofloxacin, meropenem, and piperacillin/tazobactam ranged from 55% to 60%.

Twenty-three isolates were resistant to meropenem or imipenem (MIC ≥8 μg/ml). The susceptibility profiles of these carbapenem-resistant *P. aeruginosa* (CRPA) strains are shown in Fig. S3. Amikacin is highly effective against CRPA (95.7%). No colistin-resistant strain was detected among the CRPA strains. The susceptibility of CRPA strains to imipenem/relebactam and meropenem/vaborbactam was fair (87.0% and 82.6%, respectively). Moderate (65.2%) susceptibility to cefepime was observed in CRPA; susceptibility to levofloxacin and ceftazidime was approximately 50%, and susceptibility to aztreonam, imipenem, meropenem, and piperacillin/tazobactam was less than 50%.

Teo et al. collected clinical isolates of CNPA in Singapore between 2006 and 2020 and reported that these isolates exhibited high resistance to imipenem, meropenem, aztreonam, cefepime, piperacillin/tazobactam, and levofloxacin.[9] According to Teo's report, less than 20% of CNPA isolates were sensitive to these agents. The susceptibilities of CNPA to ceftazidime, piperacillin-tazobactam and levofloxacin were 47.1%, 35.3%, and 37.2%, respectively, according to a report on clinical specimens collected from 2016 to 2017 in the US.[10] In contrast, we found a less resistant profile of CNPA in Taiwan. The CNPA we examined displayed moderate susceptibilities (greater than 50%) to meropenem, aztreonam, cefepime, piperacillin/tazobactam, and levofloxacin. Monitoring the antimicrobial susceptibility of CNPA in different regions of the world is essential since the resistance profiles of bacteria vary greatly.

In summary, we report here that clinical isolates of *P. aeruginosa* isolated in Taiwan display outstanding susceptibility to two carbapenem/β-lactamase inhibitor combinations, imipenem-relebactam, and meropenem-vaborbactam. We observed that both CNPA and CRPA isolates remain highly susceptible to these two agents. Continuous surveillance in which the trends of resistance to these two agents are monitored is vital.

Funding

This study was supported by Merck & Co., Inc. (Rahway, NJ, USA)

Declaration of Competing Interest

The authors report no conflicts of interest.

Acknowledgements

Investigators associated with the SMART Taiwan Group in 2020: Po-Ren Hsueh (China Medical University Hospital, Taichung, Taiwan), Wen-Chien Ko (National Cheng Kung University Hospital, Tainan, Taiwan), Po-Liang Lu (Kaohsiung Medical University Hospital, Kaohsiung, Taiwan), Chun-Eng Liu (Changhua Christian Hospital, Changhua, Taiwan), Hung-Jen Tang (Chi-Mei Medical Centre, Tainan, Taiwan), Fu-Der Wang (Taipei Veterans General Hospital, Taipei, Taiwan), Yao-Shen Chen (Kaohsiung Veterans General Hospital, Kaohsiung, Taiwan), Shih-Ming Tsao (Chung Shan Medical University Hospital, Taichung, Taiwan), and Mao-Wang Ho (China Medical University Hospital, Taichung, Taiwan).

Supplementary materials

Supplementary material associated with this article can be found, in the online version, at doi:10.1016/j.jinf.2022.10.038.

References

1. La Y., Hong J.Y., Lee H.S., Lee E.H., Lee K.H., Song Y.G., et al. Increase of multidrug-resistant bacteria after the COVID-19 pandemic in South Korea: time-series analyses of a long-term multicenter cohort. *J Infect* 2022 Sep 29:S0163-4453(22)00556-4.
2. Liu Y.M., Chen Y.S., Toh H.S., Huang C.C., Lee Y.L., Ho C.M., et al. In vitro susceptibilities of non-Enterobacteriaceae isolates from patients with intra-abdominal infections in the Asia-Pacific region from 2003 to 2010: results from the Study for Monitoring Antimicrobial Resistance Trends (SMART). *Int J Antimicrob Agents* 2012;**40**:S11–17 Suppl.
3. Bassetti M., Vena A., Croxatto A., Righi E., Guery B.. How to manage *Pseudomonas aeruginosa* infections. *Drugs Context* 2018;**7**:212527.
4. Moyá B., Beceiro A., Cabot G., Juan C., Zamorano L., Alberti S., et al. Pan-β-lactam resistance development in *Pseudomonas aeruginosa* clinical strains: molecular mechanisms, penicillin-binding protein profiles, and binding affinities. *Antimicrob* Agents Chemother 2012;**56**(9):4771–8.
5. Feng W., Huang Q., Wang Y., Yuan Q., Li X., Xia P., et al. Changes in the resistance and epidemiological characteristics of *Pseudomonas aeruginosa* during a ten-year period. *J Microbiol Immunol Infect* 2021;**54**(2):261–6.
6. Hsueh P.R.. Study for Monitoring Antimicrobial Resistance Trends (SMART) in the Asia-Pacific region, 2002-2010. *Int J Antimicrob Agents* 2012;**40**:S1–3 Suppl.
7. Lee Y.L., Lu M.C., Shao P.L., Lu P.L., Chen Y.H., Cheng S.H., et al. Nationwide surveillance of antimicrobial resistance among clinically important Gram-negative bacteria, with an emphasis on carbapenems and colistin: results from the Surveillance of Multicenter Antimicrobial Resistance in Taiwan (SMART) in 2018. *Int J Antimicrob Agents* 2019;**54**:318–28.
8. Jean S.S., Lu M.C., Ho M.W., Ko W.C., Hsueh P.R.. Non-susceptibilities to antibiotics against important Gram-negative bacteria, and imipenem-relebactam, meropenem-vaborbactam against carbapenem non-susceptible Enterobacterales and *Pseudomonas aeruginosa* isolates implicated in complicated intra-abdominal and urinary tract infections in Taiwan, 2019. *J Microbiol Immunol Infect* 2022;**59**(3):106521.
9. Teo J.Q., Tang C.Y., Lim J.C., Lee S.J., Tan S.H., Koh T.H., et al. Genomic characterization of carbapenem-non-susceptible *Pseudomonas aeruginosa* in Singapore. *E*merg Microbes Infect 2021;**10**(1):1706–16.
10. Lob S.H., Hoban D.J., Young K., Motyl M.R., Sahm D.F.. Activity of ceftolozane–tazobactam and comparators against *Pseudomonas aeruginosa* from patients in different risk strata - SMART United States 2016-2017. *J Glob Antimicrob Resist* 2020;**20**:209.

Yuag-Meng Liu
Department of Internal Medicine, College of Medicine, Chung Shan Medical University, Taichung, Taiwan
Department of Internal Medicine, Changhua Christian Hospital, Changhua, Taiwan

Wen-Chien Ko
Department of Medicine, College of Medicine, National Cheng Kung University, Tainan, Taiwan

Mao-Wang Ho
Division of Infectious Diseases, Department of Internal Medicine, China Medical University Hospital, Taichung, Taiwan

Yu-Lin Lee
Department of Internal Medicine, College of Medicine, Chung Shan Medical University, Taichung, Taiwan
Department of Internal Medicine, Changhua Christian Hospital, Changhua, Taiwan

Po-Ren Hsueh*
Division of Infectious Diseases, Department of Internal Medicine, China Medical University Hospital, Taichung, Taiwan
Department of Laboratory Medicine, China Medical University Hospital, Taichung, Taiwan
School of Medicine, China Medical University, Taichung, Taiwan
Ph.D. Program in Ageing, School of Medicine, China Medical University, Taichung, Taiwan

*Corresponding author at: Department of Laboratory Medicine, China Medical University Hospital, Taichung, Taiwan.

E-mail address: hsporen@gmail.com (P.-R. Hsueh)

Accepted 30 October 2022
Available online 3 November 2022

https://doi.org/10.1016/j.jinf.2022.10.038

Regdanvimab improves disease mortality and morbidity in patients with COVID-19: Too optimistic and too early to say?

Dear Editor,

We have read with great interest the recently published meta-analysis by Yang, M. et al.[1] in the *Journal of Infection* on the topic of regdanvimab use in COVID-19 patients. The authors included 7 studies in their meta-analysis and concluded that regdanvimab administration significantly reduced COVID-19 mortality and risk of disease progression according to a composite outcome. This publication is of particular interest and significance as it is currently the only meta-analysis published on the topic, however some of the authors' presented results and conclusions may potentially be misleading.

In the original meta-analysis (recreated on Fig. 1A) the authors included 4 studies in their mortality outcome analysis and concluded that regdanvimab use was associated with statistically significant lower mortality (OR = 0.14, 95% CI: 0.03 to 0.56, $P = 0.006$; I2 = 0%). In the meta-analysis, the study by Park, S. et al.[2] with a weight of 75.5% and an OR of 0.04 (95% CI: 0.00 to 0.64) contributed disproportionately more to the pooled result in comparison to other included studies. The Park, S. et al.[2] study was an observational retrospective study which explored outcomes of 377 regdanvimab treated patients and 520 standard of care controls in an overall primary cohort from which a propensity score matched cohort of 754 patients, 377 in each group, was created and analysed. In their meta-analysis, Yang, M. et al.[1] included the outcomes from the unmatched primary cohort, instead of the PS-matched cohort, which in our opinion was incorrect due to statistically significant differences between the two unmatched groups, as reported by Park, S. et al.[2], which favoured the treatment group. Patients in the control group: 1) were older (median age 65 [IQR, 57–75] vs. 61 [53–68] years, $P < 0.001$), 2) had a higher proportion of moderate COVID-19 pneumonia (54.1% vs. 45.9%, $P = 0.049$), 3) chronic lung disease (78.9% vs. 21.1%, $P = 0.007$) and 4) cardiovascular disease (73.9% vs. 26.1%, $P < 0.001$), which were all accounted for and no longer statistically significant in the PS-matched cohort. Thus, the decision to include the outcomes of the unmatched cohort seems inappropriate and presents a significant potential source of bias in the meta-analysis, especially when considering the significant weight of the Park, S. et al.[2] study. In order to eliminate the source of bias, we recreated the meta-analysis using the outcomes from the PS-matched cohort, Fig. 1B (OR = 0.49, 95% CI: 0.10 to 2.28, P = 0.38; I2 = 0%) and we also excluded the Park, S. et al.[2] study altogether due to the zero event rate, Fig. 1**C** (OR = 0.44, 95% CI: 0.08 to 2.53, P = 0.38; I2 = 0%) and we found no statistically significant impact of regdanvimab on COVID-19 mortality in either analysis. Moreover, we also recreated the composite outcome analysis, Fig. 1D and conducted an additional analysis with the PS-matched Park, S. et al.[2] cohort and found no significant difference between the results.

In conclusion, while it seems that regdanvimab may have a potential beneficial effect on COVID-19 patients based on the composite outcome, in our view, the conclusion made by Yang, M. et al.[1] that regdenvimab reduced patient mortality seems exaggerated. Finally, in all meta-analyses shown on Fig. 1, a considerable uncertainty of the results is perhaps best illustrated by the wide prediction intervals, which were present even in the original mortality outcome analysis by Yang, M. et al.[1], Fig. 1A. As the number of published studies remains small and with most current studies being retrospective in design, additional high quality, prospective, randomised trials exploring the potential beneficial effects of regdanvimab in COVID-19 patients are urgently needed.

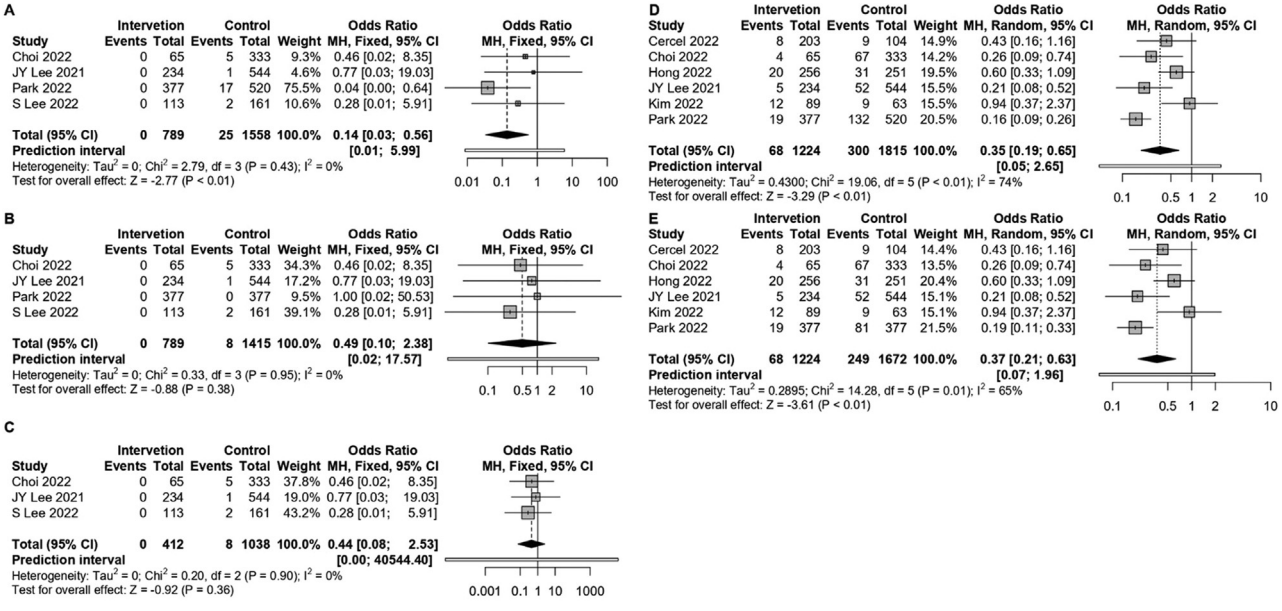

Fig. 1. Forest plots recreating the original meta-analysis results by Yang, M. et al.[1] regarding the mortality (Fig. 1A) and composite (Fig. 1D) outcomes. Reanalysis of the mortality (Fig. 1B) and composite (Fig. 1**E**) outcome meta-analysis using outcomes from the propensity score matched cohort from the Park, S. et al..[2] Mortality outcome meta-analysis (Fig. 1C) with the Park, S. et al.[2] study excluded due to a zero event rate.

Conflict of interest

No conflicts of interest to declare.

Authors' contributions

All authors participated equally in all parts of the manuscript.

Funding

No funding was received for this study.

Data disclosure statement

All analysed data is presented in the manuscript.

References

1. Yang M., et al. Regdanvimab improves disease mortality and morbidity in patients with COVID-19: a meta-analysis. *J Infect* 2022;**85**:122–4.
2. Park S., Je N.K., Kim D.W., Park M., Heo J.. Effectiveness and safety of Regdanvimab in patients with mild-to-moderate COVID-19: a retrospective cohort study. *J Korean Med Sci* 2022;**37**:1–16.

Robert Marcec, Vinko Michael Dodig
School of Medicine, University of Zagreb, Zagreb, Croatia

Robert Likic*
School of Medicine, University of Zagreb, Zagreb, Croatia
Clinical Hospital Centre Zagreb, Department of Internal Medicine, Unit for Clinical Pharmacology, Zagreb, Croatia

*Corresponding author at: University Hospital Centre Zagreb, Department of Internal Medicine, Unit of Clinical Pharmacology, Kispaticeva 12, 10000 Zagreb, Croatia.
E-mail addresses: robert.likic@mef.hr, rlikic@kbc-zagreb.hr (R. Likic)

Accepted 21 October 2022
Available online 1 November 2022

https://doi.org/10.1016/j.jinf.2022.10.030

Evaluation of clinical harm associated with Omicron hospital-onset COVID-19 infection

Dear Editor,

The COVID-19 pandemic has seen waves of hospital-onset COVID-19 infection (HOCI).[1-3] As community prevalence rose and fell, so too did the prevalence of HOCI.[2, 3] COVID-19 waves in the UK can be characterised by the variants that caused them, with the 'Omicron wave' emerging in December 2021.[4] Outcomes in hospitalised patients with COVID-19 were poor pre-Omicron.[4-7] The Omicron variant resulted in a wave of HOCI in late 2021 and early 2022. A recent article in this journal found that 'incidental' COVID-19 infection was more common during the Omicron wave than the Delta wave, accounting for approximately two thirds of cases in one London hospital group.[1] We undertook an evaluation of harms associated with HOCI caused by Omicron in order to inform future decision making about COVID-19 risk management strategies.

We reviewed patients with probable HOCI (according to UK definitions) admitted to three London hospital groups between January and mid-March 2022. Patients with 'hospital-onset probable healthcare-associated' (HOPHA) (first positive specimen date 8-14 days after admission) and patients with 'hospital-onset definite healthcare-associated' (HODHA) (first positive >=15 days after admission) were included. Patients were from Guy's and St. Thomas' NHS Foundation Trust (n=56), Royal Free London NHS Foundation Trust (n=49), and St. George's University Hospitals NHS Foundation Trust (n=24). These Trusts were testing all inpatients for SARS-CoV-2 two to three times each week, and had systems in place for real-time detection of HOCI. All COVID-19 during this period was assumed to the Omicron variant, supported by laboratory genotyping data. Patient notes and death certificates (where applicable) were reviewed and the following information was recorded: patient age, SARS-CoV-2 vaccination status, whether the patient is classified as 'vulnerable' as defined by a list used to determine eligibility for booster vaccination and treatment,[8] and whether or not the patient developed any symptoms consistent with COVID-19. The following measures of harm were chosen based on NHS guidance[9]; increased length of stay (>1 day) to manage their COVID-19 infection, new or increased requirement for supplemental oxygen, and admission to ICU or HDU for COVID-19. Death certificates of patients who died were reviewed to establish if COVID-19 was recorded as a direct cause of death (Part 1) or a condition contributing to the death (Part 2). Logistic regression was used to test whether any measure of harm (increased length of stay or new or increased requirement for supplemental oxygen or admission to ICU or HDU for COVID-19, or COVID-19 on Part 1 or Part 2 of the death certificate) was associated with age, patient vaccination status, or whether or not the patient was classified as clinically vulnerable. The review was considered service evaluation to help inform future infection prevention and control policy decisions.

Table 1
Prevalence of symptoms and harm associated with COVID-19.

COVID-19 symptoms	n	%
No	86	66.7
Yes	39	30.2
Unknown	4	3.1
Increased length of stay	**n**	**%**
No	109	84.5
Yes	15	11.6
Unknown	2	1.6
Increased O2	**n**	**%**
No	118	91.5
Yes	11	8.5
HDU/ICU admission	**n**	**%**
No	127	98.4
Yes	2	1.6

Outcome	n	%
Died by day 28 (COVID-19 not on death certificate)	13	10.1
Died by day 28 (COVID-19 on part 2 death of death certificate)	4	3.1
Died by day 28 (COVID-19 on part 1 death of death certificate)	3	2.3
Discharged or remained an inpatient at day 28	108	83.7
Unknown	1	0.8

129 patients were included in the review (Table 1). 55 (42.6%) of patients were considered fully vaccinated (three doses), and 18 (14%) unvaccinated. 43 (33.3%) were considered vulnerable. 86 (66.7%) of patients did not develop symptoms of COVID-19. 15 (11.6%) patients had an increased length of stay, 11 (8.5%) had an increased oxygen requirement, and 2 (1.6%) required ICU or HDU attributed to COVID-19. Three (2.3%) patients had COVID-19 recorded as a direct cause of death (Part 1 of the death certificate), and four (3.1%) had COVID-19 recorded as a condition contributing to death (Part 2). A further 13 patients died but COVID-19 was not recorded on their death certificates. We did not identify any significant difference in age, vaccination status, or clinically vulnerable

Table 2
Evaluation of associations with harm in patients with COVID-19.

	Harm (n=21)		No harm (n=108)		p value
	n	%	N	%	
Age (median, range)	75 (55–91)	–	74 (11–96)	–	0.216
Vaccination status					
1st dose	1	4.8	3	2.8	0.698
2nd dose	8	38.1	35	32.4	0.858
3rd dose (or more)	7	33.3	48	44.4	0.674
Unknown	2	9.5	7	6.5	0.730
Unvaccinated	3	14.3	15	13.9	Ref
Clinically vulnerable					
Yes	5	23.8	38	35.2	0.316

status for the 21 patients for whom we recorded harm compared with 108 patients for whom we did not record harm, (Table 2).

Our findings suggest a step-change reduction in harms associated with HOCI caused by Omicron, which is consistent with the reduced harms attributed to Omicron elsewhere.[1,4] Despite one-third of patients being considered vulnerable to a poor outcome from COVID-19, only a small proportion of patients required escalation of care to ICU or HDU for COVID-19 (2%), or died from COVID-19 (2%), and the majority of patients were asymptomatic (67%). This contrasts previous waves, where outcomes for patients in hospital with COVID-19 were poor.[6, 10] Indeed, in one of our centres mortality from HOCI was around 30% during the first wave.[5] Also, a retrospective observational analysis including 374, 244 adult patients in England with COVID-19 in hospitals found that adjusted mortality rates fell from 40-50% in March 2020 to 11% in August 2020.[6] A review and meta-analysis found that mortality associated with nosocomial COVID-19 between January 2020 and February 2021 was significantly higher than for community infection.[7] A large study of around 1.5m patient in England found that Omicron COVID-19 was associated with a significantly lower risk of hospital attendance, hospital admission, and death, with the risk for all three measures approximately halved or more than halved.[4]

We did not identify associations between age, vaccination status, or clinical vulnerability status and clinical harm attributed to COVID-19. This is surprising because older age, incomplete vaccination, and underlying clinical vulnerability have been associated with clinical harm from COVID-19 with each previous wave.[4, 6, 7, 10] Whilst our dataset is small, our findings may be early evidence that these variables are less important in predicting harm associated with Omicron COVID-19 in hospitalised patients than for earlier variants.

Our methods did not allow for direct comparisons of harms with previous COVID-19 variants. We also acknowledge some subjectivity in the attribution of harm, especially in deciding whether increased length of stay was due to medical care arising from COVID-19. We also only measured short-term harm associated with COVID-19, and didn't monitor long term clinical outcomes.

Our findings, from multiple hospital sites in London, suggest that when evaluating the utility of control measures for HOCI, it becomes more important to consider the indirect impacts of detecting and managing HOCI cases as the direct harms from HOCI fall. These indirect impacts include the burden of asymptomatic testing, subsequent impacts on individual patient management and discharge, and interruption to the flow of other patients due to contact isolation and bed closures.

Conflicts of interest

None.

Funding sources

None.

References

1. Rafferty H, Cann A, Daunt A, Cooke GS.. Changing patterns of clinical presentation of COVID-19 in hospital admissions: a single centre prospective cohort study. *J Infect* 2022 Online ahead of print.
2. Sommer A, Rehbock C, Vos C, Borgs C, Chevalier S, Doreleijers S, et al. Impacts and lessons learned of the first three COVID-19 waves on cross-border collaboration in the field of emergency medical services and interhospital transports in the Euregio-Meuse-Rhine: a qualitative review of expert opinions. *Front Pub Health* 2022;**10**:841013.
3. Price JR, Mookerjee S, Dyakova E, Myall A, Leung W, Weiße AY, et al. Development and delivery of a real-time hospital-onset COVID-19 surveillance system using network analysis. *Clin Infect Dis* 2021;**72**:82–9.
4. Nyberg T, Ferguson NM, Nash SG, Webster HH, Flaxman S, Andrews N, et al. Comparative analysis of the risks of hospitalisation and death associated with SARS-CoV-2 omicron (B.1.1.529) and delta (B.1.617.2) variants in England: a cohort study. *Lancet* 2022;**399**:1303–12.
5. Snell LB, Fisher CL, Taj U, Stirrup O, Merrick B, Alcolea-Medina A, et al. Combined epidemiological and genomic analysis of nosocomial SARS-CoV-2 infection early in the pandemic and the role of unidentified cases in transmission. *Clin Microbiol Infect* 2022;**28**:93–100.
6. Gray WK, Navaratnam AV, Day J, Wendon J, Briggs TWR.. COVID-19 hospital activity and in-hospital mortality during the first and second waves of the pandemic in England: an observational study. *Thorax* 2022;**77**:1113–20.
7. Ponsford MJ, Ward TJC, Stoneham SM, Dallimore CM, Sham D, Osman K, et al. A systematic review and meta-analysis of inpatient mortality associated with nosocomial and community COVID-19 exposes the vulnerability of immunosuppressed adults. *Front Immunol* 2021;**12**:744696.
8. NHS eligibility criteria for COVID-19 treatments. https://www.nhsinform.scot/illnesses-and-conditions/infections-and-poisoning/coronavirus-covid-19/coronavirus-covid-19-treatments (accessed 07/04 2022).
9. NHSEI. *Learning from hospital-onset COVID-19*; 2021.
10. Nguyen NT, Chinn J, Nahmias J, Yuen S, Kirby KA, Hohmann S, et al. Outcomes and mortality among adults hospitalized with COVID-19 at US Medical Centers. *JAMA Netw Open* 2021;**4**:e210417.

Jonathan A. Otter*
Directorate of Infection, Guy's and St. Thomas NHS Foundation Trust, St. Thomas' Hospital, Lambeth Palace Road, London, SE1 7EH, United Kingdom
National Institute for Healthcare Research Health Protection Research Unit (NIHR HPRU) in HCAI and AMR, Imperial College London & Public Health England, Hammersmith Hospital, Du Cane Road, W12 0HS, United Kingdom

William Newsholme, Luke B. Snell, Blair Merrick, Nneoma Okeke
Directorate of Infection, Guy's and St. Thomas NHS Foundation Trust, St. Thomas' Hospital, Lambeth Palace Road, London, SE1 7EH, United Kingdom

Damien J.F. Mack
Department of Microbiology, Royal Free Hospital, Royal Free London NHS Foundation Trust, Pond Street NW3 2QG, United Kingdom

Aodhán S Breathnach
Department of Infection, St George's University Hospitals NHS Foundation Trust, Tooting, London SW17 0QT, United Kingdom

Nicholas M Price
Directorate of Infection, Guy's and St. Thomas NHS Foundation Trust, St. Thomas' Hospital, Lambeth Palace Road, London, SE1 7EH, United Kingdom

*Corresponding author at: Directorate of Infection, St. Thomas' Hospital, Lambeth Palace Road, London, SE1 7EH, United Kingdom.
E-mail address: jon.otter@gstt.nhs.uk (J.A. Otter)

Accepted 21 October 2022
Available online 27 October 2022

https://doi.org/10.1016/j.jinf.2022.10.029

Red herrings in monkeypox

Dear Editor,

Since the eradication of smallpox, monkeypox became the most prominent Orthopoxvirus affecting humans, being endemic in Western and Central Africa. A rapidly emerging outbreak of monkeypox spread in Europe and in the rest of the World from May 2022, with the pathogen belonging to the West African clade, which is usually associated with milder disease compared to the Congo basin one. Most cases of the current outbreak have been diagnosed in men who have sex with men (MSM), therefore intimate contacts seem to be the prevalent route of transmission. Historically, signs and symptoms of monkeypox included a rash with several simultaneous lesions affecting multiple regions of the body, including face, arms, legs and less commonly palms, soles and genitalia. The cutaneous involvement was usually preceded by prodromal findings as fever, lymphadenopathy and flu-like symptoms.[1] Evidence from the current outbreak suggests possible atypical presentation, with rash usually involving perianal and genital areas and with only mild prodromal symptoms.[2,3] In particular, a recent paper published in your Journal by Marchese et al.[4] assessed that most of subjects attending a sexual health clinic had rash as first symptom of presentation, associated with other satellite symptoms as fever, lymphadenopathies and malaise. In these individuals, genital involvement was always associated with other systemic symptoms or usually involved also perianal region, face or oral cavity. The presentation of monkeypox as a solitary penis ulcer is therefore unusual and has never been described before.

A 29-years-old homosexual man, without anamnestic comorbidities, was admitted to our Infectious Diseases outpatient clinic for the appearance of a single, painless ulcer, with indurated borders at the level of the penis (Fig. 1A), associated with left inguinal painless lymphadenopathies. The ulcer appeared as a vesicle one week before and became gradually ulcerated. The patient denied any other symptoms or signs such as fever, headache, urethral burning, or discharge, and no other lesions or enlarged lymph nodes were found in other body regions, including oral cavity and anus. He travelled to Mykonos (Greece) one week before the appearance of the ulcer, where he had numerous unprotected sexual intercourses. The patient was tested for sexually transmitted diseases, including syphilis, HIV, Herpes Simplex 1 and 2, *Neisseria gonorrhoeae, Chlamydia trachomatis, Ureaplasma urealyticum* and *Mycoplasma genitalium*. In addition, despite of the unusual clinical picture, he was also tested for monkeypox by real-time polymerase chain reaction (RT-PCR) on a swab taken from the penis ulcer. Microbiological tests were all negative, except for Monkeypox RT-PCR. In the following days, the patient was followed-up by daily video-calls and no treatment was prescribed. No other skin or mucosal lesions occurred during follow-up; the penis ulcer gradually healed, with complete *restitutio ad integrum* in about 2 weeks (Fig. 1B).

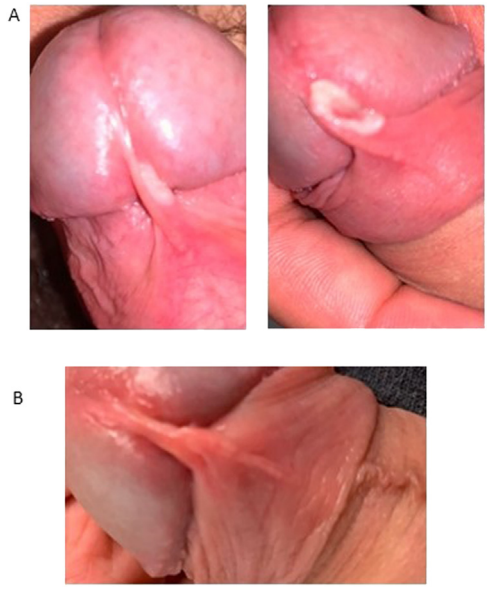

Fig. 1. Solitary ulcer of the penis due to monkeypox (Fig 1A) and its complete resolution after 2 weeks (Fig 1B).

From January to September, 22th 2022, 64,561 cases of monkeypox have been reported globally, of which 63,973 outside the African endemic regions.[4] Human-to-human transmission through intimate contacts have been identified as the most important route of transmission of this outbreak and MSM seem to be at greater risk of acquiring the infection.[2] We describe here an atypical presentation of monkeypox, presenting with an isolated, painless ulcer on the penis associated only with inguinal lymphadenopathies. There were not prodromal symptoms or other muco-cutaneous lesions at the time of presentation and during subsequent follow-up. The presence of a single, indolent ulcer of the penis usually suggests the presence of other sexually transmitted diseases, such as syphilis, venereal lymphogranuloma due to *Chlamydia trachomatis*, or chancroyd due to Haemophilus ducreyi. Consequently, the possibility of atypical presentations of monkeypox suggests that persons presenting with isolated genital ulcer, especially when referring intimate contacts, should be also tested for monkeypox, even in absence of other typical symptoms.

In conclusion, this case report underlines the importance of testing for monkeypox individuals with intimate contact with several partners in the previous 21 days and presenting with genital lesions, even in absence of other signs and symptoms.

References

1. McCollum A.M., Damon I.K.. Human monkeypox. *Clin Infect Dis* 2014;**58**(2):260–7 Epub 2013 Oct 24. Erratum in: *Clin Infect Dis*. 2014;58(12): 1792. doi:10.1093/cid/cit703.
2. Thornhill J.P., Barkati S., Walmsley S., Rockstroh J., Antinori A., Harrison L.B., et al. Monkeypox Virus Infection in Humans across 16 Countries - April-June 2022. *N Engl J Med* 2022;**387**(8):679–91.
3. Orviz E., Negredo A., Ayerdi O., Vazquez A., Munoz-Gomez A., Monzon S., et al. Monkeypox outbreak in Madrid (Spain): clinical and virological aspects. *J Infect* 2022;**S0163-4453**(22):415–17.
4. Marchese D., Pozza G., Giacomelli A., Mileto D., Cossu M.V., Beltrami M., et al. Natural history of human monkeypox in individuals attending a sexual health clinic in Milan, Italy. *J Infect* 2022. doi:10.1016/j.jinf.2022.08.019.

Marco Bongiovanni[#], Daniele Piccinini
Division of Infectious Diseases, Department of Medicine, Ente Ospedaliero Cantonale, Lugano, Switzerland

Fabian Joel Aschwanden
Emergency Department, Ente Ospedaliero Cantonale, Lugano, Switzerland

Enos Bernasconi
Division of Infectious Diseases, Department of Medicine, Ente Ospedaliero Cantonale, Lugano, Switzerland

[*]**Corresponding author:** Marco Bongiovanni, MD PhD, Division of Infectious Diseases, Ente Ospedaliero Cantonale, Lugano, Switzerland.
E-mail address: Bongiovanni@eoc.ch (M. Bongiovanni)

Accepted 16 October 2022
Available online 20 October 2022

https://doi.org/10.1016/j.jinf.2022.10.024

A complicated case of monkeypox and viral shedding characteristics

Dear Editor,

The report by Orviz et al. highlighted the relatively optimistic prognosis of monkeypox (MPX) with no serious complications in their case series from Madrid, Spain.[1] However, in another confirmed case series of 197 MPX patients, five (2.5%) had proctitis with one having a perforated rectum with HIV infection and one perianal abscess.[2] The current MPX outbreak differs from its historical antecedents and has novel features, such as sexual transmission route and genital bacterial complications. Here we report a non-HIV case of MPX with proctitis and severe refractory anal abscess who had to be relieved by colostomy. We also examined his viral shedding characteristics including the patient room and the operating room (OR) air.

A 31-year-old Canadian man visited Istanbul in July 2022. After 5 days of condomless receptive anal sexual practice with a male partner, he started to have anal pain and vesicular skin lesions. In an outpatient clinic, botulinum toxin was injected with a diagnosis of perianal fissure. With a stabbing pain, and difficulty of passing stool, a pelvic magnetic resonance imaging (MRI) was taken, which revealed proctitis and perianal abscess. He was hospitalized on August 02, 2022, in our clinic. He had history of bipolar type 2 disease and mini gastric bypass surgery. He used methamphetamine but had been clear for the last 5 months. The real-time PCR for MPX was positive from the skin and nasopharyngeal materials. He showed a lymphocytosis (max 8000 /uL) for the first 4 days, which then disappeared. An abscess drainage was applied. He was given intravenous (iv) piperacillin-tazobactam (TZP). The anal pain progressed, and an abdominopelvic computerized tomography (CT) scan revealed a deep abscess, and ESBL positive *E.coli* and *C. glabrata* were isolated. We added micafungin 1 × 100 mg iv and switched TZP to meropenem 3 × 1 gr iv. We couldn't access to the tecovirimat. He then had severe rectal bleeding with abdominal pain and high fever. In rectosigmoidocopy, rectal ulcers were observed. A new CT scan showed no perforation, but a pelvic abscess with inflammation of rectum and adjacent tissue. General surgery department applied a transverse end-loop colostomy to by-pass stool from rectum. At the last abscess drainage MPX PCR positivity with a cycle of threshold (Ct) value of 26 was detected. We accounted this low Ct value to start cidofovir iv in combination with probenecid that could be supplied 18 days after the onset of lesions. No adverse effect was observed. Psychiatric support was provided because of his mood fluctuations. His follow up continues in Montreal, Canada.

Our patient had an unfortunate course complicated by colostomy. In a case series of 181 patients, two (1%) had reported having anal abscess, who were treated conservatively,[3] and another one treated by incision and drainage.[4] In our case, both tranverse end-loop colostomy and iv cidofovir were applied in the same time. So, we could not estimate properly the true effect of each on the recovery of the abscess. He had also lymphocytosis. Atypical lymphocytes associated with MPX infection is reported in a small case series (6 out of 14 patients).[5]

A nurse was exposed to the urine of the patient while handling urinary bag (spilled over her clothes) on day 3 of admission. The nurse had no history of smallpox vaccine, and no vaccine for post-exposure was available in Turkey. She did not show any symptoms for the next 21 days.

The samples from skin lesions, anal, nasopharynx swabs, anal abscess, serum, urine, tear, and air were consecutively collected (Fig. 1). Air samples from the patient room and OR were collected by Coriolis Micro® portable biological air sampler. All samples were examined by RT-PCR for MPXV DNA and PCR positive samples were cultured on Vero-E6 cells (Fig. 1). We defined a threshold (Ct≤38; viral load, PFU/ml $\geq 10^3$) for the PCR positivity. This value can vary, ie. Paran et al. defined a threshold (Cq≥35; viral DNA≤4,300copies/mL) that predicts poorly- or non-infectious specimens.[6] In the RT-PCR, the viral load in skin lesions (the lowest Ct value: 14; 10^9 PFU/ml) was the highest, and followed by rectal smear (the lowest Ct value: 17; 10^8 PFU/ml), and nasopharyngeal swabs (the lowest Ct value: 27; 10^5 PFU/ml). No viable virus was isolated from any of the air samples. Viral culture was positive in nasopharygeal, vesiculopustular, rectal smear and rectal ulcer, and tear samples. Viral particles were visualised in rectal ulcer biopsy sample stained with anti-vaccina antibody (Fig. 2). He had also a prolonged viable virus positivity in nasopharynx until 20th day of skin rash. The latest time point at which a lesion remained positive was reported as 21 days after onset of symptom.[3, 7] In our case, we detected prolonged rectal PCR positivity until day 30. We also detected viral DNA in pelvic abscess until the day 20 with no viral growth.

We found no viable MPX virus in the room air, but detected viral DNA by PCR. Marimuthu et al. found no viable virus from the air, but yet viable MPX virus from surfaces and dust samples.[8] Gould et al. identified a replication-competent virus in air samples collected during the bed linen change.[9] We think that more studies are needed to confirm that N95 instead of surgical mask is really necessary during daily routine care of the patient. Such an information is critical because of the cost and availability of the N95 respirators.

In conclusion, anal abscess as a less, but proctitis as a more frequent manifestation in the current outbreak of MPX among men practicing anal-receptive sex should be kept in mind by the clinician. MPX could be disturbingly morbid because of its complications. MPX virus shedding dynamics with viral culture studies should be investigated much more detailed in future studies. By this case, we highlight the importance of multidisciplinary management of MPX and its expanding clinical variety.

Funding information

None declared.

Ethical approval

Koç University Institutional Review Board approved the study. The patient consented the publication.

Declaration of Competing Interest

The authors declare that they have no competing interest.

Acknowledgements

We thank our patient who had consented for clinical information to be shared in this manuscript. We also thank our great administrator Erdal Aksoy MD and his team for their unique support, and medical and nursing staff at Koc University Hospital. We are grateful to Vugar Samadlı MD from Interventional Radiology Dept. of Koç University School of Medicine (KUSOM), İrem Özdemir MD and Akın Akbulut MD from Anesthesiology Dept. of KUSOM, Aslı Ercan Doğan MD from Psychiatry Dept. of KUSOM, Pelin İrkören MD, Yağmur Nur Abik MD, Lal Sude Gucer MD, İbrahim Beyhan MD from Infectious Diseases and Clinical Microbiology Dept. of KUSOM, Sevket Ruacan, MD, Prof, and Orhun Çığ Taşkın, MD from Pathology Dept. of KUSOM for their assistance in the patient's clinical follow-up. Also thankful to Mr. Ali Pekşen

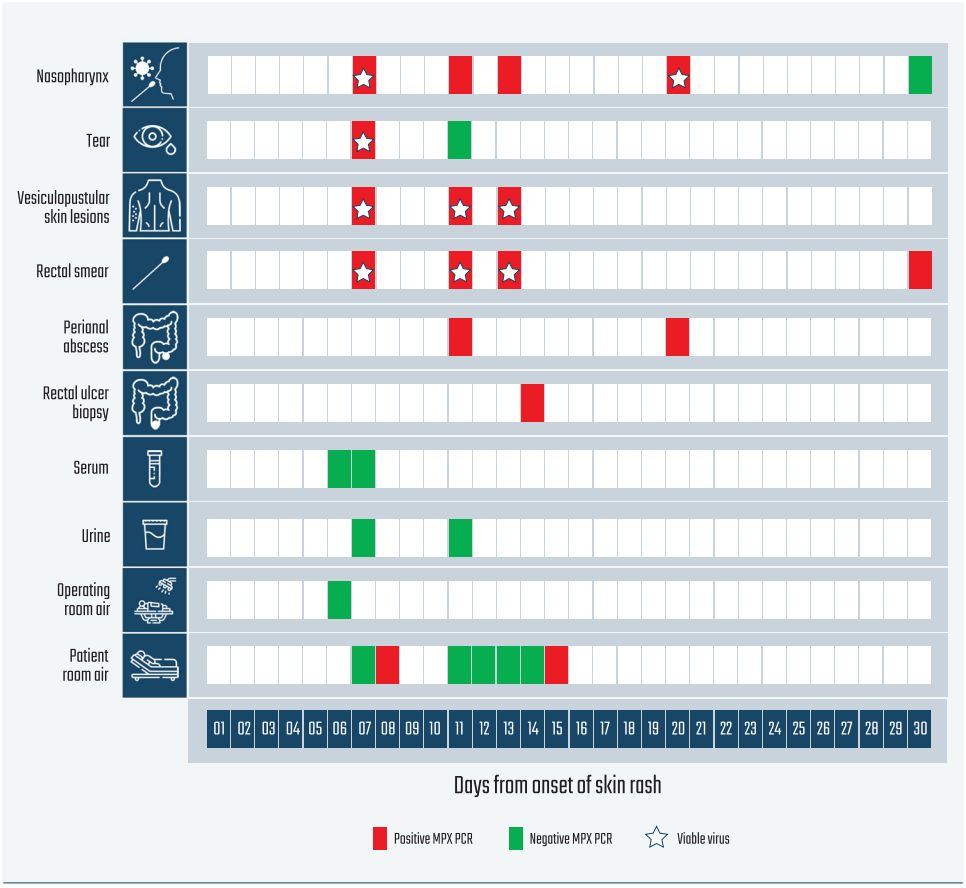

Fig. 1. Viable monkeypox (MPX) virus and viral DNA shedding in 30 days after onset of skin rash. *Green box*: Nor MPX DNA neither viable virus detected. *Red box*: MPX viral DNA detected. *Star within red box*: Viable MPX was isolated.

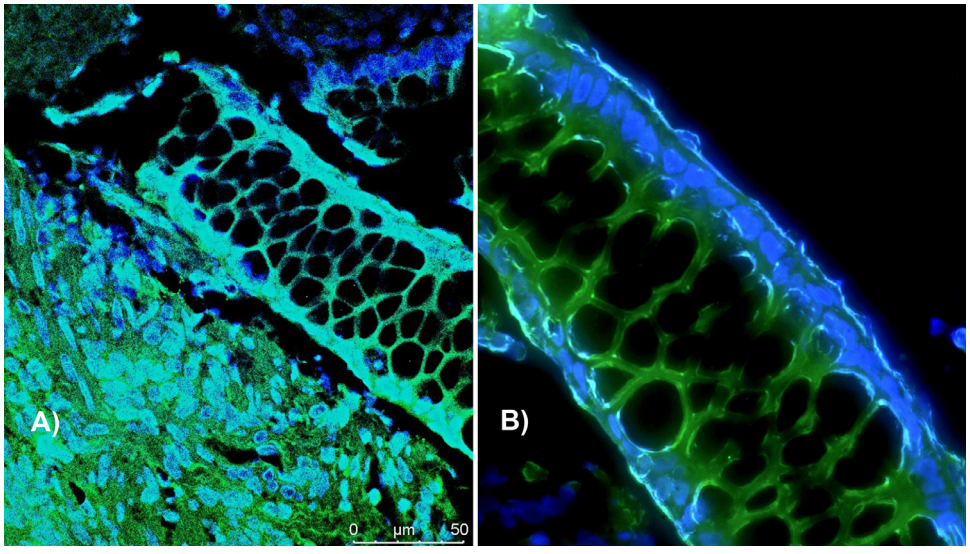

Fig. 2. Rectum epithelium in crypt infected with monkeypox (MPX) virus by using immunofluorescent staining for anti-vaccina (FITC, DAPI counterstaining). Nuclei was stained with DAPI in blue, MPX virus in green. A. 40x magnification. B. 63x magnification.

from www.dotdoc.com.tr for his unique contribution to brilliant figure designs of this study.

References

1. Orviz E., Negredo A., Ayerdi O., Vázquez A., Muñoz-Gomez A., Monzón S., Clavo P., Zaballos A., Vera M., Sánchez P., Cabello N., Jiménez P., Pérez-García J.A., Varona S., Del Romero J., Cuesta I., Delgado-Iribarren A., Torres M., Sagastagoitia I., Palacios G., Estrada V., Sánchez-Seco M.P.. Grupo Viruela del Simio Madrid CNM/ISCIII/HCSC/Sandoval. Monkeypox outbreak in Madrid (Spain): clinical and virological aspects. *J Infect.* Oct 2022;**85**(4):412–17 Epub 2022 Jul 10. PMID: 35830908; PMCID: PMC9534097. doi:10.1016/j.jinf.2022.07.005.
2. Patel A., Bilinska J., Tam J.C.H., Da Silva Fontoura D., Mason C.Y., Daunt A., Snell L.B., Murphy J., Potter J., Tuudah C., Sundramoorthi R., Abeywickrema M., Pley C., Naidu V., Nebbia G., Aarons E., Botgros A., Douthwaite S.T., van Nis-

pen Tot Pannerden C., Winslow H., Brown A., Chilton D., Nori A. Clinical features and novel presentations of human MPX in a central London centre during the 2022 outbreak: descriptive case series. *BMJ* 2022 Jul 28;**378**:e072410 PMID: 35902115; PMCID: PMC9331915. doi:10.1136/bmj-2022-072410.
3. Tarín-Vicente E.J., Alemany A., Agud-Dios M., Ubals M., Suñer C., Antón A., Arando M., Arroyo-Andrés J., Calderón-Lozano L., Casañ C., Cabrera J.M., Coll P., Descalzo V., Folgueira M.D., García-Pérez J.N., Gil-Cruz E., González-Rodríguez B., Gutiérrez-Collar C., Hernández-Rodríguez Á., López-Roa P., de Los Ángeles Meléndez M., Montero-Menárguez J., Muñoz-Gallego I., Palencia-Pérez S.I., Paredes R., Pérez-Rivilla A., Piñana M., Prat N., Ramirez A., Rivero Á., Rubio-Muñiz C.A., Vall M., Acosta-Velásquez K.S., Wang A., Galván-Casas C., Marks M., Ortiz-Romero P.L., Mitjà O.. Clinical presentation and virological assessment of confirmed human MPX virus cases in Spain: a prospective observational cohort study. *Lancet* 2022 Aug 27;**400**(10353):661–9 Epub 2022 Aug 8. PMID: 35952705. doi:10.1016/S0140-6736(22)01436-2.
4. Pfafflin F., Wendisch D., Scherer R., Jürgens L., Godzick-Njomgang G., Tranter E., Tober-Lau P., Stegemann M.S., Corman V.M., Kurth F., Schürmann D.. MPX inpatients with severe anal pain. *Infection* 2022 Aug 12 Epub ahead of print. PMID: 35960457. doi:10.1007/s15010-022-01896-7.
5. Debuysschere C., Beukinga I., Hernando C., Blairon L., Tré-Hardy M., Cupaiolo R.. Atypical lymphocytes associated with monkeypox virus infection. *Br J Haematol* 2022 Sep 21 Epub ahead of printPMID: 36128942. doi:10.1111/bjh.18480.
6. Paran N., Yahalom-Ronen Y., Shifman O., Lazar S., Ben-Ami R., Yakubovsky M., Levy I., Wieder-Feinsod A., Amit S., Katzir M., Carmi-Oren N., Levcovich A., Hershman-Sarafov M., Paz A., Thomas R., Tamir H., Cherry-Mimran L., Erez N., Melamed S., Barlev-Gross M., Karmi S., Politi B., Achdout H., Weiss S., Levy H., Schuster O.. Beth-Din A, Israely T. Monkeypox DNA levels correlate with virus infectivity in clinical samples, Israel, 2022. *Euro Surveill* Sep 2022;**27**(35):2200636 PMID: 36052723; PMCID: PMC9438394. doi:10.2807/1560-7917.ES.2022.27.35.2200636.
7. Veintimilla C., Catalán P., Alonso R., de Viedma D.G., Pérez-Lago L., Palomo M., Cobos A., Aldamiz-Echevarria T., Muñoz P.. The relevance of multiple clinical specimens in the diagnosis of MPX virus, Spain, June 2022. *Euro Surveill* Aug 2022;**27**(33) PMID: 35983771. doi:10.2807/1560-7917.ES.2022.27.33.2200598.
8. Kalisvar Marimuthu, Judith Chui Ching Wong, Poh Lian Lim, Sophie Octavia, Xiaowei Huan, Yi Kai Ng, Jun Jing Yang, Stephanie Sutjipto, Kyaw Zaw Linn, Yin Xiang Setoh, Chong Hui Clara Ong, Jane Griffiths, Sharifah Farhanah, Thai Shawn Cheok, Nur Ashikin Binti Sulaiman, Sipaco Barbara Congcong, Erica Sena Neves, Liang Hui Loo, Luqman Hakim, Shuzhen Sim, Merrill Lim, Mohammad Nazeem, Shawn Vasoo, Kwok Wai Tham, Oon Tek Ng, Lee Ching Ng Viable Monkeypox virus in the environment of a patient room medRxiv 2022.09.15.22280012; doi:10.1101/2022.09.15.22280012.
9. Susan Gould, Barry Atkinson, Okechukwu Onianwa, Antony Spencer, Jenna Furneaux, James Grieves, Caroline Taylor, Iain Milligan, Allan Bennett, Tom Fletcher, Jake Dunning, N.H.S. England Airborne HCID Network. Air and surface sampling for monkeypox virus in UK hospitals. medRxiv 2022.07.21.22277864; doi:10.1101/2022.07.21.22277864.

Mahir Kapmaz
Koç University School of Medicine, Department of Infectious Diseases and Clinical Microbiology, Istanbul, Turkey
Koç University İşbank Center for Infectious Diseases (KUISCID), Istanbul, Turkey

Derya Salim Uymaz
Koç University School of Medicine, Department of General Surgery, Istanbul, Turkey

Gulin Ozcan
Koç University İşbank Center for Infectious Diseases (KUISCID), Istanbul, Turkey
Koç University, Graduate School of Health Sciences (GSHS), Istanbul, Turkey

Tayfun Barlas, Gulen Guney-Esken
Koç University İşbank Center for Infectious Diseases (KUISCID), Istanbul, Turkey

Mete Manici
Koç University School of Medicine, Department of Anesthesiology and Reanimation, Istanbul, Turkey

Şiran Keske
Koç University School of Medicine, Department of Infectious Diseases and Clinical Microbiology, Istanbul, Turkey
Koç University İşbank Center for Infectious Diseases (KUISCID), Istanbul, Turkey

Mert Kuşkucu
Koç University İşbank Center for Infectious Diseases (KUISCID), Istanbul, Turkey

Füsun Can
Koç University İşbank Center for Infectious Diseases (KUISCID), Istanbul, Turkey
Koç University School of Medicine, Department of Medical Microbiology, Istanbul, Turkey

Önder Ergönül*
Koç University School of Medicine, Department of Infectious Diseases and Clinical Microbiology, Istanbul, Turkey
Koç University İşbank Center for Infectious Diseases (KUISCID), Istanbul, Turkey

*Corresponding author: Onder Ergonul, MD, MPH, Koç University İşbank Center for Infectious Diseases (KUISCID).
E-mail addresses: mkapmaz@kuh.ku.edu.tr (M. Kapmaz), gozcan19@ku.edu.tr (G. Ozcan), oergonul@ku.edu.tr (Ö. Ergönül)

Accepted 16 October 2022
Available online 21 October 2022

https://doi.org/10.1016/j.jinf.2022.10.020

Changes of *Haemophilus influenzae* infection in children before and after the COVID-19 pandemic, Henan, China

Dear Editor,

In this journal, Yuan et al. demonstrated *Streptococcus pneumoniae* infections among children are on a decreasing trend during the COVID-19 pandemic in Zhengzhou, China,[1] as well as carbapenemase-producing *Enterobacteriaceae* and extended-spectrum beta-lactamase *E. coli* in France.[2,3] However, no data is available regarding *Haemophilus influenzae* (*H.influenzae*) infection.

H. influenzae is a gram-negative, nonmotile, facultatively coccobacillus pathogen for human, and transmitted through respiratory secretion droplets and direct close contact.[4] *H. influenzae* mainly causes respiratory disease, bacteremia and central nervous system diseases.[5] In particular for children, it is a leading cause of children meningitis in worldwide,[6] and has been listed as one of priority pathogens by WHO. Vaccination against *H. influenzae* serotypes b (Hib) prevented the onward communication transmission of Hib, and consequently incidence of Hib infections drops considerably in many countries including China. However, archived studies showed increasing incidences of *H. influenzae* serotypes a (Hia) and non-typeable *H. influenzae* (NTHi) annually by 13% and 3%, respectively.[7] With the changing epidemiology of *H. influenza* infection, it is important to monitor the dynamic of *H. influenzae* among children during the COVID-19 pandemic. Here we evaluated the change of *H. influenzae* infection and clinical characteristics in children before and after the COVID-19 pandemic, which may help to inform the implementation of prevention strategies in clinic.

Laboratory-based surveillance of *H. influenzae* was conducted from January 1, 2018, to December 31, 2021, at Henan Children's Hospital, an affiliated hospital of Zhengzhou University with 95,000 inpatients per year, 2,200 beds in total, and located in

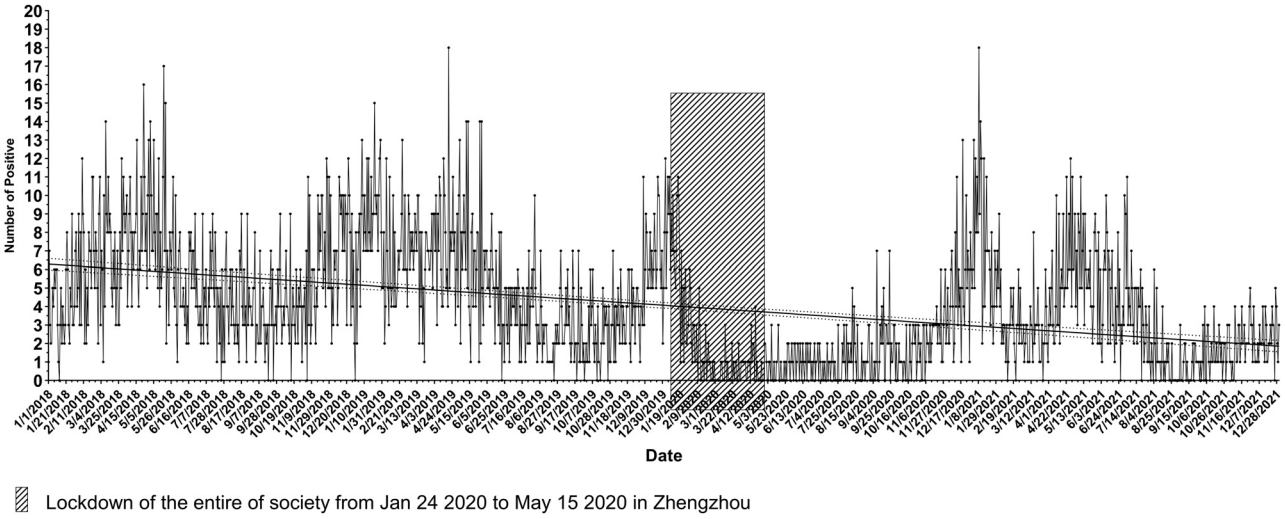

Fig. 1. The number of*H. influenzae* among Children and young people aged 0–18 years by day during2018 to 2021.

Zhengzhou, capital of Henan province, China. We present the number positive of *H. influenzae* infection among Children and young people aged 0–18 years, as well as comparisons of different age groups (0–28d, 29d-1y, 1–3y, and 3–18y).The groups are based on the traditional living habits of Chinese children and young people aged 0–18 years. Group 1 (0–28d), the baby and mom are supposed to stay at home,and avoid contact with other people except families during the first month after delivery. Group 2 (29d-1y), preschool age group at home. Group 3 (1–3y), preschool age group at home or within private nursery affiliations. Group 4 (3–18y), children and young people in kindergarten or school.

We observed that the number of positive *H. influenzae* infection in children were declined over the past four years (Fig. 1). Most likely because the government carried out a home quarantine through lockdown of the entire society from Jan 24 2020 to May 15 2020, in Zhengzhou. In particular, the decrease of *H. influenzae* infection has been sustained for five months after a lockdown strategy in Zhengzhou, which ended on May 15, 2020. Moreover, although the number positive and positive rate of *H. influenzae* infection in children began to increase since November 2020, it is still lower than that in the same period in 2018 and 2019. The positive rate of *H. influenzae* among children with respiratory disease in 2020 (6.21%) was lower than that in 2018 (11.28%) and 2019 (10.16%) ($p<0.05$), raised again in 2021 (7.37%) ($p<0.05$) and still lower than that in 2018 and 2019 ($p<0.05$). No change was observed in children with bacteremia and central nervous system diseases. Therefore the lockdown may have affected *H. influenzae* infection with respiratory disease, but not other diseases caused by *H. influenzae*. We also found that the positive rate of *H. influenzae* decreased in group 2-4 (Fig. 2), which indicated the lockdown may only contained the community based transmission of *H. influenzae*. The proportion of *H. influenzae* infection was more than 45% in group 1–2, while reach to 70% in group 1–3. It indicated that the population of *H. influenzae* infection was mainly under 3 years old (children at home), especially for those under 1 year.

In addtition, the age composition of the children with *H. influenzae* infection under 3 years old changed during the COVID-19 pandemic. The median age of children under 3 years old with *H. influenzae* infection in 2020 (8.2 months, IR 4.27–15) was older than that in 2018 (7.5 months, IR 3.8–14) and 2019 (7.5 months, IR 3.77–14) ($p<0.05$). However the median age of the hospitalized children under 3 years old in 2020 (6.1 months, IR1.77–15) was younger than that in 2018 (6.8 months, IR1.87–15) and 2019 (6.17 months, IR 1.93–15). These results way be correlated with the delay of Hib vaccinations in these years. In China, Hib vaccine should be administered starting at 2 months and completed within 1.5 years old, completed the whole inoculation in 3 doses. However, vaccinations for many children were delayed because of the 113-day lockdown during Jan 2020 to May 2020 in Henan, including Hib vaccine.

Finally, this study showed that the COVID-19 pandemic changed the epidemiological trend of *H. influenzae* infection in children in Henan, China. Several factors may have contributed to the change: the lessening of children-to-children contact during the COVID-19 pandemic (closed schools and kindergartens), hand hygiene, masks, and the limitation of travel in children. What's more, the *H. influenzae* vaccination was also delayed, which may be related to the older median age of children with *H. influenzae* infection.

In conclusion, we found a decreased tendency of *H. influenzae* infection among children during the COVID-19 pandemic. Keeping effective and continuous surveillance is of great significance to prevent endemic of *H. influenzae* infection among children under 3 years old.

Declaration of competing interest

None.

Acknowledgments

This work was funded by grants from the Key Research, Development, and Promotion Projects of Henan Province (212102310730).

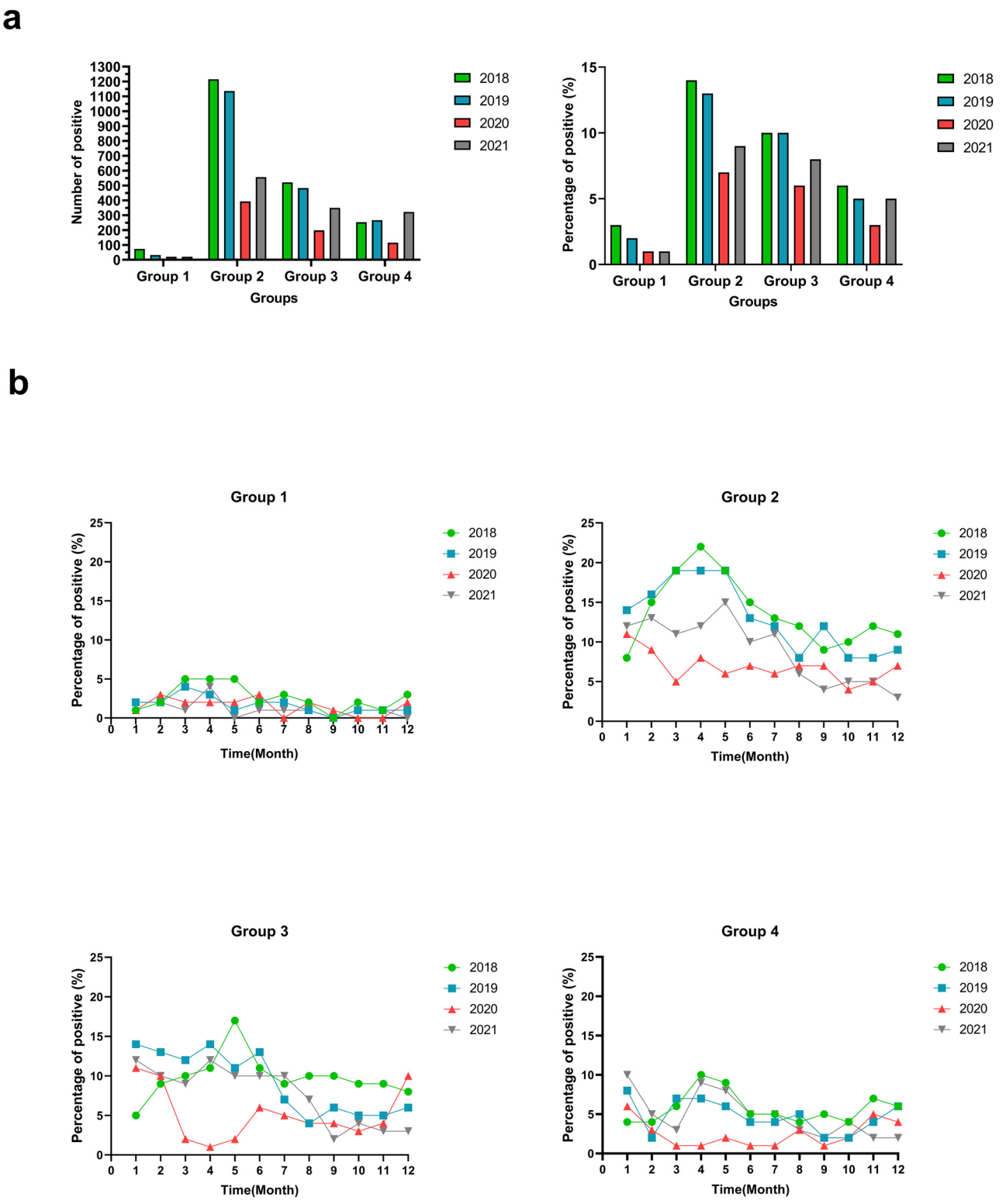

Fig. 2. a The number of positive and positive rates of *H.influenzae* infection in children by age group during 2018 to 2021. **b** The positive rate of *H.influenzae* detected in specimens by month in each age group during 2018 to 2021.

References

1. Li Y., Guo Y., Duan Y.. Changes in *Streptococcus pneumoniae* infection in children before and after the COVID-19 pandemic in Zhengzhou, China. *J Infect* 2022;**85**(3):e80–1.
2. Lemenand O., Coeffic T., Thibaut S., Colomb Cotinat M., Caillon J., Birgand G.. Clinical Laboratories of PRIMO Network. Nantes, France. Decreasing proportion of extended-spectrum beta-lactamase among *E. coli* infections during the COVID-19 pandemic in France. *J Infect* 2021;**83**(6):664–70.
3. Duverger C., Monteil C., Souyri V., Fournier S.. AP-HP Infection prevention and control teams. Decrease of carbapenemase-producing *Enterobacteriaceae* incidence during the first year of the COVID-19 pandemic. *J Infect* 2022;**85**(1):90–122.
4. McTaggart L.R., Cronin K., Seo C.Y., Wilson S., Patel S.N., Kus J.V.. Increased Incidence of Invasive *Haemophilus influenzae* Disease Driven by Non-Type B Isolates in Ontario, Canada, 2014 to 2018. *Microbiol Spectr* 2021;**9**(2):e0080321 31.
5. Brown N.E., Blain A.E., Burzlaff K., Harrison L.H., Petit S., Schaffner W., et al. Racial Disparities in Invasive *Haemophilus influenzae* Disease-United States, 2008-2017. *Clin Infect Dis* 2021;**73**(9):1617–24.

6. Bamberger E.E., Ben-Shimol S., Abu Raya B., Katz A., Givon-Lavi N., Dagan R., et al. Pediatric invasive *Haemophilus influenzae* infections in Israel in the era of Haemophilus influenzae type b vaccine: a nationwide prospective study. *Pediatr Infect Dis J* 2014;**33**(5):477–81.
7. Soeters H.M., Blain A., Pondo T., Doman B., Farley M.M., Harrison L.H., et al. Current Epidemiology and Trends in Invasive *Haemophilus influenzae* Disease-United States, 2009-2015. *Clin Infect Dis* 2018;**67**(6):881–9.

Juanjuan Zhou, Peipei Zhao, Manjie Nie, Kaijie Gao, Junmei Yang*
Zhengzhou Key Laboratory of Children's Infection and Immunity, Children's Hospital Affiliated to Zhengzhou University, Henan Children's Hospital, Zhengzhou 450018, P.R. China

Jiufeng Sun**
Guangdong Provincial Center for Disease Control and Prevention, Guangzhou, China

*Corresponding authors: Junmei Yang, Zhengzhou Key Laboratory of Children's Infection and Immunity, Children's Hospital Affiliated to Zhengzhou University, Henan Children's Hospital, Zhengzhou 450018, P.R. China.**Corresponding authors: Jiufeng Sun, Guangdong Provincial Center for Disease Control and Prevention, Guangzhou 510300, P.R.China.
E-mail addresses: yangjunmei7683@163.com (J. Yang), sunjiuf@163.com (J. Sun)

Accepted 2 October 2022
Available online 20 October 2022

https://doi.org/10.1016/j.jinf.2022.10.019

COVID-19 subgroups may slow down biological age acceleration

Dear Editor,

COVID-19 has profound health and socioeconomic impacts globally. Liu et al. suggested that older patients with COVID-19 had a higher mortality rate and were more likely to progress to severe disease.[1] Moreover, evidence indicates that chronological age is a major risk factor for COVID-19.[2–4] Cao et al. suggested that biological aging was associated with the risk of SARS-CoV-2 infection and severe COVID-19 development.[5] However, Franzen et al. reported that epigenetic clocks were not accelerated in COVID-19 patients.[6] A longitudinal study by Pang et al. showed that epigenetic clocks might be slowed down for approximately 2.06 years in young COVID-19 patients (age < 50).[7] The inconsistency of the conclusions of previous studies intrigued us to continue to explore whether there exist potential causal links between epigenetic age acceleration and COVID-19. The causal relationships between epigenetic age acceleration and various COVID-19 subgroups, especially hospitalized COVID-19 and COVID-19 diagnosed with very severe respiratory disease, remain unknown.

To further clarify the relationship between chronological age and COVID-19 subgroups, we conducted two-sample bidirectional Mendelian randomization (MR) analyses using publicly available genome-wide association studies (GWAS). Our MR analyses calculated the summary statistics of four epigenetic age acceleration measures[8] (N = 34,710) (i.e., GrimAge, HannumAge, Intrinsic HorvathAge, and PhenoAge). The four epigenetic clocks are based on DNA methylation levels at different CpG sites that capture distinctive features of biological aging.[9] HannumAge and Intrinsic HorvathAge are 'First-generation' epigenetic clocks.[10] HannumAge was trained on 71 age-related CpGs found in blood, while Intrinsic HorvathAge was based on 353 age-related CpGs found in several human tissues and cell types, and further adjustments were made for blood cell counts. GrimAge and PhenoAge are 'second-generation' epigenetic clocks.[10] The GrimAge measure combined data from 1030 CpGs associated with smoking pack-years and seven plasma proteins, and the PhenoAge measure integrated data from 513 CpGs associated with mortality and nine clinical biomarkers. Though the four epigenetic clocks measure epigenetic age acceleration differently in terms of their CpGs components, they all have been shown to assess epigenetic age accurately.[10] The COVID-19 related datasets analyzed in our study include three subgroups: COVID-19 positive (COVID-19 vs control), hospitalized COVID-19 (hospitalized vs population), and COVID-19 diagnosed with severe respiratory disease (very severe respiratory confirmed vs population) (Table S1). All the datasets were obtained from the COVID-19 Host Genetics Initiative in 2020 and were available in EBI database (https://gwas.mrcieu.ac.uk/datasets/?gwas_id__icontains=ebi-a). The severe respiratory COVID-19 dataset was derived from a comparison between very severe respiratory failure patients secondary to COVID-19 vs control. COVID-19 with signs of severe respiratory distress is defined by WHO as severe COVID-19 (https://app.magicapp.org/#/guideline/j1WBYn). Hospitalized COVID-19 datasets were obtained by comparing laboratory-confirmed SARS-CoV-2 infected patients hospitalized with symptoms of COVID-19 vs control. All participants of GWAS datasets are European ancestry.

Leveraging three stages of MR analysis, we estimated the causal effect of COVID-19 subgroups on epigenetic age accelerations. In Stage 1, we selected independent COVID-19 genetic variants in each dataset with genome-wide significance ($P < 5 \times 10^{-8}$) as instruments to satisfy the assumption that the instruments chosen for MR analysis should be strongly associated with exposure. To test the instrumental variable bias, we calculated F-statistic and R^2 ($F = (R^2 \times (N-2))/(1-R^2)$, $(R^2 = 2\beta^2 \times MAF \times (1-MAF))/2\beta^2 \times MAF \times (1-MAF)) + 2N \times MAF \times (1-MAF) \times SE^2$), MAF = effect allele frequency, β = effect estimate of the SNP in the exposure GWAS, SE = standard error, and N = sample size). All F-statistics of instruments were larger than 10, indicating that the probability of weak instrumental variable bias was minimal. In Stage 2, we extracted selected instrumental variants from four epigenetic age acceleration datasets. LD proxies ($r^2 > 0.8$) were allowed to replace the missing instrumental variants in epigenetic age acceleration datasets. Subsequently, we conducted inverse-variance weighted (IVW) MR and MR-Egger analyses. To satisfy the second and third assumptions of MR analysis, MR-Egger intercept test indicated the presence of potential pleiotropy. In Stage 3, we performed fixed effect meta-analysis to pool results across different COVID-19 subgroups, which has been applied in several studies to improve the precision of MR results. In fixed effect meta-analysis, I^2-statistic and p-value of the heterogeneity test depicted the heterogeneity across studies. The Chi-square test was used to test for subgroup differences. Furthermore, the reverse MR analysis and fixed effect meta-analysis were also performed. All statistical analyses were completed using R software version 4.1.1 with "TwoSampleMR" and "meta" R packages.

Meta-analyzed IVW MR results indicated significant causal effects between hospitalized COVID-19 and GrimAge acceleration (beta = −0.19, 95% CI −0.26 to −0.12, p = 4.68E-07), and PhenoAge acceleration (beta = −0.26, 95% CI −0.34 to −0.17, p = 8.86E-09). Interestingly, we found that COVID-19 diagnosed with very severe respiratory disease had the same casual effects as hospitalized COVID-19 (GrimAge IVW beta = −0.16, 95% CI −0.36 to −0.15, p = 7.59E-08; PhenoAge IVW beta = −0.22, 95% CI −0.30

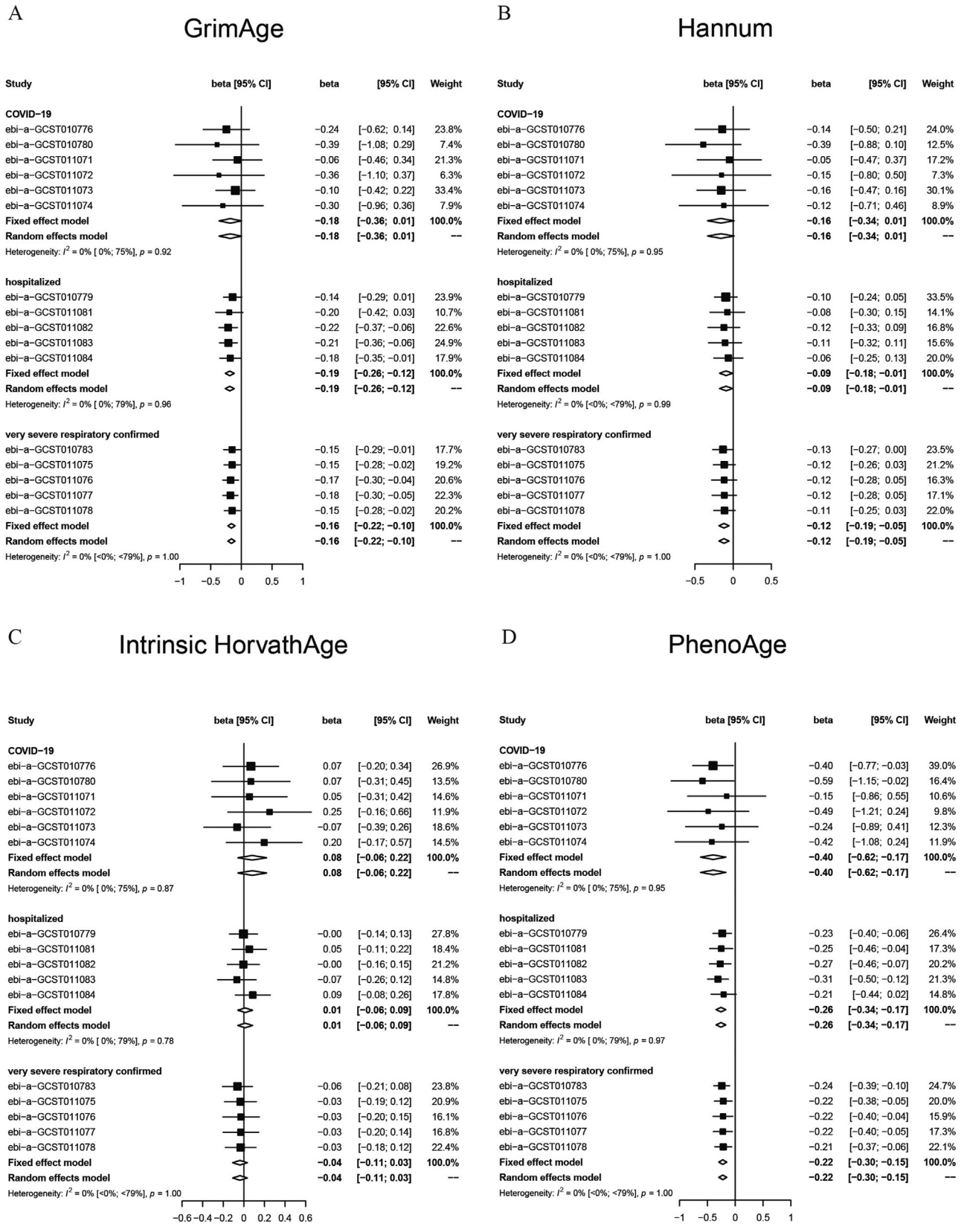

Fig. 1. Fixed effect meta-analysis of inverse-variance weighted Mendelian randomization estimates for genetically predicted effects of COVID-19 subgroups on epigenetic clocks: GrimAge acceleration (A), HannumAge acceleration (B), Intrinsic HorvathAge acceleration (C) and PhenoAge acceleration (D).

Table 1
P-value of fixed effect meta-analysis of the causal effect of COVID-19 subgroups on epigenetic clocks.

COVID-19 subgroups	GrimAge	HannumAge	Intrinsic HorvathAge	PhenoAge
COVID-19	0.057	0.071	0.253	7.06E-04
hospitalized COVID-19	4.68E-07	0.036	0.723	8.86E-09
COVID-19 with very severe respiratory confirmed	7.59E-08	0.042	0.301	1.05E-09

to −0.15, p = 1.05E-09). Besides, COVID-19 only slowed PhenoAge acceleration (beta = −0.40, 95% CI −0.62 to −0.17, p = 7.06E-04) significantly (Fig. 1, Table 1, Table S2-S5, S13). The threshold of statistically significant association between COVID-19 subgroups and epigenetic age accelerations was a Bonferroni correction ($P < 0.05/4 = 1.25E-02$). MR-Egger intercept test indicated no pleiotropy present (Table S11). Additionally, reverse MR analyses and fixed effect meta-analysis illustrated no significant casual effect of epigenetic clocks on three COVID-19 subgroups (Figure S1, Table S6-S10, S14). MR-Egger intercept test indicated no pleiotropy present (Table S12).

In conclusion, our research was initiated to further explore and investigate the conflicting views on the issue of the relationship between epigenetic aging and COVID-19 based on GWAS-based MR analysis and DNA methylation profile-based longitudinal analysis.[6,7] Taken together, our findings provided evidence to support that hospitalized COVID-19 subgroup and COVID-19 diagnosed with very severe respiratory disease may slow down GrimAge acceleration and PhenoAge acceleration. The general COVID-19 positive subgroup only slowed down PhenoAge acceleration significantly. For the reverse direction of MR analysis, we found no significant casual effect of epigenetic clocks on three COVID-19 subgroups.

Author contributions

Y.G. analyzed the data and drafted the manuscript and designed the study. Y.H. and Y.Z. helped proofread the manuscript. All authors have read and approved the final version of the manuscript.

Supplementary file 1

Table S1. Sources of GWAS summary datasets.

Table S2. Inverse-variance weighted Mendelian randomization analysis of the causal effect of COVID-19 subgroups on GrimAge acceleration.

Table S3. Inverse-variance weighted Mendelian randomization analysis of the causal effect of COVID-19 subgroups on HannumAge acceleration.

Table S4. Inverse-variance weighted Mendelian randomization analysis of the causal effect of COVID-19 subgroups on Intrinsic HorvathAge acceleration.

Table S5. Inverse-variance weighted Mendelian randomization analysis of the causal effect of COVID-19 subgroups on Intrinsic PheoAge acceleration.

Table S6. Inverse-variance weighted Mendelian randomization analysis of the causal effect of GrimAge acceleration on COVID-19 subgroups.

Table S7. Inverse-variance weighted Mendelian randomization analysis of the causal effect of HannumAge acceleration on COVID-19 subgroups.

Table S8. Inverse-variance weighted Mendelian randomization analysis of the causal effect of Intrinsic HorvathAge acceleration on COVID-19 subgroups.

Table S9. Inverse-variance weighted Mendelian randomization analysis of the causal effect of PhenoAge acceleration on COVID-19 subgroups.

Table S10. The p-value of Fixed effect meta-analysis of the causal effect of epigenetic clocks on COVID-19 subgroups.

Table S11. The result of MR-Egger intercept test for the causal effect of COVID-19 subgroups on epigenetic clocks.

Table S12. The result of MR-Egger intercept test for the causal effect of epigenetic clocks on COVID-19 subgroups.

Table S13. Genetic instruments for COVID-19 subgroups.

Table S14. Genetic instruments for epigenetic age acceleration.

Figure S1. Fixed effect meta-analysis of inverse-variance weighted Mendelian randomization estimates for genetically predicted effects of epigenetic clocks (GrimAge acceleration (A), HannumAge acceleration (B), Intrinsic HorvathAge acceleration (C) and PhenoAge acceleration (D)) on COVID-19 subgroups.

Conflicts of interest

The authors report no potential conflicts of interest.

Acknowledgements

This work was supported by the National Natural Science Foundation of China (grant number 61801147).

Supplementary materials

Supplementary material associated with this article can be found, in the online version, at doi:10.1016/j.jinf.2022.10.018.

References

1. Liu K., Chen Y., Lin R., Han K.. Clinical features of COVID-19 in elderly patients: a comparison with young and middle-aged patients. *J Infect* 2020;**80**:e14–18.
2. Wu C., et al. Risk Factors Associated With Acute Respiratory Distress Syndrome and Death in Patients With Coronavirus Disease 2019 Pneumonia in Wuhan, China. *JAMA Intern Med* 2020;**180**:934–43.
3. Onder G., Rezza G., Brusaferro S.. Case-Fatality Rate and Characteristics of Patients Dying in Relation to COVID-19 in Italy. *JAMA* 2020;**323**:1775–6.
4. Richardson S., et al. Presenting Characteristics, Comorbidities, and Outcomes Among 5700 Patients Hospitalized With COVID-19 in the New York City Area. *JAMA* 2020;**323**:2052–9.
5. Cao X., et al. Accelerated biological aging in COVID-19 patients. *Nat Commun* 2022;**13**:2135.
6. Franzen J., et al. Epigenetic Clocks Are Not Accelerated in COVID-19 Patients. *Int J Mol Sci* 2021;**22**.
7. Pang A.P.S., et al. Longitudinal Study of DNA Methylation and Epigenetic Clocks Prior to and Following Test-Confirmed COVID-19 and mRNA Vaccination. *Front Genet* 2022;**13**:819749.
8. McCartney D.L., et al. Genome-wide association studies identify 137 genetic loci for DNA methylation biomarkers of aging. *Genome Biol* 2021;**22**:194.
9. Morales Berstein F., et al. Assessing the causal role of epigenetic clocks in the development of multiple cancers: a Mendelian randomization study. *Elife* 2022;**11**.
10. Liu Z., et al. Underlying features of epigenetic aging clocks in vivo and in vitro. *Aging Cell* 2020;**19**:e13229.

Yu Guo[#]
School of Computer Science and Technology, Harbin Institute of Technology, Harbin 150001, China

Ying Zhang[#]
Beidahuang Industry Group General Hospital, Harbin, China

Yang Hu[*]
School of Computer Science and Technology, Harbin Institute of Technology, Harbin 150001, China

*Corresponding author.
E-mail address: huyang@hit.edu.cn (Y. Hu)

# These authors contributed equally to this work.
Accepted 2 October 2022
Available online 21 October 2022

https://doi.org/10.1016/j.jinf.2022.10.018

Low serum neutralization of Omicron variants a month after AZD7442 prophylaxis initiation

Dear Editor,

In this journal, Yang and colleagues recently reviewed effectiveness of monoclonal antibody therapy in organ transplant recipients with COVID-19.[1] Pre-exposure prophylaxis (PrEP) of COVID-19 is essential for immunocompromised patients who do not respond to SARS-CoV-2 vaccines. Prior to the spread of Omicron variants, a single 300 mg IM dose of AZD7442 (Tixagevimab/Cilgavimab, Evusheld) was 76.7% effective in preventing symptomatic COVID-19.[2] *In vitro* studies showed that AZD7442 has lost through various degrees part of its efficacy against all Omicron sublineages, including BA.4 and BA.5[3] which are currently becoming predominant in some parts of the world with a surge in COVID-19 cases.[4] The neutralizing activity of sera from AZD7442-treated patients against all Omicron sublineages remains poorly characterized.

The ANRS-0166s PRECOVIM prospective cohort study included severely immunocompromised patients not responding to vaccination and receiving AZD7442 300 mg IM as PrEP (NCT05216588). Here we present the first results, namely the neutralizing capacity of patients' sera one month after treatment against the Omicron variants BA.1, BA.2 and BA.5 compared to the European ancestral variant D614G.

One hundred patients (94 analyzable) from 15 French centers were included between 1/31/22 and 2/24/22 (58 solid organ transplant recipients, 20 chronic lymphocytic leukemia or non-Hodgkin lymphoma, 8 allogenic stem cell transplant recipients and 8 chronic inflammatory disorders under immunosuppressive drugs). Median age was 58 years (19–87). Using clinical replicative strains of the ancestral D614G European variant and the Omicron BA.1, BA.2 and BA.5 sublineages, we showed that the geometric mean neutralizing titers of sera from the 94 analyzable patients were respectively 5157.9, 12.7, 92.7 and 19.0 (Fig. 1). Neutralization titers were >10 (and considered positive) in 100%, 27%, 98% and 66% of patients' sera, respectively. The *in vitro* half-maximal effective concentrations (EC50) of AZD7442 against the same strains were 13.36, 580.87, 27.04 and 56.56 ng/mL, respectively.

Median anti-SARS-CoV-2 spike protein IgG antibody concentrations one month after AZD7442 administration were 2996.3 (876.1-13566.7) BAU/mL.

In this prospective cohort study including severely immunocompromised patients non-responding to SARS-CoV-2 vaccines, neutralization activity of patients' sera one month after administration of 300 mg of AZD7442 was low against both the Omicron BA.1 and BA.5 sublineages. As the serum-neutralizing capacity against SARS-CoV-2 is associated with protection against COVID-19,[5] the decreased AZD7442 *in vitro* activity against BA.1[6] had already prompted numerous regulatory agencies (FDA, MHRA, ANSM) to recommend doubling the AZD7442 dosing[4]. Our findings of low *in vivo* anti-BA.1 and -BA.5 neutralizing activity in treated patients' sera re-inforce the importance of continuous optimization of the AZD7442 dosing according to current and emerging SARS-CoV-2 variants.

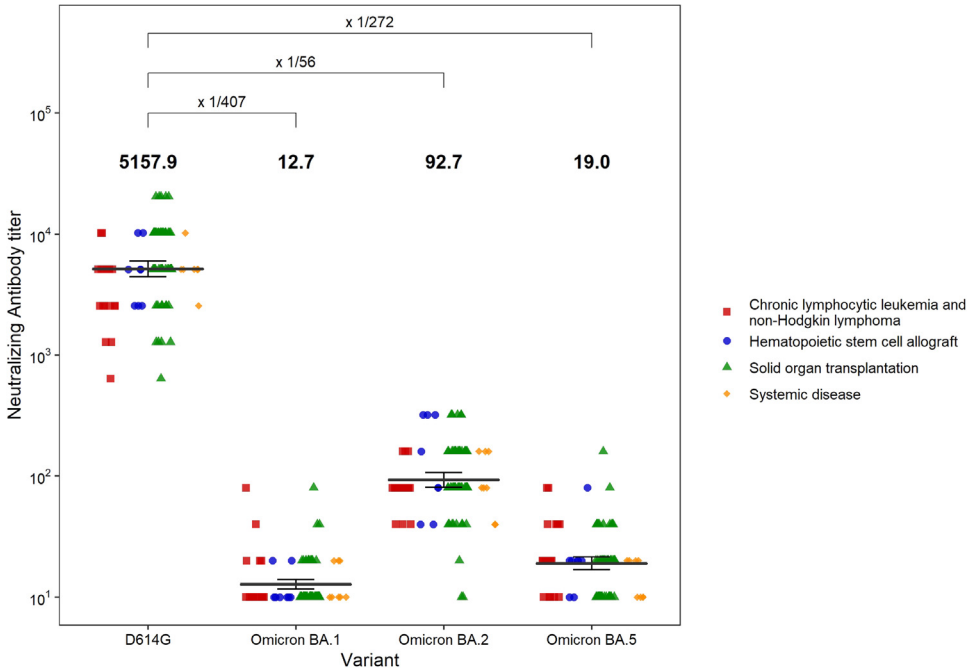

Fig. 1. Sera neutralizing titers of 94 patients one month after 150 mg Tixagevimab and 150 mg Cilgavimab administration against authentic live viruses from the D614G historical lineage and the Omicron BA.1, BA.2 and BA.5 sublineages.
Dots indicate individual samples. The serum geometric mean titers are shown with black bars and in bold characters at the *top* of the plot- I bars represent its 95% confidence intervals. Geometric means of individual ratio between viral strains neutralization are indicated in the upper part of the figure.

Declaration of Competing Interest

All authors have completed the ICMJE uniform disclosure form at www.icmje.org/coi_disclosure.pdf (available on request from the corresponding author) and declare: no support from any organization for the submitted work; no financial relationships with any organization that might have an interest in the submitted work in the previous three years; no other relationships or activities that could appear to have influenced the submitted work.

Financial disclosures

Authors have no financial disclosure to declare.

Ethical approval

This study received the ethical approval of the Comité de Protection des Personnes Sud-Ouest et Outre-Mer II.

Transparency declaration

VL (the manuscript's guarantor) affirm that the manuscript is an honest. accurate. and transparent account of the study being reported; that no important aspects of the study have been omitted; and that any discrepancies from the study as planned have been explained.

Funding

The ANRS0166s PRECOVIM cohort is conducted with the support of ANRS | MIE and funded by French ministries: Ministère des Solidarités et de la Santé and Ministère de l'Enseignement Supérieur. de la Recherche et de l'Innovation

Acknowledgments

We thank Pr Yazdan Yazdanpanah and all the ANRS-MIE team for their invaluable support and help.

Supplementary materials

Supplementary material associated with this article can be found, in the online version, at doi:10.1016/j.jinf.2022.10.006.

References

1. Yang M., Li A., Wang Y., Tran C., Zhao S., Ao G.. Monoclonal antibody therapy improves severity and mortality of COVID-19 in organ transplant recipients: a meta-analysis. *J Infect* 2022 S0163-4453(22)00384-X.
2. Levin M.J., Ustianowski A., De Wit S., et al. Intramuscular AZD7442 (Tixagevimab-Cilgavimab) for Prevention of Covid-19. *N Engl J Med* 2022;**386**:2188–200.
3. Tuekprakhon A, Huo J, Nutalai R, et al. Further antibody escape by Omicron BA.4 and BA.5 vaccine and BA.1 serum. bioRxvid 2022. doi:10.1101/2022.05.21.492554.
4. Callaway E.. What Omicron's BA.4 and BA.5 variants mean for the pandemic. *Nature* 2022;**606**:848–9.
5. Cromer D., Steain M., Reynaldi A., et al. Neutralising antibody titres as predictors of protection against SARS-CoV-2 variants and the impact of boosting: a meta-analysis. *Lancet Microbe* 2022;**3**:e52–61.
6. Bruel T., Hadjadj J., Maes P., et al. Serum neutralization of SARS-CoV-2 Omicron sublineages BA.1 and BA.2 in patients receiving monoclonal antibodies. *Nat Med* 2022;**28**:1297–302.

Xavier de Lamballerie
Unité des Virus Émergents, INSERM-120, IRD-190, Aix-Marseille University, France

Guillaume Martin-Blondel
Service des Maladies Infectieuses et Tropicales, CHU de Toulouse & Institut Toulousain des Maladies Infectieuses et Inflammatoires (Infinity), INSERM UMR1291 - CNRS UMR5051, Université Toulouse III

Axelle Dupont
Université Paris Cité and Université Sorbonne Paris Nord, Inserm, IAME, Centre d'Investigation clinique-Epidémiologie Clinique 1425. Inserm, Department of Epidemiology Biostatistics and Clinical Research, AP-HP, Hôpital Bichat, F-75018 Paris, Paris, France

Jacques Izopet
CHU Toulouse, Hôpital Purpan, Laboratoire de Virologie, National Reference Center for Hepatitis E, Inserm UMR 1291, CNRS UMR5051, Université Toulouse III, 31000, Toulouse, France

France Mentré
Université Paris Cité and Université Sorbonne Paris Nord, Inserm, IAME, Centre d'Investigation clinique-Epidémiologie Clinique 1425. Inserm, Department of Epidemiology Biostatistics and Clinical Research, AP-HP, Hôpital Bichat, F-75018 Paris, Paris, France

Nassim Kamar
Département de Néphrologie et Transplantation d'Organes, CHU Rangueil 31059 Toulouse, France

Brigitte Autran
Sorbonne-Université, Cimi-Paris, Inserm U1135. CNRS ERL8255, UPMC CR7, Team « NK and T cell immunity, infections and cancer», Paris, France

Gilles Paintaud
Université de Tours, EA4245 Transplantation, Immunology and Inflammation, Tours, France

Sophie Caillard
Department of Nephrology and Transplantation, Strasbourg University Hospital, Inserm UMR S1109 Labex Transplantex. Fédération de Médecine Translationnelle, 67000, Strasbourg, France

Amandine le Bourgeois
service d'hématologie clinique, CHU Nantes, 1 place Alexis Ricordeau 44000 Nantes, France

Christophe Richez
Hôpital Pellegrin. CHU de Bordeaux. Service de Rhumatologie. Centre de référence des maladies autoimmunes systémiques rares (RESO). UMR-CNRS 5164, Université de Bordeaux, Bordeaux, France

Lionel Couzi
Nephrologie-Transplantation-Dialyse. CHU Bordeaux. Bordeaux. France CNRS-UMR 5164 Immuno ConcEpT. Université de Bordeaux, Bordeaux, France

Aliénor Xhaard
Service d'hématologie greffe Hôpital Saint-Louis, APHP, Université de Paris Cité, Paris, France

Zora Marjanovic
Sorbonne University, Service d'Hématologie Clinique et Thérapie Cellulaire, Hôpital Saint-Antoine, AP-HP, INSERM, UMRs 938, Paris, France

Jerome Avouac
Université de Paris Service de Rhumatologie, Hôpital Cochin, AP-HP.CUP 27 rue du Faubourg Saint-Jacques 75014 Paris, France

Caroline Jacquet
Service Hématologie et Thérapies Cellulaires, CHRU Bretonneau, Tours, France

Denis Anglicheau
Department of Nephrology and kidney transplantation, Necker Hospital. APHP and Université de Paris Cité, Paris, France

Morgane Cheminant
Clinical Hematology, Necker-Enfants Malades University Hospital, AP-HP. F-75015, Université de Paris Cité, Paris, France

Yazdan Yazdanpanah
Université Paris Cité, INSERM UMRS 1137 IAME, Paris. France

Stéphanie N Guyen
Sorbonne université, Groupe Hospitalier Pitié-Salpêtrière APHP, service d'Hématologie clinique, Pavillon Georges Heuyer, 47-83 boulevard de l'Hôpital, 75651 Paris cedex 13. Sorbonne Université. Inserm CNRS 1135 « NK and T cell immunity. Virus and Cancer ». Centre d'Immunologie et des Pathologies Infectieuses (CIMI), UPMC UMRS CR7-Inserm U1135-CNRS ERL 8255, faculté de Médecine Sorbonne Université, Site Pitié-Salpêtrière, 91 boulevard de l'Hôpital, 75013 Paris, France

Benjamin Terrier
Assistance Publique-Hôpitaux de Paris, Département de Médecine Interne, Centre de Référence National pour les maladies auto-immunes systémiques rares. Hôpital Cochin Paris., Université Paris. France

Jacques Eric Gottenberg
Service de Rhumatologie, Hôpitaux Universitaires de Strasbourg, CNR RESO, Hôpitaux Universitaires de Strasbourg, Laboratoire d'Immunopathologie et de Chimie Thérapeutique. Institut de Biologie Moléculaire et Cellulaire (IBMC). CNRS UPR3572, 67000, Strasbourg, France

Caroline Besson
Université Paris-Saclay, UVSQ, CESP-INSERM1018, CH de Versailles. 78150, Le Chesnay, France

Sophie Letrou
Département d'Épidémiologie, Biostatistique et Recherche Clinique Unité de Recherche Clinique Paris Nord APHP.Nord – Université Paris Cité Hôpital Bichat – Claude-Bernard 46 rue Henri Huchard, 75877 Cedex 18, PARIS

Sabrina Kali
Clinical Research Department, ANRS | Emerging infectious disease, PariSanté Campus | 2 rue d'Oradour-sur-Glane, 75015 Paris

Denis Angoulvant
Service de Cardiologie, CHRU de Tours & EA4245 Transplantation Immunologie et Inflammation, Université de Tours. F37000 Tours, France

Ventzislava Petrov Sanchez
ANRS|Emerging Infectious Diseases, Department of Clinical Research, Paris, France

Coralie Tardivon
Departement of Epidemiology Biostatistics and Clinical Research. AP-HP. Hôpital Bichat, Paris, France

Gilles Blancho
Institut de Transplantation- Urologie – Néphrologie (ITUN) Hôtel Dieu – CHU de Nantes 30 bd Jean-Monnet, 44093, Nantes, France

Vincent Lévy*
Département de Recherche Clinique, Hôpital Avicenne. APHP, Université Sorbonne Paris Nord and CRESS INSERM U1153. ECSTRRA team

*Corresponding author at: Département de Recherche Clinique, Hôpital Avicenne, 125 rue de Stalingrad, 93000 Bobigny, France.
E-mail address: vincent.levy@aphp.fr (V. Lévy)

Accepted 2 October 2022
Available online 8 October 2022

https://doi.org/10.1016/j.jinf.2022.10.006

Rapid emergence of ceftazidime-avibactam resistance among carbapenem-resistant Enterobacterales in a tertiary-care hospital in Taiwan

Dear Editor,

We read with great interest the article by Zha *et al.* describing a nationwide survey on the management of infections caused by carbapenem-resistant *Klebsiella pneumoniae* (CRKP) in critically ill patients of tertiary hospitals in China.[1] In this study, only 16% of the participating hospitals offered ceftazidime-avibactam (CZA) for treating carbapenem-resistant *K.* pneumoniae infections. The authors recommended that routine detection of carbapenemases and *in vitro* susceptibility for CZA among all CRKP isolates are necessary, as a nationwide survey in China has demonstrated an 11.1% of CRKP isolates resistant to this agent.[1]

CZA was introduced into Taiwan in 2019 and has been widely used for the treatment of infections caused by carbapenem-resistant Enterobacterales (CRE) and *Pseudomonas* species (CRP). Resistance to CZA has been reported in isolates carrying metallo-β-lactamases (MBLs) or certain bla_{KPC} variants, resulting in treatment failure. [2] Previous surveillance revealed that CZA remained active against the CRE or CRP isolates with a resistance rate of less than 10%.[3]

In this study, we performed CZA susceptibility testing using Epsilometer tests (E test) for all CRE or CRP isolates before starting treatment from April to August 2021. We analyzed the medical records of these patients and detected five common carbapenemases (bla_{KPC}, bla_{NDM}, bla_{VIM}, bla_{IMP}, and bla_{OXA-48}) in the isolates by targeted PCR and sequencing. The genetic relatedness of CZA-resistant Enterobacterales isolates was determined by multilocus sequence typing. The *K. pneumoniae* isolates were further analyzed by pulsed-field gel electrophoresis using *Xba*I restriction enzyme digestion and *wzc* gene partial sequencing to determine relatedness and capsular types as described previously.[4]

A total of 48 patients were included in the analysis. The clinical characteristics and outcomes are summarized in Table 1 and Supplementary materials. The crude mortality rates at 28 days and 120 days were 18.8% and 50%, respectively. The antimicrobial susceptibilities are listed in Supplementary Table 1. Prior exposure to CZA within 3 months before infection episodes was a significant predictor of acquiring resistant isolates ($p = 0.039$, adjusted odds ratio: 5.14, 95% CI 1.08–24.29). Among the 48 isolates, 13 (27.1%) carried MBLs (one with two MBLs), 10 (20.8%) carried SBL, and two carried both MBL and SBL. Sixteen out of the 20 isolates (80.0%) of the CZA-resistant isolates carried at least one MBLs, including six bla_{NDM-1} (two *E. coli*, two *K. pneumoniae*, one *K. oxytoca*, one *Enterobacter cloacae* complex), two bla_{NDM-4} (*K. pneumoniae*), four bla_{IMP-8} (two *K. pneumoniae*, one ECC, one *Serratia marcescens*), one bla_{VIM-1} (*K. oxytoca*), two bla_{IMP-8}+bla_{OXA-48} (*K. pneumoniae*), and one bla_{IMP-8}+bla_{VIM-23} (one *P. alcaligenes*). One *K. pneumoniae* isolate carrying bla_{OXA-48} and four isolates (two *P. aeruginosa*, one *E. coli*, and one *K. pneumoniae*) without carbapenemases were resistant to CZA. In addition, we found that ten patients had more than one isolate identified during their admission, and 4 of the isolates from the same patients showed a 4-times elevated CZA MICs.

Table 1
Underlying characteristics and demographic data of the 48 patients infected with carbapenem-resistant Enterobacterales or carbapenem-resistant *Pseudomonas* species.

Characteristic	No. (%) of patients infected with indicated isolates		
	All isolates (n = 48)	Enterobacterales (n = 34)	*Pseudomonas* spp. (n = 14)
Age (years) Mean± S.D.	69.9 ± 16.1	69.2 ± 17.5	71.6 ± 11.9
Male	34 (70.8)	22 (64.7)	12 (85.7)
Underlying diseases			
Malignancy	26 (54.2)	15 (57.7)	11 (42.3)
Diabetes mellitus	20 (41.7)	13 (65.0)	7 (35.0)
Other endocrine diseases[a]	7 (14.6)	5 (71.4)	2 (28.6)
COPD	9 (18.8)	9 (100)	0
CKD stage ≥ 3	15 (31.3)	13 (86.7)	3 (20.0)
Cardiovascular diseases	34 (70.8)	23 (67.6)	11 (32.4)
Previous CVA	8 (16.7)	7 (87.5)	1 (12.5)
Other neurological disorders[b]	10 (20.8)	8 (80.0)	2 (20.0)
Liver diseases	11 (22.9)	6 (54.5)	5 (45.5)
Diagnosis			
Pneumonia	29 (60.4)	19 (55.9)	10 (71.4)
Bacteremia	24 (50)	13 (38.2)	11 (78.6)
UTI	10 (20.8)	9 (26.5)	1 (7.1)
IAI	7 (14.6)	6 (17.6)	1 (7.1)
Wound infection	11 (22.9)	8 (23.5)	3 (21.4)
Shock	17 (35.4)	11 (32.4)	6 (42.9)
ICU admission after onset	24 (50.0)	18 (52.9)	6 (42.9)
120-day mortality	24 (50.0)	15 (44.1)	9 (64.3)
Discharge	24 (50.0)	18 (52.9)	6 (42.9)
Discharge to another institute	9 (18.8)	8 (23.5)	1 (7.1)
Discharge to home	15 (31.3)	11 (32.4)	4 (28.6)

Abbreviations: COPD, chronic obstructive pulmonary disease; CKD, chronic kidney disease; CVA, cerebrovascular accident; UTI, urinary tract infection; IAI, intra-abdominal infection; CR, carbapenem-resistant.
[a] Including adrenal insufficiency, hyperthyroidism, hypothyroidism, and hypopituitarism
[b] Including Alzheimer's disease and Parkinson's disease

The eCIM failed to detect MBLs in *K. pneumoniae* isolates carrying $bla_{\text{IMP-8}}$+$bla_{\text{OXA-48}}$ (Supplementary Table 2).

Regarding the clonality of isolates, PFGE revealed genetic diversity especially for MBL clusters (Fig. 1). For example, four isolates carrying NDM-4 displayed pulsotypes I and IV, accounting for three different subpulsotypes. In contrast, for SBLs, four isolates carrying KPC-2 displayed pulsotype III only, which was predominant in ST11-K47. Among ST11-K47 isolates, there were three different sub-pulsotypes, indicating a local evolution rather than a single outbreak of isolates carrying KPC-2. In addition, the SBL clusters including ST11-K47 and ST11-K64 were prevalent clonalities of KPC-2 and OXA-48 in Taiwan, whereas MBL clusters such as ST307-wzc_80 carrying IMP8 seemed to be a novel clonality. Further studies are required to determine the prevalence of this condition.

The present study had three main findings. First, among carbapenemase–encoding genes, the proportion of CRE carrying MBL was higher than previous data in Taiwan,[5] and might indicate a rapid emergence of MBL resulting in reduced CZA susceptibilities. Unlike previous reports, the CZA resistance of CRE in our institute was not caused by mutations in $bla_{\text{KPC-3}}$ but by the dissemination of MBLs.[6] In addition, our study included a small number of cases infected by CRE carrying $bla_{\text{IMP-8}}$, which has not been frequently reported in Taiwan. Further studies are warranted to determine its clinical relevance by comparing it with bla_{NDM}.[7]

Second, the MBLs producing CRE not only arise from their intrinsic resistance to carbapenem and CZA, but also their location on genetic mobile elements such as plasmids, integrons, and transposons.[8] Commercial screening tools such as NG-Test CARBA 5 (NG Biotech, Guipry, France) and Xpert CARBA-R assay (Cepheid, Sunnyvale, CA, USA) might be helpful for timely and accurate detection.[9] Unfortunately, the Xpert assay could not detect the $bla_{\text{IMP-8}}$ variant in Taiwan.[9] Also, isolates containing both MBLs and SBLs further complicate the recommended phenotypic assay for the detection of MBLs as revealed by the discrepant results of mCIM and eCIM in our study.

Finally, in terms of post-infection tracing, a significant proportion of our patients were discharged into the community. Clinicians should be aware that more than half of CRE carriage can be prolonged to six months, posing a threat to long-term care facilities and communities. Considering the prolonged colonization, active surveillance may be beneficial for infection control once patients are admitted.[10]

There were three limitations in this study. First, we only collected isolates with CZA E test ordered by physicians who initiated the treatment. Not all CRE or CRP isolates were included; therefore, the resistance rate may be overestimated. Second, it remains unclear whether MBLs were already disseminated before the widespread use of CZA. Third, the sample size was small. A longer monitoring period with a larger sample size will be helpful in clarifying the resistant trend.

In conclusion, the emergence of CRE carrying various MBLs, resulting in reduced CZA susceptibility, provides an alert for clinicians in Taiwan. To prevent an outbreak of cross-infection associated with health care, measures such as contact isolation, repeated culture with the CZA E test, and timely identification of carbapenemases and the genotypes should be implemented for hospitalized patients. Moreover, the trend of CZA susceptibility should be monitored at the national level. Further research needs to be carried out to investigate zoonotic, geographical, and environmental factors that account for the emergence, so that a one-health approach can be developed for infection control.

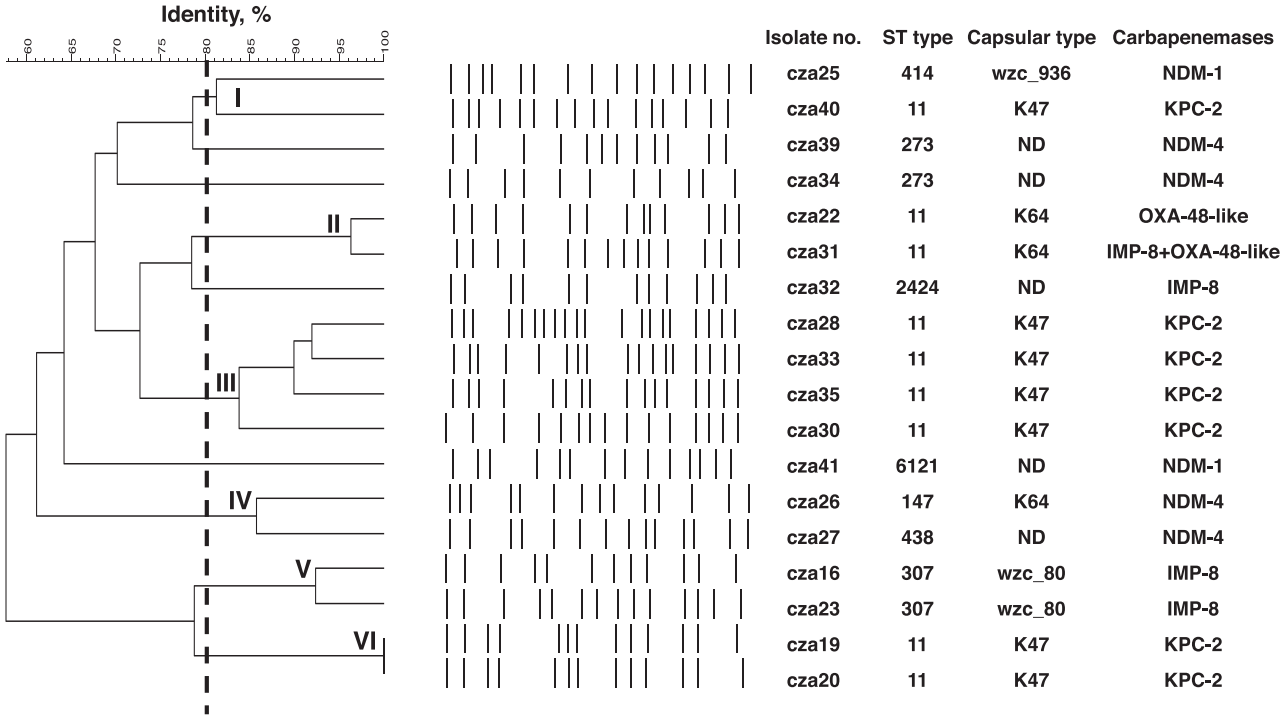

Fig. 1. Genetic relatedness of 18 carbapenemase-producing-carbapenem-resistant *Klebsiella pneumoniae* isolates by pulsed-field gel electrophoresis, multilocus sequence typing, and *wzc* capsular typing. There are six pulsotypes (I to VI) identified. The corresponding numbers from patients with multiple carbapenemase-producing-carbapenem-resistant *K. pneumoniae* isolates (Supplementary Table 2) are as following: cza16 (patient C-isolate 1), cza22 (D-1), cza23 (C-2), cza27 (F-1), cza31 (D-2), cza34 (F-2), and cza39 (F-3). The MLST-capsular types of *K. pneumoniae* isolates carrying $bla_{\text{IMP-8}}$ were ST307-wzc80 ($n = 2$; Patient C) and ST2424. Isolates carrying $bla_{\text{IMP-8}}$+$bla_{\text{OXA-48-like}}$ genes were ST11-K47 and ST11-K64. Isolates carrying $bla_{\text{NDM-4}}$ were ST147-K64, ST273 ($n = 2$, Patient F), and ST438. Isolates carrying $bla_{\text{NDM-1}}$ were ST414-wzc_936 and ST6121. *E. coli* isolates carrying $bla_{\text{NDM-1}}$ belonged to ST14 and ST69. The *E. cloacae* complex isolate with $bla_{\text{IMP-8}}$ was ST204, one *was* $bla_{\text{NDM-1}}$ ST316, and the other *was* $bla_{\text{NDM-1}}$ ST1497 (Patient B).

Funding

This study was supported by the Ministry of Science and Technology of Taiwan (MOST 111-2320-B-039-054).

Ethics approval

The institutional review board of the National Taiwan University Hospital waived the need for written informed consent because the study involved only minimal risk to the patients (IRB number: 201609066RINB).

Declaration of Competing Interest

None.

Supplementary materials

Supplementary material associated with this article can be found, in the online version, at doi:10.1016/j.jinf.2022.10.003.

References

1. Zha L., Li S., Ren Z., Li X., Zhang D., Zou Y., et al. Clinical management of infections caused by carbapenem-resistant *Klebsiella pneumoniae* in critically ill patients: a nationwide survey of tertiary hospitals in mainland China. *J Infect* 2022;**84**(6):e108–10.
2. Boyd S.E., Livermore D.M., Hooper D.C., Hope WW.. Metallo-beta-lactamases: structure, function, epidemiology, treatment options, and the development pipeline. *Antimicrob Agents Chemother* 2020;**64**(10) e00397-20.
3. Huang Y.T., Kuo Y.W., Teng L.J., Liao C.H., Hsueh PR.. Comparison of E test and broth microdilution for evaluating the susceptibility of *Staphylococcus aureus* and *Streptococcus pneumoniae* to ceftaroline and of carbapenem-resistant Enterobacterales and *Pseudomonas aeruginosa* to ceftazidime/avibactam. *J Global Antimicrob Resist* 2021;**26**:301–7.
4. Liao C.H., Huang Y.T., Hsueh PR.. Multicenter surveillance of capsular serotypes, virulence genes, and antimicrobial susceptibilities of *Klebsiella pneumoniae* causing bacteremia in Taiwan, 2017–2019. *Front Microbiol* 2022;**13**:783523.
5. Wang C.H., Ma L., Huang L.Y., Yeh K.M., Lin J.C., Siu L.K., et al. Molecular epidemiology and resistance patterns of $bla_{\text{OXA-48}}$ *Klebsiella pneumoniae* and *Escherichia coli*: A nationwide multicenter study in Taiwan. *J Microbiol Immunol Infect* 2021;**54**(4):665–72.
6. Coppi M., Di Pilato V., Monaco F., Giani T., Conaldi P.G., Rossolini GM.. Ceftazidime-avibactam resistance associated with increased $bla_{\text{KPC-3}}$ gene copy number mediated by pKpQIL plasmid derivatives in sequence type 258 *Klebsiella pneumoniae*. *AntimicrobAgents Chemother* 2020;**64**(4):e01816–19.
7. Huang Y.S., Tsai W.C., Li J.J., Chen P.Y., Wang J.T., Chen Y.T., et al. Increasing New Delhi metallo-beta-lactamase-positive *Escherichia coli* among carbapenem non-susceptible Enterobacteriaceae in Taiwan during 2016 to 2018. *Sci Rep* 2021;**11**(1):2609.
8. Nordmann P., Poirel L.. Epidemiology and diagnostics of carbapenem resistance in Gram-negative bacteria. *Clin Infect Dis* 2019;**69**(7):S521–S5S8 Suppl.
9. Huang Y.T., Kuo Y.W., Lee N.Y., Tien N., Liao C.H., Teng L.J., et al. Evaluating NG-Test CARBA 5 multiplex immunochromatographic and Cepheid Xpert CARBA-R assays among carbapenem-resistant Enterobacterales isolates associated with bloodstream infection. *Microbiol Spectr* 2022;**10**(1) e01728-21.
10. Chen H.Y., Jean S.S., Lee Y.L., Lu M.C., Ko W.C., Liu P.Y., et al. Carbapenem-resistant Enterobacterales in long-term care facilities: a global and narrative review. *Front Cell Infect Microbiol* 2021;**11**:601968.

Jia-Arng Lee, Shin-Hei Du, Tai-fen Lee
Department of Laboratory Medicine, National Taiwan University Hospital, National Taiwan University College of Medicine, Taipei, Taiwan

Yu-Shan Huang
Department of Internal Medicine, National Taiwan University Hospital, National Taiwan University College of Medicine, Taipei, Taiwan

Chun-Hsing Liao
Colleague of Medicine, National Yang-Ming University, Taipei, Taiwan

Department of Internal Medicine, Far Eastern Memorial Hospital, New Taipei City, Taiwan

Yu-Tsung Huang*
Department of Laboratory Medicine, National Taiwan University Hospital, National Taiwan University College of Medicine, Taipei, Taiwan
Graduate Institute of Clinical Laboratory Sciences and Medical Biotechnology, National Taiwan University, Taipei, Taiwan

Po-Ren Hsueh**
Departments of Laboratory Medicine and Internal Medicine, School of Medicine, China Medical University Hospital, China Medical University, Taichung, Taiwan
Ph.D Program for Aging, College of Medicine, China Medical University, Taichung, Taiwan

*Corresponding author at: Department of Laboratory Medicine, National Taiwan University Hospital, National Taiwan University College of Medicine, Taipei, Taiwan. **Corresponding author at: Departments of Laboratory Medicine and Internal Medicine, China Medical University Hospital, School of Medicine, China Medical University, Taichung, Taiwan.
E-mail addresses: yutsunghuang@gmail.com (Y.-T. Huang), hsporen@gmail.com (P.-R. Hsueh)

Accepted 2 October 2022
Available online 17 October 2022

https://doi.org/10.1016/j.jinf.2022.10.003

Efficacy and safety of Paxlovid for COVID-19:a meta-analysis

Dear Editor,

We read with interest a recent article reported by Wang Y et al. [1]. The authors reported a case of COVID-19 rebound in a severe COVID-19 patient during long term (20 days) treatment of Paxlovid. Paxlovid is a recommended treatment for mild-moderate COVID-19 and risk factors for severe disease. With wide-spread use of Paxlovid, there have been case reports of individuals experiencing virologic rebound. Hence, meta-analysis of the efficiency and safety of Paxlovid in patients with COVID-19 is of great importance.

An extensive literature search was performed in PubMed, Web of Science, EMBASE, and Cochrane Library to find all for relevant studies published from December 1, 2021, to September 20, 2022. We screened the references of the retrieved studies and restricted the language of the search to English. Following keywords were used in the search: Paxlovid (nirmatrelvir/ritonavir) and COVID-19 (SARS-CoV-2, SARS2, SARS Coronavirus 2, Coronavirus Disease 2019, 2019-nCoV, 2019 Novel Coronavirus). The inclusion criteria were as follows: (1) the article reported the clinical results of Paxlovid, including the total number of participants and the specific number of deaths, hospitalization, rebound or adverse events; (2) English language. The exclusion criteria were as follows: (1) irrelevant to the research direction, (2) no relevant data, (3) case reports, (4) review papers, (5) repeated articles.

The analysis was conducted using the Review Manager statistical software, version 5.3. A binary controlled study was used to calculate the number of deaths, hospitalization, rebound or adverse events. Odds ratio (OR) and 95% confidence interval (CI) were used to assess the effect in a whole random-effects meta-analysis model. The I^2 and P value was used to quantify the heterogeneity of the effects among the included studies.

A total of 13 studies involving 186,306 patients were identified in the final analysis, and the detail of the included studies are shown in Table 1[2-14]. Three studies described the rebound of COVID-19 patients in Paxlovid group and control group. The overall OR of rebound among COVID-19 patients in the Paxlovid vs. control group was 0.99 (95% CI, 0.28–3.57; I^2 =59%), $P = 0.99$ (Fig. 1A). Five studies described adverse events in Paxlovid group and control group. The overall OR of adverse events among COVID-19 patients in the Paxlovid vs. control group was 1.07 (95% CI, 0.49–2.34; I^2 =90%), $P = 0.87$ (Fig. 1B). There is no significant difference of rebound and adverse events in Paxlovid group and control group.

In addition, we analyze the efficacy of Paxlovid on death and hospitalization for COVID-19 patients. Seven studies described the

Table 1
Basic information of the included studies.

Study	Events	Paxlovid Group		Placebo group	
		Events (n)	Total (n)	Events (n)	Total (n)
Dryden-Peterson S, 2022[2]	Death	0	6036	39	24,286
	Hospitalization	40	6036	223	24,286
Ganatra S, 2022[3]	Death	0	1130	10	1130
	Hospitalization	10	1130	23	1130
Hammond J, 2022[4]	Death	0	697	9	682
	Hospitalization	5	697	44	682
	Adverse events	476	1109	525	1115
Hedvat J, 2022[5]	Death	0	28	3	75
	Hospitalization	3	28	23	75
Pfizer; 2021[6]	Death	0	607	10	612
	Hospitalization	6	607	41	612
	Adverse events	10	607	40	612
Saravolatz LD, 2022[7]	Death	0	1039	12	1046
	Hospitalization	8	1039	66	1046
	Adverse events	67	1039	22	1046
Wong CKH, 2022[8]	Death	31	890	83	890
Yip TCF, 2022[9]	Hospitalization	172	4921	1931	83,154
Dai EY, 2022[10]	Rebound	3	11	1	25
Wang L, 2022[11]	Rebound	609	11,270	204	2374
Li HY, 2022[12]	Rebound	2	258	3	244
Anderson AS, 2022[13]	Adverse events	23	990	17	980
Yan GF, 2022[14]	Adverse events	2	5	7	30

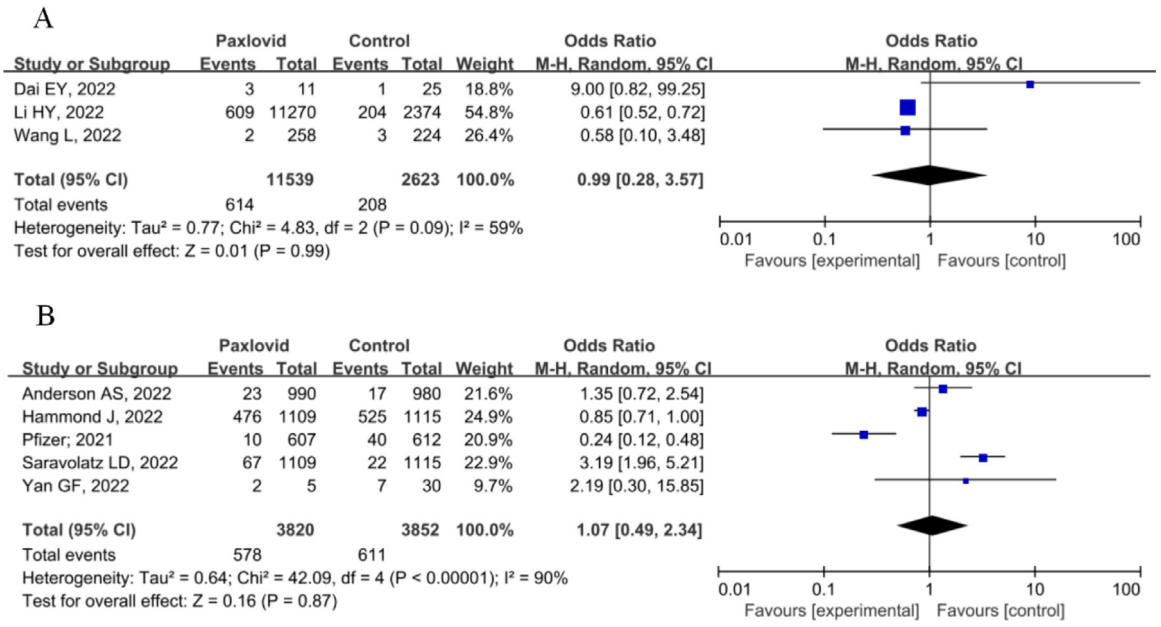

Fig. 1. Incidence of rebound (A) and adverse events (B) in Paxlovid group and control group.

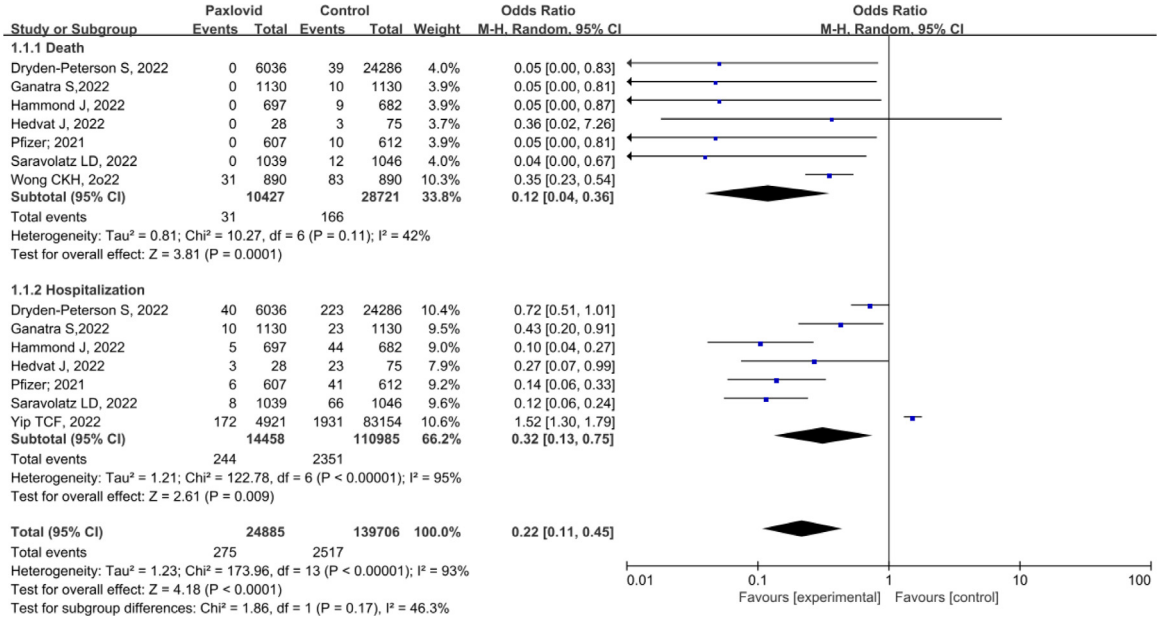

Fig. 2. Subgroup analysis: impact of Paxlovid on mortality and hospitalization rates of COVID-19 patients.

death of COVID-19 patients in the Paxlovid group and control group, and seven studies described the hospitalization of COVID-19 patients. Our study showed that the overall OR for death and hospitalization among COVID-19 patients in the Paxlovid vs. control group was 0.22 (95% CI, 0.11–0.45; I^2 =93%), P <0.0001. The result indicates that the Paxlovid treatment is effective for patients with COVID-19, reducing the mortality or hospitalization rate by 78% (Fig. 1). Subtype analysis shows that the OR of mortality for COVID-19 patients in the Paxlovid vs. control group was 0.12 (95% CI, 0.04–0.36; I^2 =42%), P = 0.0001, indicating an 88% reduction in mortality. The OR of hospitalization for COVID-19 patients in the Paxlovid vs. control group was 0.32 (95% CI, 0.13–0.75; I2 =95%), P = 0.009, a 68% reduction in hospitalization rate.

In conclusion, our research shows that Paxlovid for COVID-19 is effective and safe. COVID-19 rebound is not unique to Paxlovid. There is no significant difference of rebound in Paxlovid group and control group. There has been more attention to COVID-19 rebounds following Paxlovid treatment, which may be attributable to more people being treated with Paxlovid. However, the phenomenon of rebounds following Paxlovid treatment reinforces the importance of testing for individuals with recurrent symptoms after Paxlovid treatment.

Funding

This work was supported by Science and Technology Fund of Guizhou Health Commission (No.gzwkj2021-024), and the cultivate project 2021 for National Natural Science Foundation of China, Affiliated Hospital of Guizhou Medical University (No.gyfynsfc-2021-14).

Declaration of Competing Interest

All authors report that they have no potential conflicts of interest.

References

1. Wang Y., Chen X., Xiao W., Zhao D., Feng L.. Rapid COVID-19 rebound in a severe COVID-19 patient during 20-day course of Paxlovid. *J Infect* 2022. doi:10.1016/j.jinf.2022.08.012.
2. Dryden-Peterson S., Kim A., Kim A.Y., Caniglia E.C., Lennes I., Patel R., Gainer L., Dutton L., Donahue E., Gandhi R.T., Baden L.R., Woolley A.E.. Nirmatrelvir plus ritonavir for early COVID-19 and hospitalization in a large US health system. *medRxiv* 2022. doi:10.1101/2022.06.14.22276393.
3. Ganatra S., Dani S.S., Ahmad J., Kumar A., Shah J., Abraham G.M., McQuillen D.P., Wachter R.M., Sax P.E.. Oral Nirmatrelvir and Ritonavir in Non-hospitalized Vaccinated Patients with Covid-19. *Clin Infect Dis* 2022. doi:10.1093/cid/ciac673.
4. Hammond J., Leister-Tebbe H., Gardner A., Abreu P., Bao W., Wisemandle W., Baniecki M., Hendrick V.M., Damle B., Simon-Campos A., Pypstra R., Rusnak J.M.E.-H. Investigators Oral Nirmatrelvir for High-Risk, Nonhospitalized Adults with Covid-19. *N Engl J Med* 2022;**386**(15):1397–408. doi:10.1056/NEJMoa2118542.
5. Hedvat J., Lange N.W., Salerno D.M., DeFilippis E.M., Kovac D., Corbo H., Chen J.K., Choe J.Y., Lee J.H., Anamisis A., Jennings D.L., Codispodo G., Shertel T., Brown R.S. Jr., Pereira M.R.. COVID-19 therapeutics and outcomes among solid organ transplant recipients during the Omicron BA.1 era. *Am J Transplant* 2022. doi:10.1111/ajt.17140.
6. Mahase E.. Covid-19: pfizer's paxlovid is 89% effective in patients at risk of serious illness, company reports. *BMJ* 2021;**375**:n2713. doi:10.1136/bmj.n2713.
7. Saravolatz L.D., Depcinski S., Sharma M.. Molnupiravir and Nirmatrelvir-Ritonavir: oral COVID Antiviral Drugs. *Clin Infect Dis* 2022. doi:10.1093/cid/ciac180.
8. Wong C.K.H., Au I.C.H., Lau K.T.K., Lau E.H.Y., Cowling B.J., Leung G.M.. Real-world effectiveness of early molnupiravir or nirmatrelvir-ritonavir in hospitalised patients with COVID-19 without supplemental oxygen requirement on admission during Hong Kong's omicron BA.2 wave: a retrospective cohort study. *Lancet Infect Dis* 2022. doi:10.1016/S1473-3099(22)00507-2.
9. Yip T.C.F., Lui G.C.Y., Lai M.S.M., Wong V.W.S., Tse Y.K., Ma B.H.M., Hui E., Leung M.K., Chan H.L.Y., Hui D.S.C., Wong G.L.H.. Impact of the use of oral antiviral agents on the risk of hospitalization in community COVID-19 patients. *Clin Infect Dis* 2022. doi:10.1093/cid/ciac687.
10. Dai E.Y., Lee K.A., Nathanson A.B., Leonelli A.T., Petros B.A., Brock-Fisher T., Dobbins S.T., MacInnis B.L., Capone A., Littlehale N., Boucau J., Marino C., Barczak A.K., Sabeti P.C., Springer M., Stephenson K.E.. Viral Kinetics of Severe Acute Respiratory Syndrome Coronavirus 2 (SARS-CoV-2) Omicron Infection in mRNA-Vaccinated Individuals Treated and Not Treated with Nirmatrelvir-Ritonavir. *medRxiv* 2022. doi:10.1101/2022.08.04.22278378.
11. Wang L., Berger N.A., Davis P.B., Kaelber D.C., Volkow N.D., Xu R.. COVID-19 rebound after Paxlovid and Molnupiravir during January-June 2022. *medRxiv* 2022. doi:10.1101/2022.06.21.22276724.
12. Li H., Gao M., You H., Zhang P., Pan Y., Li N., Qin L., Wang H., Li D., Li Y., Qiao H., Gu L., Xu S., Guo W., Wang N., Liu C., Gao P., Niu J., Cao J., Zheng Y.. Association of nirmatrelvir/ritonavir treatment on upper respiratory SARS-CoV-2 RT-PCR negative conversion rates among high-risk patients with COVID-19. *Clin Infect Dis* 2022. doi:10.1093/cid/ciac600.
13. Anderson A.S., Caubel P., Rusnak J.M.E.-H.T. Investigators Nirmatrelvir-Ritonavir and Viral Load Rebound in Covid-19. *N Engl J Med* 2022. doi:10.1056/NEJMc2205944.
14. Yan G., Zhou J., Zhu H., Chen Y., Lu Y., Zhang T., Yu H., Wang L., Xu H., Wang Z., Zhou W.. The feasibility, safety, and efficacy of Paxlovid treatment in SARS-CoV-2-infected children aged 6-14 years: a cohort study. *Ann Transl Med* 2022;**10**(11):619. doi:10.21037/atm-22-2791.

Qian Zheng, Pengfei Ma
Department of Neurology, Affiliated Hospital of Guizhou Medical University, Guiyang, China

Mingwei Wang
Department of Cardiology, Affiliated Hospital of Hangzhou Normal University, Hangzhou, China

Yongran Cheng
School of Public Health, Hangzhou Medical College, Hangzhou, China

Mengyun Zhou
Shinshu University School of Medicine, Matsumoto, Japan

Lan Ye
Engineering Research Center for Molecular Medicine, School of Basic Medical Science, Guizhou Medical University, Guiyang, China

Zhanhui Feng*
Department of Neurology, Affiliated Hospital of Guizhou Medical University, Guiyang, China

Chunlin Zhang**
Engineering Research Center for Molecular Medicine, School of Basic Medical Science, Guizhou Medical University, Guiyang, China

*Correspondence: Zhan-Hui Feng, Department of Neurology, Affiliated Hospital of Guizhou Medical University, Guiyang, China.
**Chunlin Zhang, Engineering Research Center for Molecular Medicine, School of Basic Medical Science, Guizhou Medical University, Guiyang, China.
E-mail addresses: h9450203@126.com (Z. Feng), zcl@gmc.edu.cn (C. Zhang)

Accepted 26 September 2022
Available online 30 September 2022

https://doi.org/10.1016/j.jinf.2022.09.027

Resurgence of influenza virus activity during COVID-19 pandemic in Shanghai, China

Dear Editor,

Recent study by Han et al., reported the dramatic impact of nonpharmaceutical interventions (NPIs) introduced during the coronavirus disease 2019 (COVID-19) pandemic on influenza and other common respiratory virus detections among children in Hangzhou, China.[1] Their results demonstrated that the influenza virus activity had apparent seasonality before COVID-19 pandemic, while it was suppressed and the seasonality was not fully highlighted during COVID-19 pandemic (From February 2020 to October 2021). Besides, a study conducted in Singapore also reported that although rhinoviruses, parainfluenza, respiratory syncytial viruses and other common respiratory viruses have returned, the activity of influenza remains absent in circulation during COVID-19 pandemic.[2] Herein, we presented a resurgence of influenza virus activity among children during COVID-19 pandemic in Shanghai, China.

In this cross-sectional study, pediatric patients with respiratory disease symptoms (fever, cough, rhinitis, sore throat or myalgia) in the outpatient clinic at Children's Hospital of Fudan University from Jan 1, 2014 to Aug 31, 2022 were enrolled. Nasopharyngeal swabs were collected from all enrolled outpatients and tested by chromatographic immunoassay for influenza A/B virus (Standard Diagnostics, Yongin, Republic of Korea). Time series models of seasonal autoregressive integrated moving average (SARIMA) were trained using data from Jan 2014 to Jan 2020 (pre-COVID-19) to forecast the monthly positive rates of influenza A/B virus from February 2020 to August 2022 (COVID-19 pandemic). Goodness-of-fit tests of models were performed by comparing Akaike's information criterion (AIC) and Schwarz Bayesian Criterion (SBC). Smaller AIC and SBC indicate the better fitting model.[3] For comparisons between different periods, Chi-squared test was used for categorical data and Mann-Whitney U test for numeric data.

A total of 452,552 patients were enrolled in the study, including 328,220 (72.5%) patients in the pre-COVID-19 period and 124,332 (27.5%) patients in the COVID-19 pandemic period. The median age of patients in the pandemic period (6 years) was older than in the

Table 1
Comparison of demographics and positive rates (%) of influenza viruses between pre-COVID-19 and COVID-19 pandemic.

	Whole study period*	pre-COVID-19*	COVID-19 pandemic*	*P* value#
Demographics				
Total patients	452,552	328,220	124,332	
Male sex, n (%)	244,946 (54.1)	177,467 (54.1)	67,479 (54.3)	0.221
Age, median	5y (16m-9y)	4y (7m-8y)	6y (3m-10y)	<0.001
Virus detections, n (%)				
Influenza A	42,293 (9.3)	39,950 (12.2)	2343 (1.9)	<0.001
Influenza B	32,634 (7.2)	26,519 (8.1)	6115 (5.9)	<0.001
Total	74,927 (16.6)	66,469 (20.3)	8458 (6.8)	<0.001

* Whole study period: Jan 1, 2014 to Aug 31, 2022; pre-COVID-19: Jan 1, 2014 to Jan 31, 2020; COVID-19 pandemic: Feb 1, 2020 to Aug 31, 2022.
# Comparison between pre-COVID-19 and COVID-19 pandemic;Abbreviations: y, years; m, months.

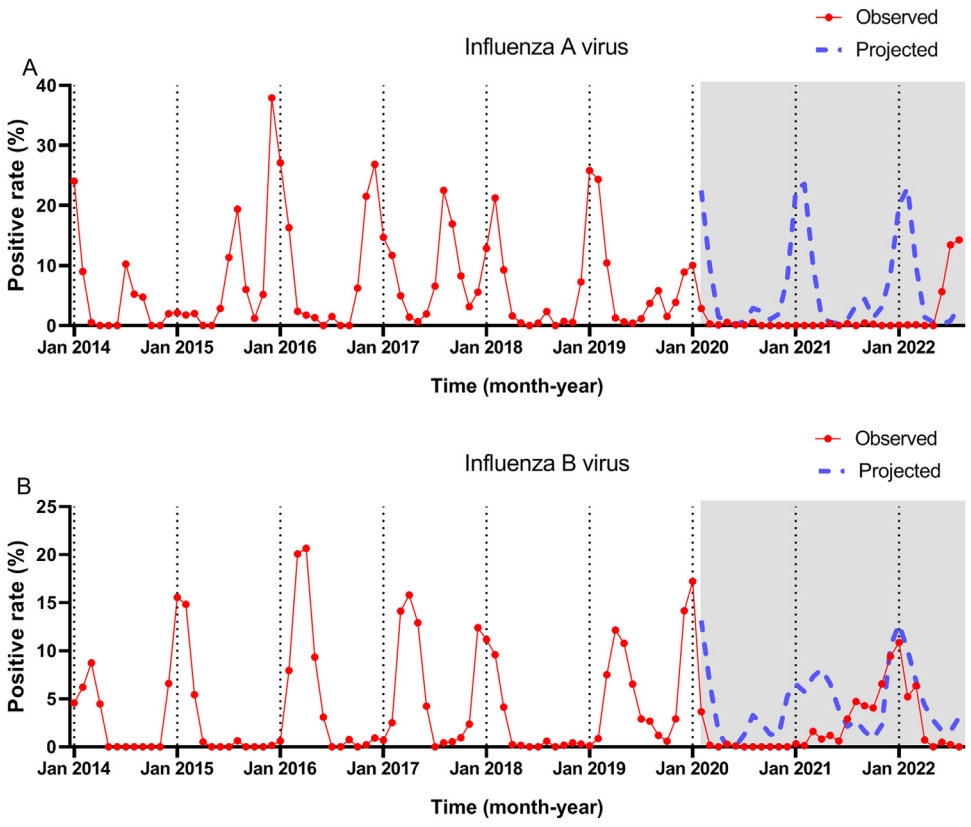

Fig. 1. *Observed and model-fitted time series of monthly influenza activity between Jan, 2014 and Aug, 2022.* (A) influenza A virus; (B) influenza B virus. Hypothetical positive rates during Feb, 2020-Agu, 2022 (blue) in the absence of NPIs was projected using the SARIMA model based on Jan 2014-Jan 2020. Gray block represents the period of the "COVID-19 pandemic" when NPIs were implemented. NPIs, nonpharmaceutical interventions; SARIMA, seasonal autoregressive integrated moving average.

pre-pandemic period (4 years), and no qualitative difference was found between the two sexes (Table 1). A significant decline in influenza A/B activity was observed in the pandemic period compared to the pre-COVID-19 period from a positive rate of 20.3 to 6.8% (Table 1). The usual bimodal peaks of influenza A activity, in summer (June to August) and winter (December to February) were present in the pre-COVID-19 period. However, the seasonality of influenza A was interrupted after the introduction of tight nationwide NPIs in February 2020. The peaks disappeared completely in the year of 2020 and 2021. Whereas, a resurgence of influenza A activity was observed in the summer of 2022, and the actual activity significantly exceeded model-projected levels in the hypothetical scenario without COVID-19 related NPIs (Fig. 1A).

The annual peak of influenza B activity occurred in winter or early spring (January to March) in the pre-COVID-19 period and it was also flattened or suppressed after the implementation of NPIs. However, the resurgence of influenza B was earlier than influenza A. The activity increased from July 2021 and peaked in January 2022, which was almost in agreement with the model-projected seasonality (Fig. 1B).

Early studies conducted in both Southern Hemisphere and Northern Hemisphere reported that influenza seasons were entirely suppressed during the COVID-19 pandemic.[4–6] Likewise, the activity of influenza declined sharply and was reduced to near zero during the early stage of pandemic in our study. Influenza virus can be transmitted by contact, droplet, or aerosol.[7] Leung et al. reported that surgical face masks significantly reduced the detection of influenza virus RNA in respiratory droplets, indicating that surgical face masks could prevent the transmission of influenza viruses from symptomatic individuals.[8] These results demonstrated that

the current NPIs, including international mobility restriction and mask-wearing, social distancing, increased hand hygiene, could be highly effective against influenza activity. This positive effect in the short term is welcome. However, the lack of immune stimulation due to the reduced circulation of influenza and the related reduced vaccine uptake may induce an "immunity debt" which could have negative consequences and may render the population more vulnerable in the following season.[9] Unsurprisingly, after a relative absence during the pandemic period, a large resurgence of influenza activity was observed in July 2021 for influenza B and June 2022 for influenza A in Shanghai, China. These findings raise concerns for influenza control. The eventual cancelation of COVID-19 related NPIs may herald a more significant rise in influenza activity. Vaccination is one of the most effective measures in influenza control. Identifying and developing universal vaccines, as well as increasing the vaccination coverage are of primary importance after influenza's long-term absence. Additionally, further studies are still needed to better understand the circulation patterns change of influenza viruses during COVID-19 pandemic in the different stages and regions.

Funding

This study was funded by Key Development Program of Children's Hospital of Fudan University (No: EK2022ZX05).

Declaration of Competing Interest

All authors claim no conflict of interest.

References

1. Han X., Xu P., Wang H., Mao J., Ye Q.. Incident changes in the prevalence of respiratory virus among children during COVID-19 pandemic in Hangzhou, China. *J Infect* 2022;**84**(4):579–613.
2. Chan H.C., Tambyah P.A., Tee N., Somani J.. Return of other respiratory viruses despite the disappearance of influenza during COVID-19 control measures in Singapore. *J Clin Virol* 2021;**144**:104992.
3. Benvenuto D., Giovanetti M., Vassallo L., Angeletti S., Ciccozzi M.. Application of the ARIMA model on the COVID-2019 epidemic dataset. *Data Brief* 2020;**29**:105340.
4. Olsen S.J., Azziz-Baumgartner E., Budd A.P., et al. Decreased influenza activity during the COVID-19 pandemic-United States, Australia, Chile, and South Africa, 2020. *Am J Transplant* 2020;**20**(12):3681–5.
5. Sohn S., Hong K., Chun B.C.. Decreased seasonal influenza during the COVID-19 pandemic in temperate countries. *Travel Med Infect Dis* 2021;**41**:102057.
6. Lagace-Wiens P., Sevenhuysen C., Lee L., Nwosu A., Smith T.. Impact of non-pharmaceutical interventions on laboratory detections of influenza A and B in Canada. *Can Commun Dis Rep* 2021;**47**(3):142–8.
7. Brankston G., Gitterman L., Hirji Z., Lemieux C., Gardam M.. Transmission of influenza A in human beings. *Lancet Infect Dis* 2007;**7**(4):257–65.
8. Leung N., Chu D., Shiu E., et al. Respiratory virus shedding in exhaled breath and efficacy of face masks. *Nat Med* 2020;**26**(5):676–80.
9. Cohen R., Ashman M., Taha M.K., et al. Pediatric Infectious Disease Group (GPIP) position paper on the immune debt of the COVID-19 pandemic in childhood, how can we fill the immunity gap? *Infect Dis Now* 2021;**51**(5):418–23.

Pengcheng Liu
Department of Clinical Laboratory, Children's Hospital of Fudan University, National Children's Medical Center, Shanghai 201102, China

Jin Xu*
Department of Clinical Laboratory, Children's Hospital of Fudan University, National Children's Medical Center, Shanghai 201102, China
Shanghai Institute of Infectious Disease and Biosecurity, Fudan University, Shanghai, China

*Corresponding author at: Department of Clinical Laboratory, Children's Hospital of Fudan University, 399 Wanyuan Rd, Minhang District, Shanghai 201102, China.
E-mail address: jinxu_125@163.com (J. Xu)

Accepted 24 September 2022
Available online 30 September 2022

https://doi.org/10.1016/j.jinf.2022.09.025

Genome characterization of monkeypox cases detected in India: Identification of three sub clusters among A.2 lineage

Dear Editor,

In this journal, Jolly and Scaria, reported distinct phylogenetic cluster of monkeypox virus (MPXV) genomes suggesting an early spread of virus.[1] Since May 2022, monkeypox cases have been reported in more than 102 countries indicating expansion of its geographic range. Recent studies have also reported microevolution of MPXV genome of 2022 outbreak compared to earlier outbreaks.[2–5] Here, we report the complete genome analysis of monkeypox cases detected in India.

The clinical specimens i.e., orophryngeal swab, nasopharyngeal swab, lesion crust and lesion fluids of 96 suspected Monkeypox cases were referred to ICMR-National Institute of Virology, Pune, India for diagnosis of Monkeypox. Of all the cases, MPXV infection was confirmed in ten cases (Kerala=5, Delhi=5) using Monkeypox specific real time PCR. [6] Cases from Delhi had no international travel history; while cases from Kerala had travel history from United Arab Emirates to India.[5] All the cases were immunocompetent with no comorbidities and their clinical presentations are described in supplementary Table 1.

The genomic characterization of these MPXV positive samples were carried out using next generation sequencing.[7] The Maximum-Likelihood phylogenetic tree analysis placed ten genome sequences (Retrieval 90 to 99%) from India (highlighted in blue) and eight genomes from USA ($n = 3$), UK ($n = 2$) and Thailand ($n = 3$) under lineage A.2 of clade IIb (Fig. 1). Further, they diverge into three sub clusters of A.2 lineage consist of total eighteen sequences. The seven sequences (Kerala $n = 5$, Delhi $n = 2$) grouped into sub cluster I showing highest similarity with MPXV_USA_2022_FL001. In this sub cluster, five sequences from Kerala were designated as A.2.1 based on the lineage defining mutations in the position C 25072 T, A 140492 C, C 179537 T. Two sequences from Delhi are lacking these three mutations hence still defined into A.2 lineage. These mutations were also lacking in the 3 sequences of Delhi from sub cluster II which aligned with sequences of lineage A.2 reported from USA 2022 (USA_2022_VA001). Apparently, Delhi MPXV sequences in sub cluster I and II are showing divergence which needs to be further explored.

The sub cluster III has monkeypox sequences reported from UK, Thailand during current outbreak of 2022 and USA during 2021. These sequences have many shared mutations that separated them from other two sub cluster including India (A.2) and travel-associated cases from 2017 to 2021 of other lineages (A, A.1, A.1.1). The A.2 lineage MPXV sequences from India showed a divergence from the MPXV sequences reported from Germany, Italy, Portugal, Switzerland and France (lineage B.1) and earlier outbreak sequences from Nigeria, Israel and Singapore 2017/18 (lineage A.1). The findings of our study are in concordance with the recent study

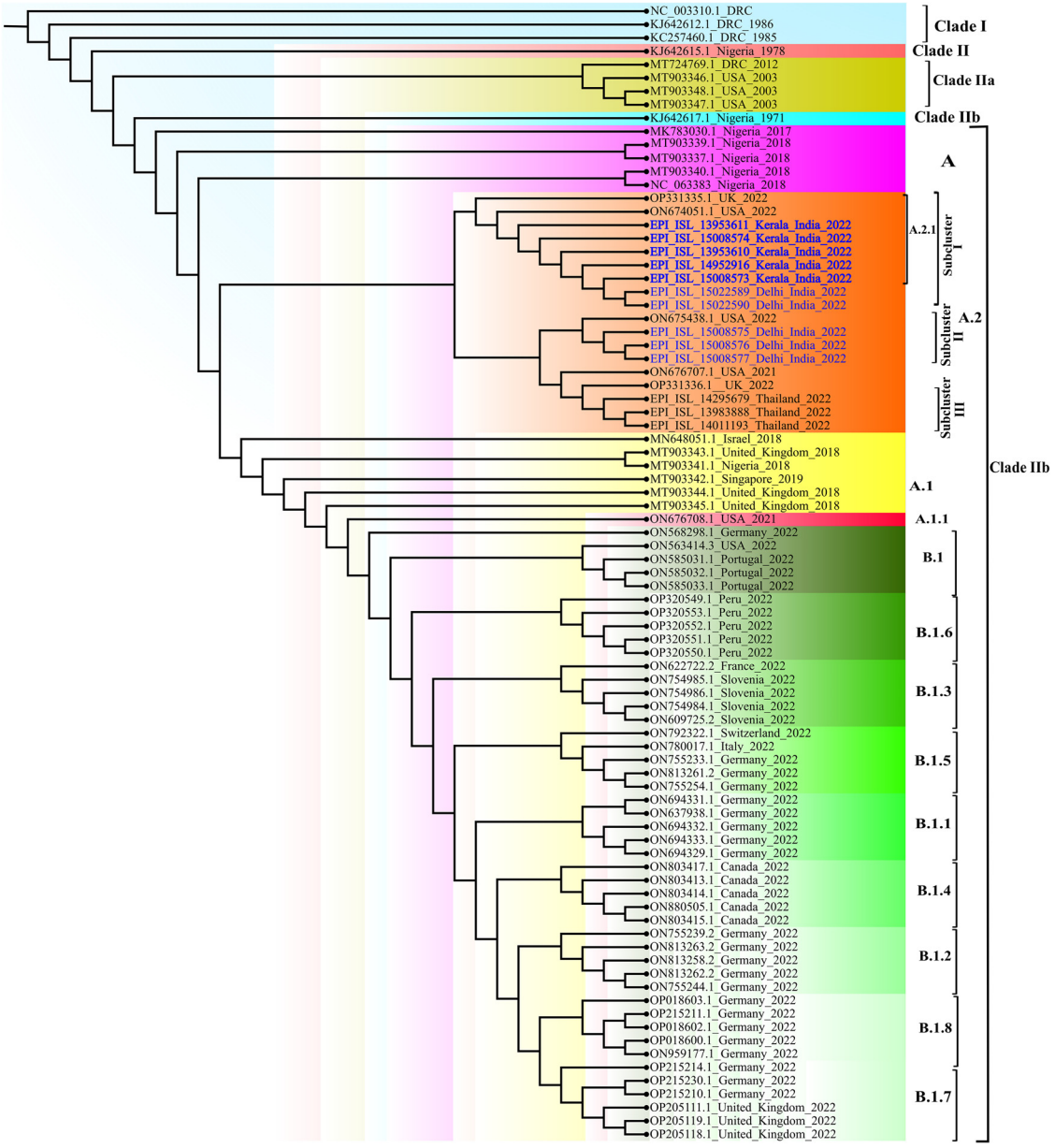

Fig. 1. The maximum-likelihood phylogenetic tree of MPxV/hMPxV genome constructed using software IQ TREE with 1000 ultra bootstrap replication cycle. The retrieved sequences from ten monkeypox cases from India belong to A.2 lineage of Clade IIb (Highlighted in red color).

of Gigante et al, which reported the circulation of both A.2 and B.1 lineages in current outbreak in USA with similarity to MPXV sequences of traveler from Nigeria to Texas in 2021.[3]

Analysis of Clusters of Orthologous Genes for orthopox viruses (OPG) revealed that the sub cluster I of seven sequences from India showed 07 synonymous mutations (OPG055, OPG071, OPG074, OPG093, OPG124, OPG163, OPG187) and 11 non-synonymous mutations (OPG040, OPG062, OPG063, OPG069, OPG074, OPG116, OPG160 and OPG208). Sub cluster II included three sequences from India which indicated 04 non synonymous mutations (OPG025, OPG082, OPG084, OPG099) and 08 synonymous mutations (OPG037, OPG038, OPG105, OPG111, and OPG135). Mapping the A.2 sequences with the reference genome (NC_063383 strain) indicated total fifteen mutations (OPG031, OPG047, OPG053, OPG103, OPG113, OPG145, OPG174, OPG176, OPG180, OPG188, OPG190 and OPG205) which were common throughout all the three sub clusters of the A.2 lineage (Fig. 2A). We have also noted a seven-nucleotide deletion in all three A.2 sub clusters in OPG 174 gene. It is known to play role in influencing virulence by suppressing immune system; further studies are needed to determine the impact of this deletion on virulence of A.2 lineage.

We have also observed single nucleotide polymorphisms (SNPs) specific to sub cluster III compared to reference (NC 063383.1) which were not found in the sequences of sub cluster I and II. There were total 27 non synonymous changes observed in Thailand sequences.

APOBEC 3 mutation analysis indicated presence of 13 mutations in A.2 sequences from the current MPXV outbreak 2022. These could be A.2 lineage defining mutations apart from OPG053; C 34472 T reported during earlier studies (https://master.clades.nextstrain.org) (Fig. 2B). Further, we identified 25 additional APOBEC 3 mutations from the MPXV strain circulating in India. Besides this, 21 synonymous and non-synonymous APOBEC-3 mutations were also noted in sub cluster

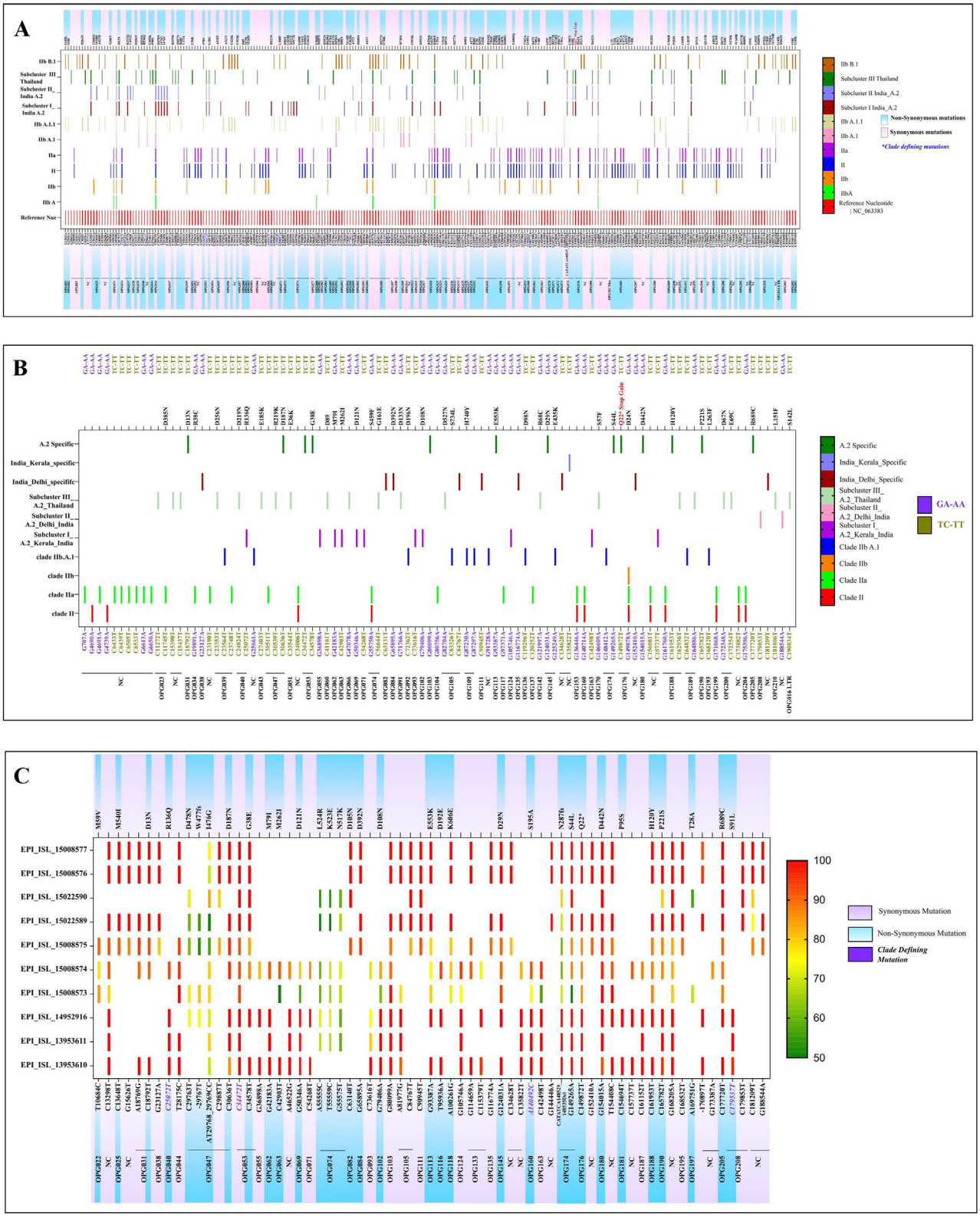

Fig. 2. (A) The variant analysis of MPXV genome was done using software MEGA 10 w.r.t reference sequence NC_063383. The depicted figure showed the synonymous and non-synonymous mutations in Clade II and lineages. The A.2 lineage is further characterized into sub-cluster I, II and III. All the clade defining mutations are marked with blue color positions. (B) The APOBEC 3 mutation analysis was done using software MEGA 10.0. The mutations (GA-AA, TC-TT) were marked for all the clades. (C) The variant analysis of MPXV genome of all the retrieved sequences was done using CLC genomics workbench with 50% frequency. The reference positions marked with synonymous and non-synonymous mutations for all the sequences with the respective frequencies.

III. Recently O'Toole and Rambaut reported that the APOBEC3 with cytidine deaminase activity could be significant factor in the short-term evolution of MPXV since 2017.[8] Our APOBEC3 mutation analysis supported a strong inclination for GA to AA and TC to TT mutations, indicating cytosine deaminase functioning reported only in Clade II since 2017 and not in Clade I.[4] A recent study Isidro et al. also demonstrated microevolution and divergence of MPXV sequences of 2022 outbreak pertaining to APOBEC3 and other proteins.[2]

Variant analysis of all sequences of A.2 lineage indicated a total of 34/67 synonymous mutations and 33/67 non synonymous mutations. Fourteen mutations are found in the non coding region and 53 mutations were observed in coding region of different ORFs. Most of the mutations are observed in gene OPG 047 which is closer to the middle of the genome followed by OPF 053, OPG 074 and OPG 105. Earlier reported clade defining mutation was observed (C 34472 T) in all the retrieved sequences from India. During complete genome analysis, we have observed insertions; one in OPG 047 (insertion of T at 29767), and other in non coding region (insertion of T at 170897). A deletion of CATATCA was also noted at 148529- 148535 in gene OPG 174 [9] (Fig. 2C).

Interestingly, one di-nucleotide substitution of AT-CC in OPG 047 at position 29768 leading to amino acid change (I 476 G) was observed in the retrieved sequences of ten monkeypox cases. Of 67, a total 63 substitution mutations were observed in cluster from India in which 58 are transitions and 05 are transversion (Non synonymous 30 and synonymous 33). One substitution mutation which led to stop gain at position 149872 was also recorded in gene OPG 176. No mutations were noted on H3L (OPG 108), glycosil transferase which plays important role in pox virus entry into host cell. We have also observed four non synonymous and two synonymous SNPs in OPG 31 and OPG 174 genes that are predicted to modulate the host immune response.

The 2022 Monkeypox outbreak demonstrates accelerated microevolution of MPXV leading to divergence in viral phylogeny.[2–5] Gigante et al., demonstrated 80 nucleotide changes in lineage A.2 compared to the B.1 lineage which has been predominant lineage of 2022 suggesting an independent virus strain emergence.[3] The genomic research on the 2022 MPXV outbreak has also grabbed attention depicting divergence of lineage B.1 from lineage A.1 of 2018–2019 outbreaks.[2] Hence, genome evolution mechanisms and importance of gene functions needs to be studied further to understand evolution of the MPXV genome. As B.1 is found to be the predominant lineage of 2022 Monkeypox outbreak globally, the introduction event of A.2 lineage specifically in the USA, UK, India and Thailand is the question of further exploration.

Ethical approval

The study was approved by the Institutional Human Ethics Committee of ICMR-NIV, Pune, India under the project 'Providing diagnostic support for referred samples of viral hemorrhagic fever and other unknown etiology and outbreak investigation'. The clinical data collected were anonymized. The informed consents were obtained for the use of the clinical details in the study.

Financial support & sponsorship

The intramural grant was provided from ICMR-National Institute of Virology, Pune for conducting this study.

Supplementary information

Supplementary Table-1. Clinico-demographic, viral load and outcome of ten monkey pox cases from India, July-August 2022

Declaration of Competing Interest

Authors do not have a conflict of interest among themselves.

Acknowledgement

Authors extend gratitude to Smt. Veena George [Hon'ble Minister for Health and Family Welfare, Kerala], for efficient coordination of the monkeypox virus disease control activities, and "The Team Kerala Health," the district administration. We would also extend our gratitude towards Dr. Asha Thomas, Additional Chief secretary of Medical Education, Mrs. Tinku Biswal, Principal Secretary for Health Kerala, Dr. Thomas Mathew, Director of Medical Education and Dr. Preetha PP, Director of Health Services, Kerala. The authors would like to thank Dr. Lakshmi Geetha Gopalkrishnan, State Epidemiologist, and District Surveillance Officers of Thiruvananthapuram [Dr. Preethi James], Kannur [Dr. Shaj MK], Kollam [Dr. Sandhya], and Thrissur [Dr. Anoop TK and Dr. Kavya Karunakaran]. Dr. Kala Kesavan P, Principal; Dr. Nizarudeen A, Medical superintendent; Dr. Aravind Reghukumar, HOD Infectious Diseases and Dr. Manjusree Suresh, from Government Medical College Thiruvananthapuram. The authors are thankful to Dr. Prathap Somanath, Principal, Dr. Sudeep, HOD Infectious Diseases; Dr. Manasi Ravindranath from Government Medical College Kannur; Dr. Shinas, Government Medical College, Manjeri. The authors also acknowledge the support from Dr. Fazil Abubaker from Daya General Hospital and Specialty Surgical Centre, Thrissur.

Authors extend sincere thanks to Dr. Bijayalaxmi Sahoo, Professor and Head, and resident doctors Dr. Abhinav Kumar, Dr. Aneet Kaur, Dr. Bhawna Solanki, Dr. Anjali Bagrodia of Dermatology; Dr. Sonal Saxena, Professor, and Head, Department of Microbiology from Maulana Azad Medical College and Lok Nayak Hospital, New Delhi for providing support for sample collection and transportation. We are also grateful to Dr. Lalit Dar, Professor, Department of Microbiology; Dr. Aashish Choudhary, Dr. Megha Brijwal, from All India Institute of Medical Sciences, New Delhi. The authors are thankful to Dr. Avdesh Kumar, State Surveillance Officer, New Delhi and his team for coordination. The authors are extremely grateful to Dr. Nivedita Gupta, Scientist 'F' and Head, Epidemiology and Communicable Diseases, ICMR, New Delhi for her constant support.

We also acknowledge the excellent technical support from Dr. Kannan Sabarinath PS, Dr. Rajlaxmi Jain, Ms. Jyoti Yemul, Mr. Sunil Shelkande, Ms. Pratiksha Vedhpathak, Mrs. Shubhangi Sathe, Ms. Vaishnavi Kumari, Ms. Nandini Shende, Mr. Raj Hawale for the diagnosis and data management for the diagnosis and data management. The authors also would like to thank and express immense gratitude to the monkeypox cases and family members, who willingly agreed and provided consent to be part of the study.

Supplementary materials

Supplementary material associated with this article can be found, in the online version, at doi:10.1016/j.jinf.2022.09.024.

References

1. Jolly B., Scaria V.. A distinct phylogenetic cluster of Monkeypox genomes suggests an early and cryptic spread of the virus. *J Infect* 2022 Aug 19.
2. Isidro J., Borges V., Pinto M., Sobra D., Santos J.D, Nunes A., et al. Phylogenomic characterization and signs of microevolution in the 2022 multi-country outbreak of monkeypox virus. *Nat Med* 2022:1–4 Jun 24.
3. Gigante C.M., Korber B., Seabolt M.H., Wilkins K., Davidson W., Rao A.K., et al. Multiple lineages of Monkeypox virus detected in the United States, 2021-2022. *BioRxiv* 2022 Jan 1.
4. O'Toole A., Rambaut A.. *Initial observations about putative APOBEC3 deaminase editing driving short-term evolution of MPXV since 2017*. ARTIC Network; 2022.
5. Yadav P.D., Reghukumar A., Sahay R.R., Sudeep K., Shete A.M, Raman A., et al. First two cases of Monkeypox virus infection in travellers returned from UAE to India, July 2022. *J Infect* 2022;**S0163-4453**(22):00471–6.

6. Li Y., Olson V.A., Laue T., Laker M.T., Damon I.K.. Detection of monkeypox virus with real-time PCR assays. *J Clin Virol* 2006;**36**(3):194–203.
7. Yadav P.D., Nyayanit D.A., Shete A.M., Jain S., Majumdar T., Chaubal G.Y, et al. Complete genome sequencing of Kaisodi virus isolated from ticks in India belonging to *Phlebovirus* genus, family *Phenuiviridae*. *Ticks Tick-Borne Dis* 2019;**10**(1):23–33.
8. Senkevich T.G., Yutin N., Wolf Y.I., Koonin E.V, Moss B.. Ancient gene capture and recent gene loss shape the evolution of orthopoxvirus-host interaction genes. *Mbio* 2021;**12**(4) e01495-21.
9. Nguyen L.T., Schmidt H.A., Von Haeseler A., Minh B.Q. IQ-TREE: a fast and effective stochastic algorithm for estimating maximum-likelihood phylogenies. *Mol Biol Evolut* 2015;**32**(1):268–74.

Anita M. Shete[1], Pragya D. Yadav[1]*, Abhinendra Kumar, Savita Patil, Deepak Y. Patil, Yash Joshi, Triparna Majumdar
Maximum Containment Facility, National Institute of Virology, Indian Council of Medical Research-National Institute of Virology, Sus Road, Pashan, Pune, Maharashtra 411021, India

Vineet Relhan
Maulana Azad Medical College and Lok Nayak Hospital, New Delhi 110002, India

Rima R. Sahay
Maximum Containment Facility, National Institute of Virology, Indian Council of Medical Research-National Institute of Virology, Sus Road, Pashan, Pune, Maharashtra 411021, India

Meenakshy Vasu
Public Health Department of Kerala, Directorate of Health Services, Thiruvananthapuram 695035, India

Pranita Gawande, Ajay Verma
Maximum Containment Facility, National Institute of Virology, Indian Council of Medical Research-National Institute of Virology, Sus Road, Pashan, Pune, Maharashtra 411021, India

Arbind Kumar, Shivram Dhakad
All India Institute of Medical Sciences, New Delhi 110029, India

Anukumar Bala Krishnan
Indian Council of Medical Research-National Institute of Virology, Alappuzha, Kerala 688005, India

Shubin Chenayil
State Surveillance Unit (IDSP), Directorate of Health Services (IDSP), Malappuram, Kerala 688005, India

Suresh Kumar
Maulana Azad Medical College and Lok Nayak Hospital, New Delhi 110002, India

Priya Abraham
Maximum Containment Facility, National Institute of Virology, Indian Council of Medical Research-National Institute of Virology, Sus Road, Pashan, Pune, Maharashtra 411021, India

*Corresponding author.
E-mail address: hellopragya22@gmail.com (P.D. Yadav)

[1] These authors contributed equally to this work and are first authors

Accepted 22 September 2022
Available online 28 September 2022

https://doi.org/10.1016/j.jinf.2022.09.024

Genetic characterization of a novel quadruple reassortant influenza A (H1N2) virus from swine, China, 2021

Dear Editor,

We read with interest a recent letter in the Journal of Infection, which reported the emergence of novel H5N6 reassortant and it's threat to both birds and humans.[1] Pigs are susceptible to human, swine, and avian influenza A viruses (IAVs) and considered as intermediate hosts or "mixing vessels" for generating novel viruses with pandemic potential.[2] Moreover, China has a complicated ecosystem of swine influenza viruses (SIVs) in which H1N1, H1N2, and H3N2 subtypes with classical swine (CS), North America triple-reassortant (TR), Eurasian avian-like (EA), and H1N1 pandemic/2009 (pdm/09) lineages are co-circulating throughout the swine population. This co-circulation has led to frequent emergence of novel reassortments or genotypes.[3] In this study, we report a novel influenza virus A(H1N2) virus, A/swine/Henan/417/2021(H1N2) (HN/21) that was isolated from a swine farm in December 12, 2021 in Henan, China.

We collected 168 nasal swab samples from pigs for swine influenza surveillance from November 2021 to December 2021. For virus isolation, nasal swabs were taken and placed in spread medium (50% glycerol in phosphate-buffered saline [PBS] vol/vol) containing antibiotics. All samples were individually inoculated into Madin-Darby canine kidney (MDCK) cells for virus isolation. The total RNA was extracted according to the instruction of the RNAfast200 purification kit (Fastagen Biotech, Shanghai, China). Polymerase chain reaction (PCR) was conducted using Uni12 and universal primers for influenza viruses.[4] The PCR products were recovered and cloned into the pMD-19T vector (Takara Bio Inc., Beijing, China) for sequencing. Sequencing data were spliced using the Seqman program of Lasergene (Version 7.1). GISAID accession numbers were assigned to the gene sequences of the analysed virus: 1) polymerase basic 2 (PB2) (EPI2129631), 2) polymerase basic 1 (PB1) (EPI2129632), 3) polymerase acid (PA) (EPI2129633), 4) hemagglutinin (HA) (EPI2129634), 5) nucleoprotein (NP) (EPI2129637), 6) neuraminidase (NA) (EPI2129636), 7) matrix protein (M) (EPI2129635), and 8) nonstructural protein (NS) (EPI2129638).

The homology was analysed by comparison with the sequences available in GenBank (http://www.ncbi.nlm.nih.gov/). At the nucleotide level, the PB2, PB1, NP, and NA genes of HN/21 showed high similarity to A/Guangdong/YueFang277/2017(H3N2), which caused human infection with 99.80%, 99.87%, 99.93%, and 99.78% agreement, respectively as shown in Supplementary Table S1.[5] All coding regions of all HN/21's segments were obtained based on the G + C content from 41.84% to 46.64%. It is noteworthy that all H1N2 SIVs contained at least 1 of 4 amino acid mutations (158E, 190D, 225E, and 226Q) in HA gene and 1 of 6 amino acid mutations (251K, 271A, 431T, 591R, 627K, and 701N) in the PB2 gene, which were associated with increasing viral mammalian-adapting, replication, and pathogenicity (Supplementary Table S2).

Sequence alignments were constructed separately for eight segments using the MAFFT (version 7.149) program.[6] Phylogenetic trees were inferred using the maximum likelihood method in the IQ-TREE 1.68 software with 1,000 bootstraps.[7] Phylogenetic analyses of the eight genes of H1N2 SIVs revealed that the HA, NA, PB2, PB1, PA, NP, M, and NS genes were classified into four (Supplementary Fig. 1A), four (Supplementary Fig. 1B), six (Supplementary Fig. 1C), six (Supplementary Fig. 1D), six (Supplementary Fig. 1E), six (Supplementary Fig. 1F), seven (Supplementary Fig. 1G), and six (Supplementary Fig. 1H) separate lineages, respectively.

To reveal H1N2's evolutionary characteristics, we conducted molecular clock phylogenetic analysis and genotype characterisation (Fig. 1). We computed marginal likelihoods using path

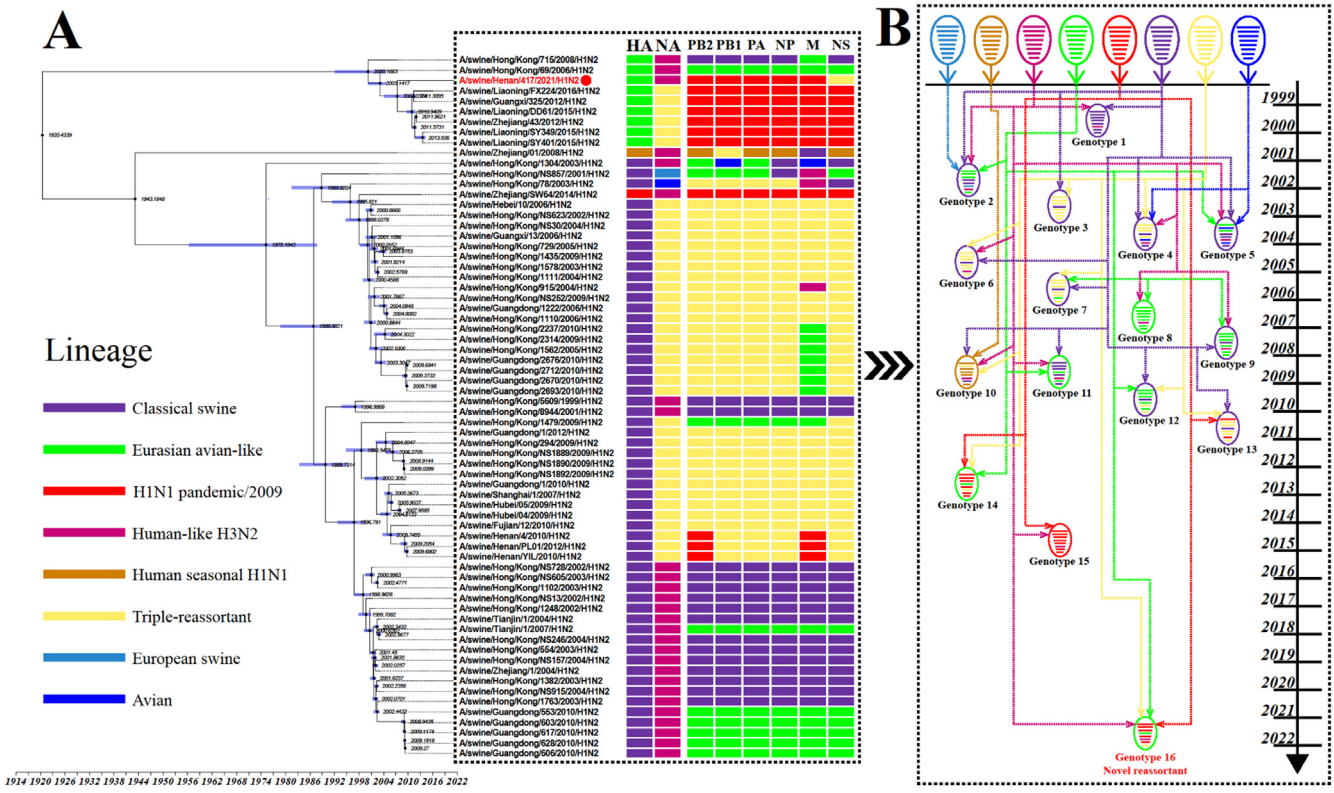

Fig. 1. Molecular clock phylogenetic analysis of SIVs in China. (A) The phylogenetic tree of HA gene using BEAST (version 1.10.4) under the Exponential coalescent tree prior model, "GTR+F+G4" substitution mode, and a "uncorrelated relaxed clock" model. The IAVs sequenced in this study were marked with red dots. The lineages of SIVs genes were marked by colored boxes. Purple node bars represented 95% credible intervals of lineage divergence times. (B) Diagrammatic representation of the detection of different H1N2 reassortants. Viral particles are represented by coloured ovals containing horizontal bars representing the 8 gene segments (from top to bottom: PB2, PB1, PA, HA, NP, NA, M, and NS). Fragments in the descendant viruses are colored according to their corresponding source viruses (top) to account for genetic ancestry through reassortment events. Possible donor viruses are adjacent to arrow tails; arrowheads point to the resulting reassortants. The timeline on the right indicates the year in which the novel recombinant was detected. Different colours represent different lineages. Detailed genotypes are available as the Supporting Information Table S1.

sampling and stepping-stone sampling to compare the constant-size, exponential-growth, and Bayesian skyline coalescent tree priors and to compare the strict molecular clock and uncorrelated lognormal relaxed clock.[8] The best-fit model was chosen to construct maximum clade credibility (MCC) trees using 200,000,000 total steps for each set with sampling every 1,000 steps (Supplementary Table S3). The convergence (effective sample sizes > 200) of relevant parameters was assessed using Tracer version1.7.[9] Based on genomic diversity, China's H1N2 SIVs were classified into sixteen different genotypes (G1–G16) from 1999 to 2021 with nine reassortants of the CS lineage, five reassortants of the EA lineage, one reassortant of the pdm/09 lineage, and one reassortant of human seasonal influenza lineage. HN/21 classified into genotype 16 is a novel quadruple reassortant-derived HA gene from the EA lineage, the NA gene from human-like H3N2 lineage, the NS gene from TR lineage. and the PB2, PB1, PA, and M genes from pdm/09 lineage (Fig. 1).

N-linked glycosylation (abbreviates G) of HA and NA, which add oligosaccharides to Asn-residue by N-glycosidic linkages, plays an important role in multiple biological activities of IAV. According to the consensus N-X-S/T (X can be any amino acid except proline) glycosylation motif, HN/21 had six (28G+, 40G +, 291G+, 498G+, 502G+, and 557G+) and three (66G+, 82G+, and 142G+) N-linked glycosylation sites on HA (Fig. 2C) and NA (Fig. 2D), respectively. In contrast, the phenotype of genotype 15 was 104G+/291G−/313G+/502G− and 230+ on HA and NA genes, respectively. Our results suggested there are variations in the glycosylation sites at the residues 104, 291, 313, and 551 of HA gene and 230 of NA gene during the evolution of H1N2 SIVs. The HN/21 lost a glycosylation site at residue 230 of NA. Remarkably, glycosylation at the residue 230 of NA was absent in the H1N1 pandemic/2009 virus and was suggested as a pandemic associated signature (Supplementary Table 2). The 230 G shift in the glycosylation site of NA could serve as a potential characteristic of the pandemic.

To further detect the replication ability of HN/21 *in vitro*, the growth curves were measured in MDCK, A549, and 3D4/21 cells. It was found that HN/21 virus efficiently replicated in MDCK, A549, and 3D4/21 cells. In MDCK, A549, and 3D4/21 of HN/21, viral titres peaked at 72, 60, and 24 hpi with titres of 7.8, 3.5, and 3.85 lgTCID$_{50}$/mL, respectively (Supplementary Fig. 2). Thus, this novel reassortant poses the potential to infect human, as was observed human cases infection with EA lineage SIVs.[10] Our results demonstrate that emerging reassortants have the potential risk for adaptation to humans or mammals, thus necessitating continuous surveillance and development of effective vaccine for SIVs.

Ethics Statement

All sampling procedures were approved by the Animal Ethics Committee of South China Agricultural University and conducted under the guidance of the South China Agricultural University Institutional Animal Care and Use Committee (SCAU-AEC-2021L015).

Author Contribution

Hailiang Sun and Hanlin Liu contributed equally to this work. Hailiang Sun, Ming Liao and Hanlin Liu designed the research; Data collection and paper writing were performed by Hanlin Liu, Zifeng

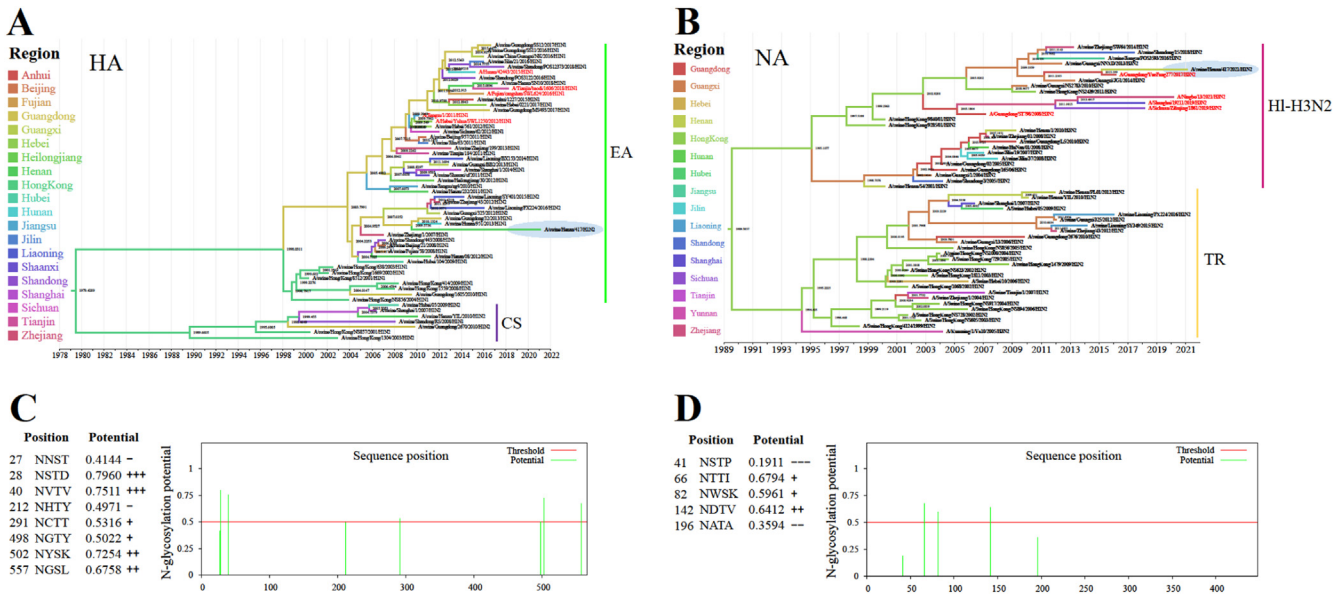

Fig. 2. Phylogenetic and glycosylation analyses of the HA and NA gene sequences from swine influenza viruses. Virus name with red represents human isolates. (A) Phylogenetic tree of HA gene for swine influenza viruses. (B) Phylogenetic tree of NA gene for swine influenza viruses. The light blue oval highlights the novel reassortant isolated in this study. (C) Glycosylation analyses of the HA gene for A/swine/Henan/417/2021. (D) Glycosylation analyses of the NA gene for A/swine/Henan/417/2021. Glycosylation sites were predicted by the consensus N-X-S/T glycosylation motif. The potential of the glycosylation sites was calculated by the NetNGlyc 1.0 Server (http://www.cbs.dtu.dk/services/NetNGlyc/). The reference sequences were retrieved from the GISAID (https://www.gisaid.org). Abbreviation: Classical swine (CS), Eurasian avian-like (EA), Human-like H3N2 (Hl-H3N2), and North America triple-reassortant (TR).

Pang and Yinglin Jiang. Hanlin Liu, Yanwei Liu and Zifeng Pang conducted the phylogenetic and data analysis. Laboratory detection was performed by Yanwei Liu. The final version was approved by all authors.

Declaration of Competing Interest

The authors declare no conflict of interest.

Acknowledgments

This work was supported by special fund for scientific innovation strategy-construction of high level Academy of Agriculture Science-Distinguished Scholar (R2020PY-JC001).

Supplementary materials

Supplementary material associated with this article can be found, in the online version, at doi:10.1016/j.jinf.2022.09.009.

References

1. Sun R, Jiang W, Liu S, Peng C, Yin X, Liu H, et al. Emergence of novel reassortant H5N6 influenza viruses in poultry and humans in Sichuan Province, China, 2021. *J Infect* 2022;**84**(5):e50–ee2 May PubMed PMID:35259421 Epub 2022/03/09. eng.
2. Ma W, Lager KM, Vincent AL, Janke BH, Gramer MR, Richt JA.. The role of swine in the generation of novel Influenza viruses. *Zoonoses Public Health* 2009;**56**(6-7):326–37.
3. Vijaykrishna D, Smith GJ, Pybus OG, Zhu H, Bhatt S, Poon LL, et al. Long-term evolution and transmission dynamics of swine influenza A virus. *Nature* 2011;**473**(7348):519–22 May 26. PubMed PMID:21614079 Epub 2011/05/27. eng.
4. Hoffmann E, Stech J, Guan Y, Webster RG, Perez DR.. Universal primer set for the full-length amplification of all influenza A viruses. *Arch Virol* 2001;**146**(12):2275–89 Dec. PubMed PMID:11811679 Epub 2002/01/29.
5. Lu J, Yi L, Jing Y, Tan H, Mai W, Song Y, et al. A human infection with a novel reassortant H3N2 swine virus in China. *J Infect* 2019;**79**(2):174–87 Aug. PubMed PMID:31051185 Epub 2019/05/06. eng.
6. Katoh K, Standley DM.. MAFFT multiple sequence alignment software version 7: improvements in performance and usability. *Mol Biol Evol* 2013;**30**(4):772–80 Apr. PubMed PMID:23329690 Pubmed Central PMCID: PMC3603318. Epub 2013/01/19.
7. Nguyen LT, Schmidt HA, von Haeseler A, Minh BQ. IQ-TREE: a fast and effective stochastic algorithm for estimating maximum-likelihood phylogenies. *Mol Biol Evol* 2015;**32**(1):268–74 Jan. PubMed PMID:25371430 Pubmed Central PMCID: PMC4271533. Epub 2014/11/06.
8. Baele G, Li WL, Drummond AJ, Suchard MA, Lemey P.. Accurate model selection of relaxed molecular clocks in bayesian phylogenetics. *Mol Biol Evol* 2013;**30**(2):239–43 Feb. PubMed PMID:23090976 Pubmed Central PMCID: PMC3548314. Epub 2012/10/24. eng.
9. Rambaut A, Drummond AJ, Xie D, Baele G, Suchard MA.. Posterior summarization in bayesian phylogenetics using tracer 1.7. *Syst Biol* 2018;**67**(5):901–4 Sep 1. PubMed PMID:29718447 Pubmed Central PMCID: PMC6101584. Epub 2018/05/03. eng.
10. Li X, Guo L, Liu C, Cheng Y, Kong M, Yang L, et al. Human infection with a novel reassortant Eurasian-avian lineage swine H1N1 virus in northern China. *Emerg Microbes Infect* 2019;**8**(1):1535–45 PubMed PMID:31661383 Pubmed Central PMCID: PMC6830285. Epub 2019/10/30. eng.

Hailiang Sun[1], Hanlin Liu[1], Yanwei Liu, Zifeng Pang, Yinglin Jiang
College of Veterinary Medicine, South China Agricultural University, Guangzhou 510642, China
Key Laboratory of Zoonosis Control and Prevention of Guangdong Province, South China Agricultural University, Guangzhou 510642, China
National and Regional Joint Engineering Laboratory for Medicament of Zoonosis Prevention and Control, South China Agricultural University, Guangzhou 510642, China

Quan Liu, Ming Liao*
Institute of Animal Health, Guangdong Academy of Agricultural Sciences, Guangzhou 510640, China
Key Laboratory for Prevention and Control of Avian Influenza and Other Major Poultry Diseases, Ministry of Agriculture and Rural Affairs, Guangzhou 510640, China

*Corresponding author.
E-mail addresses: hsun@scau.edu.cn (H. Sun), liuhanlin0050@163.com (H. Liu), liuyanwei2412@163.com (Y. Liu), pangzf0075@163.com (Z. Pang), a1031411823@163.com (Y. Jiang), liuquan1973@hotmail.com (Q. Liu), mliao@scau.edu.cn (M. Liao)

[1] These authors contributed equally to this work.

Accepted 6 September 2022
Available online 12 September 2022

https://doi.org/10.1016/j.jinf.2022.09.009

Dynamics of immune responses to inactivated COVID-19 vaccination over 8 months in China

Dear Editor,

In this Journal, Lazarus and colleagues recently reported results of a randomized controlled trial of a novel inactivated SARS-CoV-2 vaccine (VLA2001) in healthy adults.[1] They found that the highest dose group showed statistically significantly stronger immunogenicity with similar tolerability and safety. We also investigated dynamics of immune responses to inactivated COVID-19 vaccination over 8 months among healthy adults in China. Studies from Israel, UK, Chile and Denmark on the decay of anti-SARS-CoV-2 antibodies elicited by BNT162b2 (mRNA vaccine) and ChAdOx1-nCoV19 (adenovirus-vectored vaccine) revealed that mRNA vaccines could induce robust antibody response but started a rapid decay shortly after vaccination.[2-5] Modeling of the antibody decay uncovered factors such as age, sex, comorbidity, and the interval between vaccine doses that could influence the dynamics of humoral responses.[3-5] Yet, long-term surveillance study is needed to supplement studies of immune responses for inactivated COVID-19 vaccines.[2,6] In addition, the relationship between humoral and cellular immune responses to inactivated vaccine has been rarely investigated.

We conducted a large-scale longitudinal study with 6646 serum samples from 4359 eligible participants, including many healthcare workers, who received a 2-dose immunization of inactivated SARS-CoV-2 vaccine (BBIBP-CorV or CoronaVac) at Yunnan University Affiliated Hospital (74.4% were female; average age 33±11 years [±SD]) to evaluate immunogenicity kinetics(Fig.S1). We used comprehensive immune indexes including anti-SARS-CoV-2 receptor-binding domain (RBD) IgG, anti-RBD-IgM, neutralizing antibodies (NAbs) as well as T cell responses (for a subset of participants) to analyze immunogenicity kinetics according to various demographics and disease states. Baseline characteristics of the participants are well-balanced across groups (Table 1). To assess the humoral response to inactivated SARS-CoV-2 vaccines, we measured NAbs titers using competitive inhibition method, while anti-RBD-IgG and anti-RBD-IgM using magnetic particle chemiluminescence immunoassay (MCLIA, Bioscience Co., Tianjin, China). We performed FluoroSpot assay to estimate T cell response (Human IFN-g/IL-2 SARS-CoV-2 FluoroSpot^{PLUS} kit, Mabtech AB, Sweden). The study was approved by the Committee on Medical Ethics of Affiliated Hospital of Yunnan University (Approval number: 2021078), and Informed Consent Forms were signed by all participants.

We analyzed the seroprevalence of SARS-CoV-2-specific IgM or IgG among 2,4705 participants prior to the massive vaccination campaign in China (Table S1). We observed very low IgG seroprevalence among local hospital patients and healthcare workers (0.11–0.62%) and significantly elevated seroprevalence among healthcare workers who have worked as temporary support team at Wuhan during the early pandemic outbreak (2.35%). This data indicates a very low local natural infection rate before vaccination campaign.

We then assessed antibody levels for the vaccine study population cohort spanning from receiving the first dose to over 200 days after the second vaccination (Table 1). After the first dose of inactivated vaccine, a minority of participants showed significant increase of anti-RBD-IgG, anti-RBD-IgM, and NAbs (108 [9.6%], 156 [13.9%], and 140 [12.5%], respectively). A second dose elicited a sharp increase in antibody concentrations among most people (Fig. 1A, 1B and 1C). The average NAbs, anti-RBD-IgG, and anti-RBD-IgM concentration increased 12, 45, and 4 folds, respectively, after 1-2 weeks of the second dose compared to the first dose. The concentration and seropositive rate of NAbs and anti-RBD-IgG peaked at the 4th week after the second dose (236.3 IU/mL, 94.6% and 47.6 S/CO, 94.1%, respectively) (Fig. 1A and 1B). From the 5th week, NAbs levels decreased sustainably and culminated in a 4-fold decrease in NAbs level reaching 58.5% seropositivity at the 21st week. Anti-RBD-IgG levels significantly decreased by a factor of 9.3 with a 50.7% seropositivity at the 21th week. Anti-RBD-IgM level also dropped by a factor of 11.3 with 4.8% seropositivity during 9-12th weeks, but the decline from the 9th week to the end of study was much slower, with an overall decrease by a factor of 1.3. Importantly, we noted anti-RBD-IgG and NAbs kinetics were consistent in their degree of immunogenicity ($R = 0.89$, $P < 2\times10^{-16}$, Fig. S2).

Although most people showed a significant waning antibodies after two-dose inactivated vaccine immunization, cellular responses developed in majority of individuals, especially Th1 cell responses (Fig. 1D), suggesting that a second vaccination could effectively promote SARS-CoV-2-specific T cells immunity. Moreover, humoral immune response represented by antibody levels positively correlated with Th1 responses represented by IFN-γ and IL2 secreting cells (Fig. S3).

We found that age, sex, BMI, health condition, vaccine products, the days since the second-dose vaccination were significantly related to the antibody waning kinetics by linear regression analysis (Fig. S4-S7). Therefore, we estimated the dynamics of anti-RBD-IgG and NAbs over 27 weeks after the second dose and associated changes of SARS-CoV-2 specific antibodies with demographic characteristics of participants by linear mixed models (Table. S2 and S3). Mixed model analysis revealed that individuals with diabetes, obesity (BMI ≥ 23.9), older age (≥ 48 years-old), and male sex significantly associated with lower NAbs and anti-RBD-IgG concentrations. Conversely, vaccine product CoronaVac was associated with higher NAbs and anti-RBD-IgG concentrations compared to BBIBP-CorV (Table S4). We also observed an age-by-sex interaction in affecting antibodies titers, suggesting age-dependent antibody kinetics vary differently condition on sex.

Our analysis showed that antibody levels decline at different rates depending on age, sex, BMI, diabetes, vaccine products, and the time since the second-dose vaccination. Although antibody levels drop sharply, the cellular immunity was activated in most people and T cell immune memory induced by inactivated vaccines could last over 6 months post vaccination.[7] The finding provides valuable insights of humoral response dynamics and advice to vaccination strategy with inactivated COVID-19 vaccine.

Funding

This study was funded and supported by Yunnan Provincial Science and Technology Department (202102AA100051 and 202003AC100010, China), National Natural Science Foundation of China (81960116; 82060368, China), Reserve Talents Project for Young and Middle-Aged Academic and Technical Leaders of Yunnan Province (202205AC160023), Yunnan Natural Science Foundation (202001AT070085, China). Spring City Plan:the High-level Talent Promotion and Training Project of Kunming.

Table 1
Participants demographic characteristics. The study population includes volunteers who provided blood samples after the first dose and after the second dose (Whole study population). Participants who provided at least one blood sample following the second vaccination were subject to analysis (Population in model).

Characteristics		Whole study population (n=4359) Population in model (n=4314) Total	Before2Dose	week1–2	week3–4*	week5–8*	week9–12	week13–16	week17–20	week21+
Age, median (IQR)		31 (24–41)	34(29-43)	32(27-42)	35(28-45)	30(23-42)	24(22-32)	28(23-38)	31(25-41)	33(29-42)
Age n (%)	18–27	1717 (39.4)	207(20.6)	183(29.7)	459(24.3)	163(43.6)	460(63.6)	556(48.8)	142(36.5)	53(18.7)
	27–38	1235 (28.3)	369(36.8)	215(34.8)	621(32.9)	91(24.3)	161(22.3)	289(25.4)	114(29.3)	132(46.5)
	38–47	748 (17.2)	247(24.6)	141(22.9)	402(21.3)	54(14.4)	67(9.3)	182(16.0)	78(20.1)	56(19.7)
	≥48	659 (15.1)	153(15.3)	78(12.6)	406(21.5)	66(17.7)	35(4.8)	111(9.8)	55(14.1)	43(15.1)
Sex n (%)	male	1117 (25.6)	239(23.8)	172(27.9)	556(29.5)	85(22.7)	170(23.5)	235(20.7)	85(21.9)	54(19.0)
	female	3242 (74.4)	764(76.2)	445(72.1)	1332(70.6)	289(77.3)	553(76.5)	903(79.3)	304(78.1)	230(81.0)
BMI n (%)	≤18.5	536 (12.3)	99(9.9)	62(10.0)	174(9.2)	44(11.8)	129(17.8)	156(13.7)	42(10.8)	34(12.0)
	18.5–23.9	3093 (71.2)	626(62.4)	374(60.6)	1137(60.7)	237(63.5)	478(66.1)	731(64.2)	270(69.4)	193(68.0)
	≥23.9	712 (16.5)	268(26.7)	177(28.9)	562(30.0)	92(24.7)	116(16.1)	251(22.1)	77(17.8)	57(20.0)
Body condition n (%)	health	1818 (43.2)	543(54.1)	382(62.0)	1252(66.3)	135(36.1)	129(17.8)	262(23.0)	136(35.0)	71(25.0)
	comorbidity	2386 (56.8)	460(45.9)	235(38)	636(33.7)	239(63.9)	594(82.2)	876(77.0)	253(65.0)	213(75.0)
Seropositivity N (%)	NAbs	4817(72.5)	140(12.5)	525(84.4)	1802(94.6)	336(89.8)	625(86.3)	922(81.0)	301(77.3)	166(58.5)
	IgG	4753(73.5)	108(9.6)	517(83.1)	179(94.1)	339(90.6)	622(85.9)	939(82.5)	296(76.1)	144(50.7)
	IgM	1465(22.0)	156(13.6)	292(46.9)	875(46.0)	57(15.2)	35(4.8)	29(0.8)	13(3.3)	8(2.8)

n: Number of participants; N:Sample size;
* :Some individuals did not provide online survey.

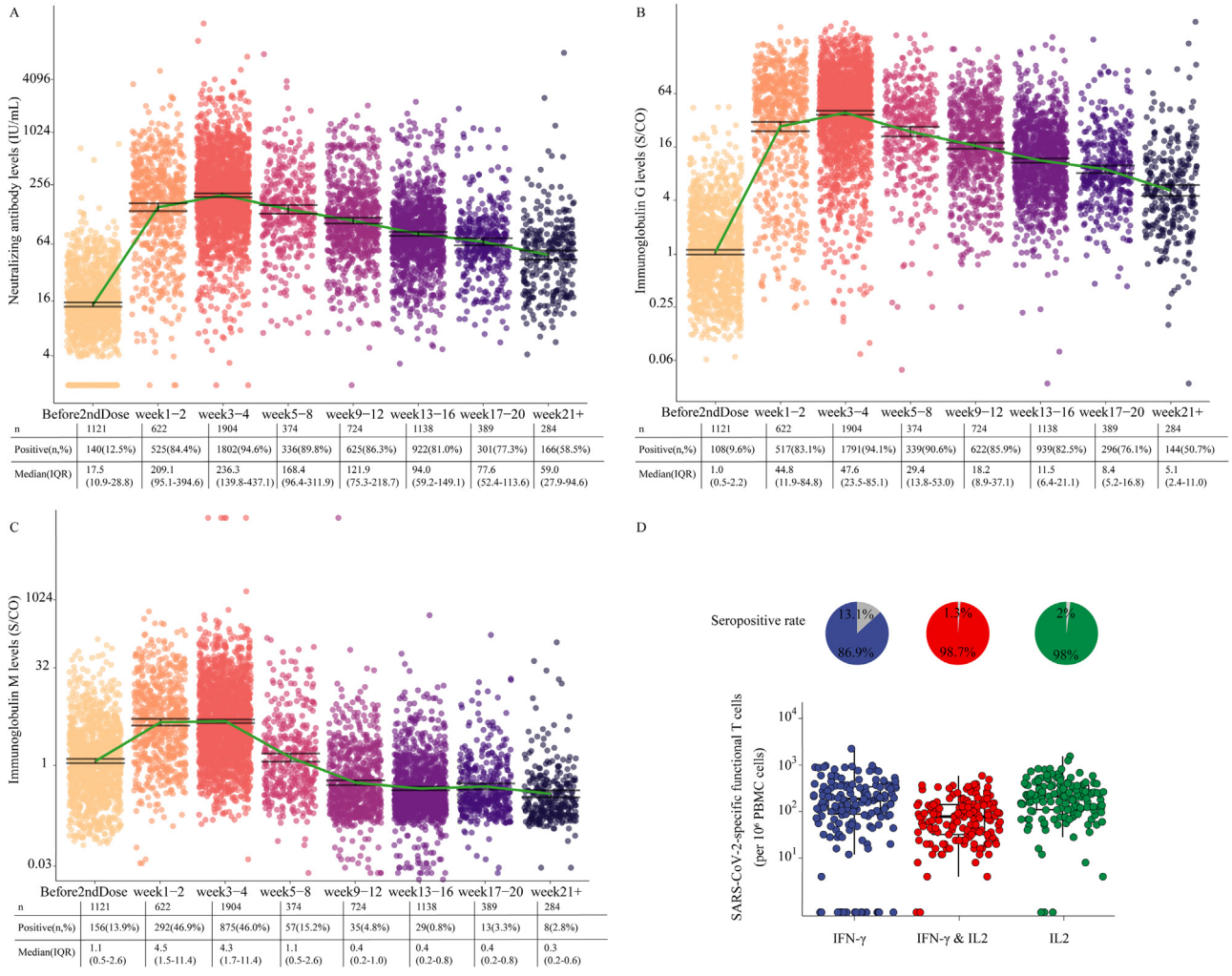

Fig. 1. Antibody kinetics and T-cells responses following vaccination. (A) shows the neutralizing antibody levels following vaccination. The cutoff level of positive neutralizing concentration is 50 IU/mL. (B) shows the IgG levels following vaccination. The cutoff level of positive antibody concentration is 5 S/CO. (C) shows the IgM levels following vaccination. The cutoff level of positive antibody concentration is 5 S/CO. Each point represents a serum sample. The error-bar indicates 95% confidence interval (CI) of geometrical mean concentrations(GMTs). (D) Distribution of IFN-γ and IL2 levels from activated T-cells upon recognition of S peptides. Samples were collected at the 30th day after a second vaccination. Data reported as the median and interquartile range (box), whiskers represent 1.5 times the interquartile range.

Declaration of Competing Interest

Z.Z. served as a PI in a phase 4 clinical study sponsored by Sinovac Biotech Ltd. The funder has no role in study design, implementation and manuscript writing in this study.

Acknowledgments

The authors thank the study participants, and clinical staff and nurses who providing help for their participation and sampling. We thank technicians (Yongcui Ma and Hu Yang) from Tianjin Bioscience Diagnostic Technology Co, Ltd. for technical support of antibodies detection. We also thank all volunteers in the study.

Supplementary materials

Supplementary material associated with this article can be found, in the online version, at doi:10.1016/j.jinf.2022.08.041.

References

1. Lazarus R, Taucher C, Brown C, Čorbic Ramljak I, Danon L, Dubischar K, et al. Valneva Phase 1 trial group. Safety and immunogenicity of the inactivated whole-virus adjuvanted COVID-19 vaccine VLA2001: A randomized, dose escalation, double-blind phase 1/2 clinical trial in healthy adults. *J Infect* 2022 Sep;**85**(3):306–17 PubMed PMID: 35718205; Pubmed Central PMCID: PMC9212764. Epub 2022/06/16.eng.
2. Sauré D, O'Ryan M, Torres JP, Zuniga M, Santelices E, Basso LJ.. Dynamic IgG seropositivity after rollout of CoronaVac and BNT162b2 COVID-19 vaccines in Chile: a sentinel surveillance study. *Lancet Infect Dis* 2022 Jan;**22**(1):56–63 PubMed PMID: 34509185. Pubmed Central PMCID: PMC8428469. Epub 2021/09/13. eng.
3. Lustig Y, Sapir E, Regev-Yochay G, Cohen C, Fluss R, Olmer L, et al. BNT162b2 COVID-19 vaccine and correlates of humoral immune responses and dynamics: a prospective, single-centre, longitudinal cohort study in health-care workers. *Lancet Respir Med* 2021 Sep;**9**(9):999–1009 PubMed PMID: 34224675. Pubmed Central PMCID: PMC8253545. Epub 2021/07/06. eng.
4. Levin EG, Lustig Y, Cohen C, Fluss R, Indenbaum V, Amit S, et al. Waning immune humoral response to BNT162b2 Covid-19 vaccine over 6 months. *N Engl J Med* 2021 Dec 9;**385**(24):e84 PubMed PMID: 34614326. Pubmed Central PMCID: PMC8522797. Epub 2021/10/07. eng.
5. Pérez-Alós L, Armenteros JJA, Madsen JR, Hansen CB, Jarlhelt I, Hamm SR, et al. Modeling of waning immunity after SARS-CoV-2 vaccination and influencing factors. *Nat Commun* 2022 Mar 28;**13**(1):1614 PubMed PMID: 35347129. Pubmed Central PMCID: PMC8960902. Epub 2022/03/30. eng.
6. Zhou T, Shi T, Li A, Zhu L, Zhao X, Mao N, et al. A third dose of inactivated SARS-CoV-2 vaccine induces robust antibody responses in people with inadequate response to two-dose vaccination. *Natl Sci Rev* 2022 nwac066,PubMed PMID: 35958680.Pubmed Central PMCID: PMC9362758.eCollection 2022 Jul.
7. C Li , A Li, H Bi, J Fu, F Yang, T Zhou et al., Immunogenicity and safety of the CoronaVac inactivated SARS-CoV-2 vaccine in people with underlying medical conditions in China: a retrospective study. PREPRINT (Version 1) available at Research Square https://doiorg/1021203/rs3rs-1794955/v1. 18 July 2022.

Tianpei Shi
Central Lab, Liver Disease Research Center and Department of Infectious Disease, The Affiliated Hospital of Yunnan University, Kunming, Yunnan 650021, China
State Key Laboratory of Genetic Resources and Evolution, and Yunnan Laboratory of Molecular Biology of Domestic Animals, Kunming Institute of Zoology, Chinese Academy of Sciences, Kunming 650223, China
College of Life Science, University of Chinese Academy of Sciences, Beijing 100049, China
State Key Laboratory for Conservation and Utilization of Bio-resource and School of Life Sciences, Yunnan University, Kunming, Yunnan 650091, China

Mu-Xian Dai, Feng-Wei Liu
Central Lab, Liver Disease Research Center and Department of Infectious Disease, The Affiliated Hospital of Yunnan University, Kunming, Yunnan 650021, China

Jun Hu
Preventive medicine department, The Affiliated Hospital of Yunnan University, Kunming, Yunnan 650021, China

Mu-Hua Feng, Gang-Xu Xu, Ya-Jing Wang
Central Lab, Liver Disease Research Center and Department of Infectious Disease, The Affiliated Hospital of Yunnan University, Kunming, Yunnan 650021, China

Li-Hong Zhang
Preventive medicine department, The Affiliated Hospital of Yunnan University, Kunming, Yunnan 650021, China

Liang Zhang
Central Lab, Liver Disease Research Center and Department of Infectious Disease, The Affiliated Hospital of Yunnan University, Kunming, Yunnan 650021, China

Zijie Zhang*
Central Lab, Liver Disease Research Center and Department of Infectious Disease, The Affiliated Hospital of Yunnan University, Kunming, Yunnan 650021, China
State Key Laboratory for Conservation and Utilization of Bio-resource and School of Life Sciences, Yunnan University, Kunming, Yunnan 650091, China

Tai-Cheng Zhou**, Jia Wei**
Central Lab, Liver Disease Research Center and Department of Infectious Disease, The Affiliated Hospital of Yunnan University, Kunming, Yunnan 650021, China

*Corresponding author at: Central Lab, Liver Disease Research Center and Department of Infectious Disease, The Affiliated Hospital of Yunnan University, Kunming, Yunnan 650021, China.
**Corresponding authors.
E-mail addresses: zijiezhang@ynu.edu.cn (Z. Zhang), zhoutc@ynshhyy.com (T.-C. Zhou), weijia19631225@163.com (J. Wei)

Accepted 29 August 2022
Available online 3 September 2022

https://doi.org/10.1016/j.jinf.2022.08.041

Pseudomonas aeruginosa bloodstream infection in patients with hematological diseases: Clinical outcomes and prediction model of multidrug-resistant infections

Dear Editor,

We read with interest the article by Metais et al.,[1] which reported that short-term antibiotic treatment during febrile neutropenia (FN) in patients with acute myeloid leukemia was as effective as prolonged therapy for bloodstream infection (BSI), with very few relapses over 30 days. Patients with hematological diseases are susceptible to BSI due to long-term neutropenia, and *P. aeruginosa* presents one of the major cause of hospital acquired infections.[2] *P. aeruginosa* is intrinsically resistant to a variety of antibiotic agents, and it is easy to develop resistance under the overuse of antibiotics. The spreading of carbapenem-resistant (CR) and multidrug resistant (MDR) infections brings great difficulties to clinical treatment and becomes a challenge topic with increasing costs[3] and mortality.[4]

Table 1
Clinical characteristics of patients with PA BSI, According to multidrug resistance of isolates.

Characteristic	MDR (n= 58)	Non-MDR (n= 371)	Univariate Analysis *P* value
Age	42.5(29.0-51.3)	43.0(29.0-52.0)	0.980
Female	21 (36.2)	175 (47.2)	0.156
Severe neutropenia	28 (48.3)	159 (42.9)	0.478
Neutropenia	53 (91.4)	349 (94.1)	0.390
Duration of neutropenia before BSI	7.5 (3.0-13.0)	4.0(2.0-8.0)	0.005
Prior hospital admission	44 (75.9)	242(65.2)	0.134
Corticosteroid use	10 (17.2)	72 (19.4)	0.858
HSCT	7 (12.1)	29 (7.8)	0.305
Chemotherapy	45 (77.6)	315 (84.9)	0.178
Diabetes mellitus	10 (17.2)	26 (7.0)	0.018
BSI occurring during antibiotic therapy	31 (53.4)	31 (8.4)	<0.001
Prior antibiotic therapy within 3 months			
Quinolones	17 (29.3)	37 (10.0)	<0.001
Anti-pseudomonal cephalosporins	35 (60.3)	181 (48.8)	0.067
Piperacillin/tazobactam	17 (29.3)	52 (14.0)	0.006
Carbapenems,	43 (74.1)	192 (51.8)	0.002
Aminoglycoside	7 (12.1)	25 (6.7)	0.175
Length of hospital stay before BSI, days	16.0(10.8-26.0)	16.0(13.0-22.0)	0.696
Duration of antibiotic treatment, days	14.0(10.0-23.0)	11.0(8.0-17.0)	0.063
Complications			
Oral mucositis	20 (34.5)	91 (24.5)	0.110
Diarrhea	9 (15.5)	53 (14.3)	0.841
Septic shock within 48 h	0 (0.0)	16 (4.3)	0.145
Pulmonary infection	22 (37.9)	108 (29.1)	0.218
Perianal infection	8 (13.8)	39 (10.5)	0.496
Hypoalbuminemia	25 (43.1)	129 (34.8)	0.240
IET within 48h	24(41.4)	25(6.7)	<0.001
30-day mortality	17 (29.3)	27 (7.3)	<0.001
7-day mortality	6 (10.3)	15 (4.0)	0.050

Notes: BSI, bloodstream infection; HSCT: hematopoietic stem cell transplantation; MDR, multidrug resistant; CR, carbapenems resistant; IET, inadequate empirical therapy.

Rational use of antibiotics is essential to reduce antibiotic resistance and improve patient outcome. Therefore, there is an urgent to find a way to balance the coverage of active antibiotic agents and avoiding further development of antibiotic resistance under overuse of antibiotics. To this end, we conducted an analysis of 429 consecutive episodes of *P. aeruginosa* BSI in patients with hematological diseases at our hospital from January 2014 to December 2020, to compare the clinical risk factors for MDRPA BSI and prognostic factors of PA BSI.

Patient characteristics were detailed in Table S1, all patients received empirical treatment immediately after the collection of blood samples. None of the patients in this study received prophylactic antibiotic treatment. Most patients with acute myeloid leukemia, 80.4% of the patients received at least one antimicrobial agent with in vitro activity within 24 hours after the onset of BSI, 88.6% of patients received adequate empirical therapy (AET) after the adjustment based on clinical response within 48 hours, and 421 patients received adequate definitive therapy. The median antimicrobial treatment length was 11 days, overall 30-day mortality rate was 10.3%, higher mortality was found in MDR group (P<0.001; Table 1), and there was no significant difference in mortality between the empirical monotherapy and combination therapy (P=0.686). Early AET be of great importance to patient outcome[5] and cost.[6] In this study, inadequate empirical therapy (IET) was more frequent in patients with MDR *P. aeruginosa* BSI, it reached up to 41.4% within 48 hours after the onset of BSI, and multivariate analysis revealed IET was an independent risk factor for 30-day mortality (Table 1 and S2). As shown in Fig. 1A, the longer a patient waits to receive AET, the worse the prognosis, and the 30-day mortality rate was 33.3%, 51.0% and 80.0%, respectively, for patients received IET within 24 hours, 48 hours and 72 hours after the onset of BSI. Therefore, patients with *P. aeruginosa* BSI could benefit from an early use of active agents.

P. aeruginosa exhibits multiple antibiotic resistance mechanisms, the efflux pump mechanism can generate cross-resistance to multiple classes of antimicrobials, and may work in conjunction with other resistance mechanisms.[7] Quinolones is the substrate of all efflux pumps for *P. aeruginosa*, which may trigger cross-resistance to many other important antibiotics.[8] The prior use of antibiotics is a well-known factor for resistant infections, medication time and the serum concentrations are important factors related to patient outcome.[9] In the current study, previous antibiotic therapy was defined as the use of antibiotics for at least 72 hours within 3 months before the onset of BSI. We found that the previous use of quinolones was an independent predictor of MDR *P. aeruginosa* BSI, and we further revealed the association between time of previous quinolone exposure and subsequent MDR infections. Notably, among patients previously treated with quinolones(n=54) or carbapenems (n=235), the cumulative duration of quinolone and carbapenem use was longer in patients with MDR infection than in non-MDR infection. (median, days: 8.0 vs4.0, *P*=0.010;12.5 vs8.0, *P*=0.006). In other words, duration of antibiotic use was associated with MDR infections, rather than antibiotic use alone. Furthermore, no one received antibiotic prophylaxis. In addition to antibiotic exposure, duration of neutropenia and diabetes mellitus are associated with MDR BSI (P=0.005, P=0.018; Table 1). Therriault et al.[10] demonstrated that levofloxacin prophylaxis may contribute to the development of antibiotic resistant infections in patients received allo-HSCT. In this study, 30-day mortality was lower than most recent reports,[5] and the low mortality and the relatively low incidence of MDR *P. aeruginosa* BSI in this study underscore the safety of neutropenic patients not receiving prophylactic therapy and the side effects of long-term antibiotic use.

CR and MDR infections were recorded in 85(19.8%) and 58(13.5%) patients. The incidence of MDR P. aeruginosa trended upward during the study period (Fig. 1B). As illustrated in Fig. 1C, there were still many agents have in vitro activity against CR

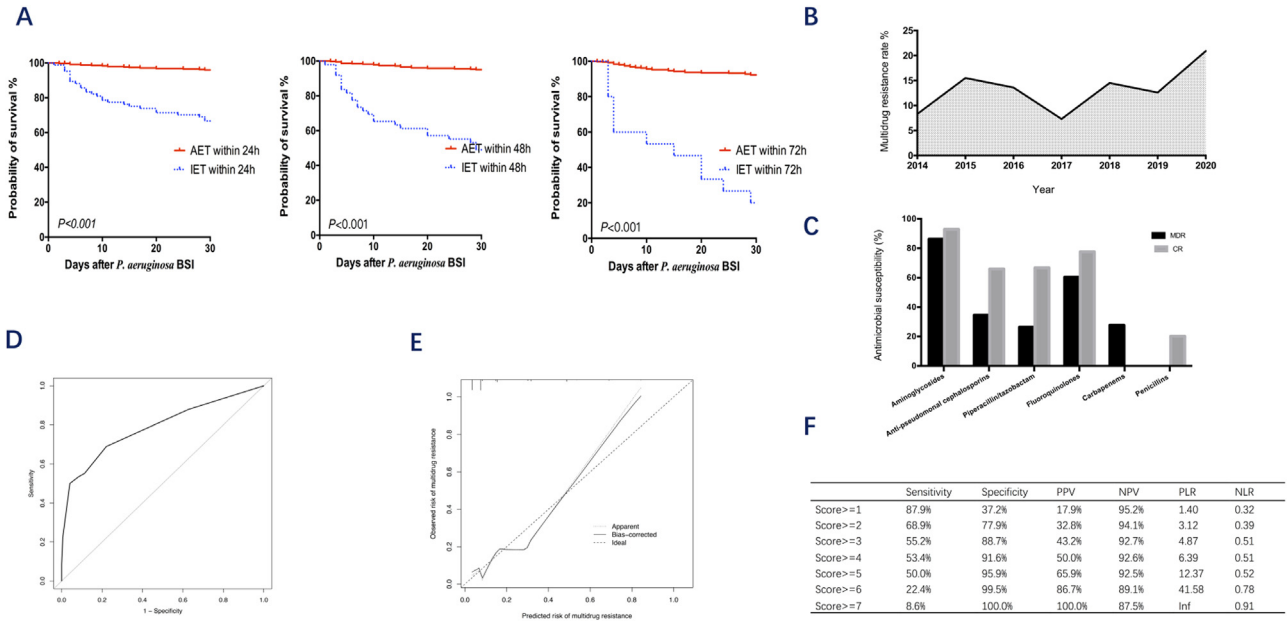

F

	Sensitivity	Specificity	PPV	NPV	PLR	NLR
Score>=1	87.9%	37.2%	17.9%	95.2%	1.40	0.32
Score>=2	68.9%	77.9%	32.8%	94.1%	3.12	0.39
Score>=3	55.2%	88.7%	43.2%	92.7%	4.87	0.51
Score>=4	53.4%	91.6%	50.0%	92.6%	6.39	0.51
Score>=5	50.0%	95.9%	65.9%	92.5%	12.37	0.52
Score>=6	22.4%	99.5%	86.7%	89.1%	41.58	0.78
Score>=7	8.6%	100.0%	100.0%	87.5%	Inf	0.91

Fig. 1. Clinical outcomes and antibiotic resistant characteristics of *P. aeruginosa* bloodstream infection. (A) Association between empirical therapy and survival among patients with *P. aeruginosa* bloodstream infection. *Abbreviations: BSI, bloodstream infection; AET, adequate empirical therapy; IET, inadequate empirical therapy.* (B) Evolution of multidrug resistant *P. aeruginosa* bloodstream infection from 2014 to 2020. (C) Antimicrobial susceptibility of *P. aeruginosa* isolates in different resistance patterns. *Abbreviations: MDR, multidrug resistant; CR, carbapenems resistant.* (D) Internal discrimination of the prediction model of multidrug resistant in patients with *P. aeruginosa* bloodstream infection demonstrated by receiver operating characteristics curves. The overall predictive model showed a good discrimination with a C-index of 0.79 (95% CI, 0.71 to 0.86) and the goodness of fit of the model is satisfying, with a P-value of the Hosmer-Lemeshow test of 0.53; (E) Internal calibration of prediction model by levels of predicted risk versus observed risk. Internal validation after bootstrap re-sampling showed good calibration, the C-index is calculated using the score after coefficient transformation, with a very minimal decrease in the C-index (0.793 to 0.773), indicates a low over-optimism of the final model and good consistency between prediction probabilities and observation probabilities. (F) Sensitivity and specificity of the prediction model for different cut off. *Abbreviations: PPV, positive predictive value; NPV, negative predictive value; PLR, positive likelihood ratio; NLR, negative likelihood ratio.*

strains in this study, and more than 60% of CR strains were susceptible to antipseudomonal cephalosporins (Ceftazidime and Cefepime) and piperacillin/tazobactam, and MDR strains were most sensitive to aminoglycosides. In addition, we collected 274 non-repetitive CR strains from clinical samples between October 2017 and April 2021. Most of the isolates were obtained from throat swabs (23.7%, 65/274), followed by anal swabs (23.7%, 65/274) and blood (20.8%, 57/274), and only 13 isolates were found to express carbapenemase, IMP was the most prevalent type (92.3%, 12/13) , followed by NDM (7.7%, 1/13). which provides an explanation for the susceptibility of CR *P. aeruginosa* strains to other antimicrobials in this study.

To facilitate the rapid identification of high-risk MDR infections, we developed a quick scoring prediction rule based on a few straightforward clinical factors. Prior treatment with carbapenems (OR, 2.066; 95%CI, 1.024–4.171), piperacillin-tazobactam (OR, 2.500; 95% CI, 1.162–5.380), quinolones (OR, 2.275; 95% CI, 1.016–5.094) and BSI occurring during antibiotic treatment (OR, 12.957; 95% CI, 6.581–25.514) were independent risk factors for MDR *P. aeruginosa* BSI in multivariate analysis (Table S2), one point was assigned to each predictor, except for BSI occurring during antibiotic treatment (4 points). The model showed a good discrimination and calibration (Fig. 1D and E). Patients with a score≥6 were classified as high-risk group, with a positive predictive value of 86.7% (Fig. 1F).

In conclusion, the present study of a large number of patients with blood diseases revealed the association between long-term antibiotic use and subsequent infection with MDR *P. aeruginosa*. Then we demonstrated a strong link between clinical data and microbiological outcomes, as well as antibiotic resistance patterns and adverse outcomes of delaying appropriate treatment. Finally, a quick scoring rule based on clinical factors was established to identify patients at risk for MDR *P. aeruginosa* BSI. This could be a quick tool to identify patients at high risk for multidrug-resistant infections who could benefit from a broad-spectrum regimen, thereby optimizing antibiotic therapy based on local resistance patterns, improving clinical outcomes, and reducing antibiotic overuse in low-risk patients. Furthermore, reducing the development and spread of resistance.

Declaration of Competing Interest

Yuanqi Zhao and Qingsong Lin contributed equally to this article. All authors have no reported conflicts.

Funding

This work was supported by the Chinese Academy of Medical Sciences Innovation Fund for Medical Sciences (grant number 2021-I2M-1-017) and the Nonprofit Central Research Institute Fund of Chinese Academy of Medical Sciences (grant number 2018PT32034).

Supplementary materials

Supplementary material associated with this article can be found, in the online version, at doi:10.1016/j.jinf.2022.08.037.

References

1. Metais A, Torregrosa Diaz JM, Gallego Hernanz MP, et al. Efficacy of antibiotic short course for bloodstream infections in acute myeloid leukemia patients with febrile neutropenia: A retrospective comparative study. *J Infect* 2022;**84**:1–7.
2. Thaden JT, Park LP, Maskarinec SA, Ruffin F, Fowler VG Jr., van Duin D. Results from a 13-Year Prospective Cohort Study Show Increased Mortality Associated with Bloodstream Infections Caused by Pseudomonas aeruginosa Compared to Other Bacteria. *Antimicrob Agents Chemother* 2017;**61**(6) Jun.

3. Riu M, Chiarello P, Terradas R, et al. Cost Attributable to Nosocomial Bacteremia. Analysis According to Microorganism and Antimicrobial Sensitivity in a University Hospital in Barcelona. *PLoS One* 2016;**11**(4):e0153076.
4. Righi E, Peri AM, Harris PN, et al. Global prevalence of carbapenem resistance in neutropenic patients and association with mortality and carbapenem use: systematic review and meta-analysis. *J Antimicrob Chemother* 2017 Mar 1;**72**(3):668–77.
5. Martinez-Nadal G, Puerta-Alcalde P, Gudiol C, et al. Inappropriate Empirical Antibiotic Treatment in High-risk Neutropenic Patients With Bacteremia in the Era of Multidrug Resistance. *Clin Infect Dis* 2020 Mar 3;**70**(6):1068–74.
6. Merchant S, Proudfoot EM, Quadri HN, et al. Risk factors for Pseudomonas aeruginosa infections in Asia-Pacific and consequences of inappropriate initial antimicrobial therapy: A systematic literature review and meta-analysis. *J Glob Antimicrob Resist* 2018;**14**:33–44 Sep.
7. Poole K.. Efflux-mediated antimicrobial resistance. *J Antimicrob Chemother* 2005;**56**(1):20–51 Jul.
8. Masuda N, Sakagawa E, Ohya S, Gotoh N, Tsujimoto H, Nishino T.. Substrate specificities of MexAB-OprM, MexCD-OprJ, and MexXY-oprM efflux pumps in Pseudomonas aeruginosa. *Antimicrob Agents Chemother* 2000;**44**(12):3322–7 Dec.
9. Roberts JA, Paul SK, Akova M, et al. DALI: defining antibiotic levels in intensive care unit patients: are current beta-lactam antibiotic doses sufficient for critically ill patients? *Clin Infect Dis* 2014;**58**(8):1072–83 Apr.
10. Therriault BL, Wilson JW, Barreto JN, Estes LL.. Characterization of bacterial infections in allogeneic hematopoietic stem cell transplant recipients who received prophylactic levofloxacin with either penicillin or doxycycline. *Mayo Clin Proc* 2010;**85**(8):711–18 Aug.

Yuanqi Zhao
State Key Laboratory of Experimental Hematology, National Clinical Research Center for Blood Diseases, Institute of Hematology & Blood Diseases Hospital, Chinese Academy of Medical Sciences & Peking Union Medical College, Tianjin, China
Fujian Institute of Hematology, Fujian Provincial Key Laboratory on Hematology, Fujian Medical University Union Hospital, Fuzhou, China

Qingsong Lin, Tingting Zhang, Sisi Zhen, Jieru Wang, Erlie Jiang, Yingchang Mi, Lugui Qiu, Mingzhe Han, Jianxiang Wang, Sizhou Feng*
State Key Laboratory of Experimental Hematology, National Clinical Research Center for Blood Diseases, Institute of Hematology & Blood Diseases Hospital, Chinese Academy of Medical Sciences & Peking Union Medical College, Tianjin, China

*Corresponding author at: Hematopoietic Stem Cell Transplantation Center, State Key Laboratory of Experimental Hematology, National Clinical Research Center for Blood Diseases, No. 288 Nanjing Road, Tianjin, China.
E-mail addresses: doctor_szhfeng@163.com, szfeng@ihcams.ac.cn (S. Feng)

Accepted 29 August 2022
Available online 3 September 2022

https://doi.org/10.1016/j.jinf.2022.08.037

Comparative analysis of transmission and vaccine effectiveness in Omicron and Delta variant outbreaks in China

Dear Editor,

In this Journal, Yidun Zhang et al. compared Ct value difference between Omicron BA.1 and BA.2 variants and showed that Omicron BA.2 more transmissible than BA.1[1]. Previous letter by Yue Yin et al. announced that inactivated COVID-19 vaccines (CoronaVac, Sinovac) is less effective against Omicron than against Delta, and its protection against Omicron[2]. However, the transmission characteristics of infection in Delta and Omicron mutant strains have not been fully defined. The goal of this study is to examine the characteristics of Delta and Omicron variants, including transmission, Ct value, and effectiveness of vaccine, to provide additional information about the COVID-19 pandemic in China.

We examined three outbreaks caused by the different SARS-CoV-2 variants and located in Southern China (Fig. S1). A total of 202 infections due to SARS-CoV-2 variants in three outbreaks were included in our analysis. Of these infections, 33 (16.34%) were caused by the Omicron BA.2 variant, 38 (18.81%) were caused by the Omicron BA.1 variant, and 129 (63.86%) were caused by the Delta variant. The median age of infections for Omicron BA.2, Omicron BA.1 and Delta variant was varied (21.5 years *vs.* 31.0 years *vs.* 34.0 years), and 137 (67.82%) infections were in adults (19–64 years). 31 (88.57%) infections of Omicron BA.2 have been completed vaccine, higher than Delta (68.42%) and Omicron BA.1 (29.46%). In addition, the proportion of asymptomatic infections decreased from 15% in the Delta outbreak to 6%–8% in the Omicron outbreak (Table S1, Fig. 1A-C).

The distribution of epidemiological parameters was fitted to Gamma distribution, the Lognormal distribution and Weibull distribution were used as well and showed similar goodness-of-fit as measured by log-likelihood (Table S2, Fig. S2). Compared with the Delta variant, Omicron BA.2 and BA.1 variants were transmitted with a shorter serial interval (SI), (5.70days *vs.* 3.00 days *vs.* 2.24 days) (Fig. 1D), and incubation period (IP) (7.63 days *vs.* 4.35 days *vs.* 3.07days) (Fig. 1E) in the outbreaks examined. Approximately 35.09% cases where SIs were shorter than IPs were recorded in individuals infected with Omicron BA.1; similarly, 70.98% cases were recorded in those infected with Omicron BA.2, and 75.00% cases in those infected by Delta (Fig. 1F). The estimation of generation time (GT) was based on a review of the exposed period and probable time of infection. Omicron BA.1 displayed a shorter GT than the Delta variant (1.76 days *vs.* 2.52 days), and a similar GT to Omicron BA.2 (2.93 days *vs.* 2.52 days). Transmission generation (TG) of variants, defined as the period between the positive test results of infector and infectee which did not relay on the recall of infectee, were also varied. Delta and Omicron BA.1 showed similar TG values (3.61 days *vs.* 3.56 days), and Omicron BA.2 displayed a TG of 1.95 days (Fig. 1G-H). R_{eff} of Delta at increased stage was 1.93 (95% CI: 1.3–2.72), 2.94 (95% CI: 1.41–5.30) for Omicron BA.1, and 3.56 (95% CI: 1.20–7.94) for Omicron BA.2 (Fig. 1I). We also compared IP, SI, TG, and GT values between adults (older than 19 years) and children (0–18 years) and found that children had shorter IP in the Omicron BA.1 outbreak (4.00 days *vs.* 4.89 days) and shorter TG values in both the Omicron BA.1 (3.11 days *vs.* 4.14 days) and Delta (2.37 days *vs.* 4.06 days) outbreaks (Fig. S3). This may be related to a deficient vaccine coverage in children, in part (Fig. 1A-C). However, the difference between the epidemiological parameters of Omicron BA.2, as opposed to other variants, cannot be explained entirely by deficient vaccine coverage in children.

A total of 21,716 contacts were introduced by 202 infections and tracked by local CDC health workers (Table S3). Full vaccine coverage of contacts in Delta, Omicron BA.1, and BA.2 outbreaks was 44.33%, 79.77%, and 68.72%, respectively. Booster dose coverage was 40.84% and 29.62% in Omicron BA.1 and Omicron BA.2 outbreaks, respectively. Vaccine coverage of children (aged 0–18 years) and older adults (aged 65 years or older) was lower than that of younger adults (Fig. 2A-C). More than 99% of the vaccines received by contacts were produced by 5 manufacturers, including Sinovac Biotech Ltd., Sinopharm Group Co. Ltd., CanSino Biologics Inc., Anhui Zhifei Longcom Biopharmaceutical Co. Ltd., and Shenzhen Kangtai Biological Products Co., Ltd. The mixed vaccine strategy was also observed in each outbreak, but 98.27% of vaccinations were a dosing combination of CoronaVac (Sinovac Biotech

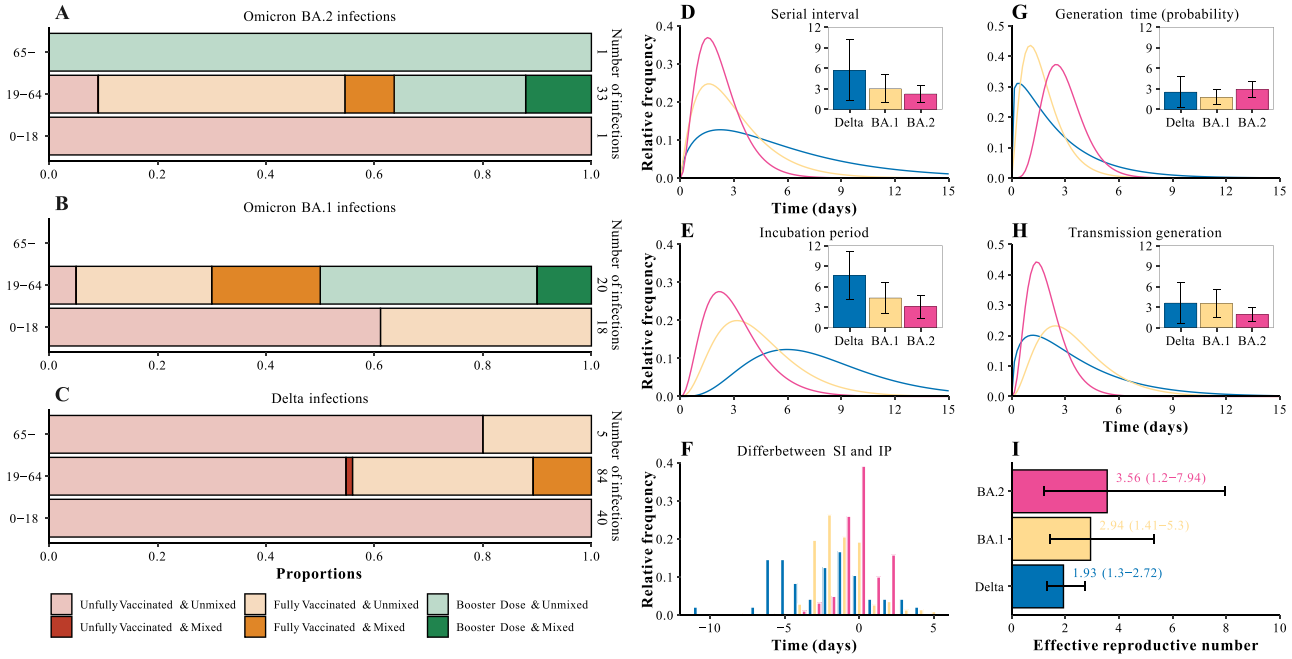

Fig. 1. Vaccination status and epidemiological parameters estimation of infections in COVID-19 outbreaks caused by Omicron BA.2, Omicron BA.1 and Delta. Vaccination status of infections from Omicron BA.2 (A), Omicron BA.1 (B) and Delta (C), respectively, and grouped by age. (D), Fitted serial interval (SI) distribution of paired cases of Delta (n = 83), Omicron BA.1 (n = 31) and BA.2 (n = 19). (E), Fitted incubation period (IP) distribution of cases of Delta (n = 74), Omicron BA.1 (n = 35) and BA.2 (n = 33). (F), The difference between IP and related SI of cases. (G), Fitted probability generation time (GT) distribution of infections of Delta (n = 58), Omicron BA.1 (n = 33) and BA.2 (n = 20). (H), Fitted transmission generation (TG) distribution of infections of Delta (n = 90), Omicron BA.1 (n = 32) and BA.2 (n = 20). (I), Effective reproductive number of difference outbreaks, estimated using R0 package.

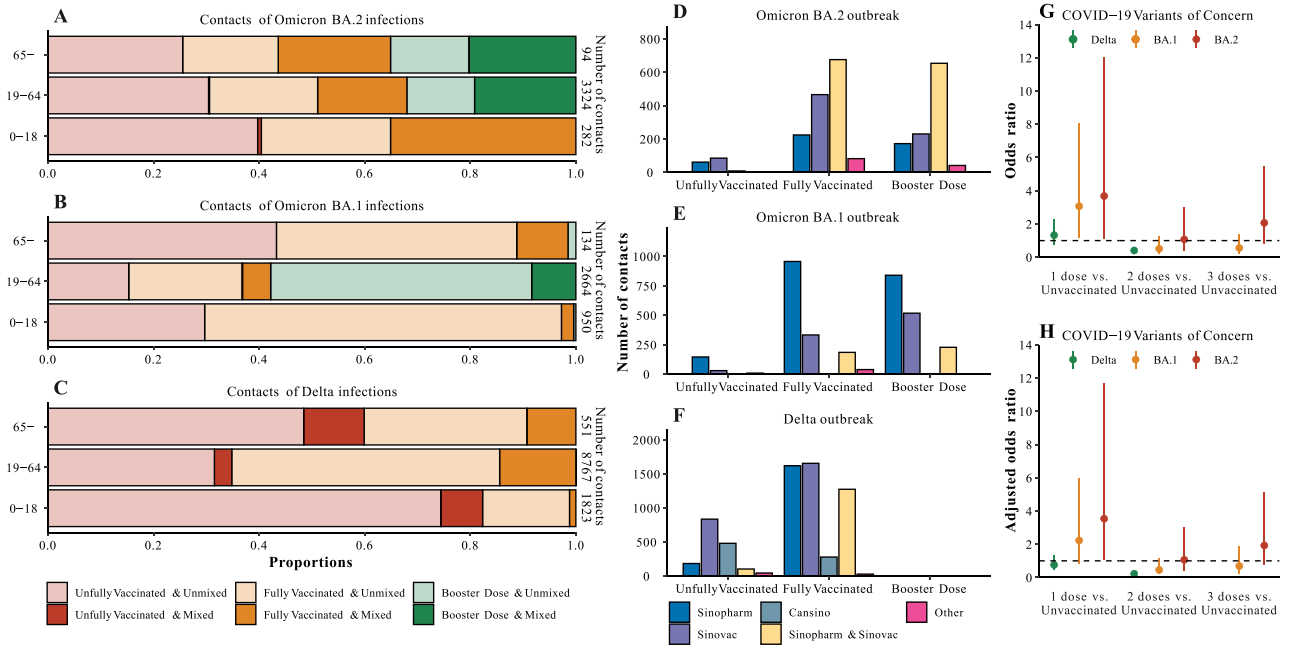

Fig. 2. Vaccination status of contacts and vaccine effectiveness against infections in COVID-19 outbreaks caused by Omicron BA.2, Omicron BA.1 and Delta. Vaccination status of contacts from Omicron BA.2 (A), Omicron BA.1 (B) and Delta (C), respectively, and grouped by age. Vaccine manufacturers with contacts in Omicron BA.2 (D), Omicron BA.1 (E) and Delta outbreaks (F), respectively. (G), Comparison of vaccine effectiveness against infection using a logistic regression model. (H), Comparison of vaccine effectiveness against infection using conditional logistic regression model, adjusted for age group.

Ltd.) and COVILO (Sinopharm Group Co. Ltd.) (Fig. 2D-F). Overall effectiveness of vaccine against the Delta variant in fully vaccinated individuals was 51.68% (95% CI: 28.90–67.16%) (Fig. 2G). In conditional logistic regression model, the vaccine effectiveness against Delta variant infection adjusted by age group was 67.87% (95% CI: 51.67–78.64%) (Fig. 2H). For Omicron BA.1 and BA.2, difference in vaccine effectiveness against infection was not observed, regardless of adjustment by age group.

Our findings imply that Omicron's transmissibility is 1.5–1.8 times higher than that of Delta in terms of viral transmission. This is lower than the value reported by other studies, which claim that Omicron has a transmissibility 2.5 to 4 higher than that of Delta[3,4].

This might be attributable to the rising rate of fully vaccinated and booster-vaccinated people. Meanwhile, the geographic variability is also linked to inconsistencies in the implementation of COVID-19 prevention and control measures in different regions. We also saw that the transmissibility of the two Omicron sub-lineages differed, with Omicron BA.2 being 1.2 times more transmissible than BA.1, which is similar to the results of several studies that suggest that BA.2 is 30 to 40 percent more infectious than BA.1[5-7]. In comparison to Delta, applying a dynamic zero-COVID policy for interrupting Omicron transmission may necessitate greater preventative and control efforts.

Funding

This study was partly supported by the National Key Research and Development Program of China (2021YFC2301604), The Bill & Melinda Gates Foundation (Grant INV-005834 to T.C.) and Zhuhai Science and Technology Program (ZH22036302200077PWC).

Ethical statement

This study was approved by the institutional ethics committee of the Zhuhai Center for Disease Control and Prevention (CDC), Guangdong, China. Written consent was obtained from patients or their guardian(s) when samples were collected. The Hunan Provincial CDC, China and the Xiamen CDC, Fujian, China have a data-sharing agreement of infections and contacts in 2021–10 Delta outbreaks and 2022–2 Omicron BA.2 outbreaks.

Author contributions

Conceptualization: TMC, FR, ZNG. Investigation: FR, XBZ, ZNG, XLY, WHM. Methodology: KGL, ZYZ, TMC. Software: KGL. Validation: TMC. Writing - original draft: ZYZ, KGL, SSY, ZMY, BA. Writing - review & editing: ZYZ, KGL, BA.

Data and source code availability

Source code and data of analysis procedure is accessible at GitHub repository (https://github.com/xmusphlkg/zhuhai_omicron).

Declaration of competing interest

The authors declare no competing interests.

Acknowledgments

We thank staff at Zhuhai, Xiamen and Hunan Center for Disease Control and Prevention, China for accessing the various data sources. The opinions expressed are those of the authors and not necessarily the institutions to which they are affiliated.

Supplementary materials

Supplementary material associated with this article can be found, in the online version, at doi:10.1016/j.jinf.2022.08.018.

References

1. Zhang Y., Li J., Jiang L., et al. Comparison of SARS-CoV-2 aerosol emission from patients with Omicron BA.1 or BA.2 subvariant infection. *J Infect* 2022;**85**(2) e37-e9. doi:10.1016/j.jinf.2022.05.035.
2. Yin Y., Li X., Qian C., Cheng B., Lu F., Shen T.. Antibody efficacy of inactivated vaccine boosters (CoronaVac) against Omicron variant from a 15-month follow-up study. *J Infect* 2022. doi:10.1016/j.jinf.2022.06.018.
3. Nishiura H., Ito K., Anzai A., Kobayashi T., Piantham C., Rodriguez-Morales A.J.. Relative Reproduction Number of SARS-CoV-2 Omicron (B.1.1.529) compared with delta variant in South Africa. *J Clin Med* 2021;**11**(1). doi:10.3390/jcm11010030.
4. Liu Y., Rocklov J.. The effective reproduction number for the omicron SARS-CoV-2 variant of concern is several times higher than Delta. *J Travel Med* 2022. doi:10.1093/jtm/taac037.
5. Johnson H. New Omicron variant: symptoms of Covid subvariant BA.2, how contagious is it and does it cause severe illness? 2022. https://www.nationalworld.com/health/new-omicron-variant-symptoms-of-covid-subvariant-ba2-how-contagious-is-it-and-does-it-cause-severe-illness-3612480 (accessed 15 April 2022).
6. Skydsgaard N. Omicron subvariant BA.2 more infectious than 'original', Danish study finds. 2022. https://www.reuters.com/business/healthcare-pharmaceuticals/omicron-subvariant-ba2-more-infectious-than-original-danish-study-finds-2022-01-31/ (accessed 30 January 2022).
7. Kimball S. Omicron B.A. 2 subvariant is more contagious and can reinfect people, but isn't more severe, studies find. 2022. https://www.cnbc.com/2022/02/25/covid-transmissibility-severity-reinfection-of-omicron-bapoint2-subvariant.html (accessed 25 January 2022).

Kangguo Li[1]
State Key Laboratory of Molecular Vaccinology and Molecular Diagnostics, School of Public Health, Xiamen University, Fujian, China

Feng Ruan[1]
Zhuhai Center for Disease Control and Prevention, Guangdong, China

Zeyu Zhao[1]
State Key Laboratory of Molecular Vaccinology and Molecular Diagnostics, School of Public Health, Xiamen University, Fujian, China
CIRAD, Intertryp, Montpellier, France, IES, Université de Montpellier-CNRS, Montpellier, France

Zhinan Guo[1]
Xiamen Center for Disease Control and Prevention, Fujian, China

Zimei Yang, Shanshan Yu, Buasiyamu Abudunaibi
State Key Laboratory of Molecular Vaccinology and Molecular Diagnostics, School of Public Health, Xiamen University, Fujian, China

Xuebao Zhang, Xiling Yin, Wenhua Mei*
Zhuhai Center for Disease Control and Prevention, Guangdong, China

Tianmu Chen*
State Key Laboratory of Molecular Vaccinology and Molecular Diagnostics, School of Public Health, Xiamen University, Fujian, China

*Corresponding authors.
E-mail addresses: 1297648405@qq.com (W. Mei), 13698665@qq.com (T. Chen)

[1] These authors contributed equally to this study.

Accepted 18 August 2022
Available online 22 August 2022

https://doi.org/10.1016/j.jinf.2022.08.018

Highly accurate protein structure prediction and drug screen of monkeypox virus proteome

Dear Editor,

We recently came accross an interesting article published in this journal by Usman Ayub Awan et al.,[1] which highlighted that the monkeypox virus had become another global emergency threatening human health under the COVID-19 pandemic. An out-

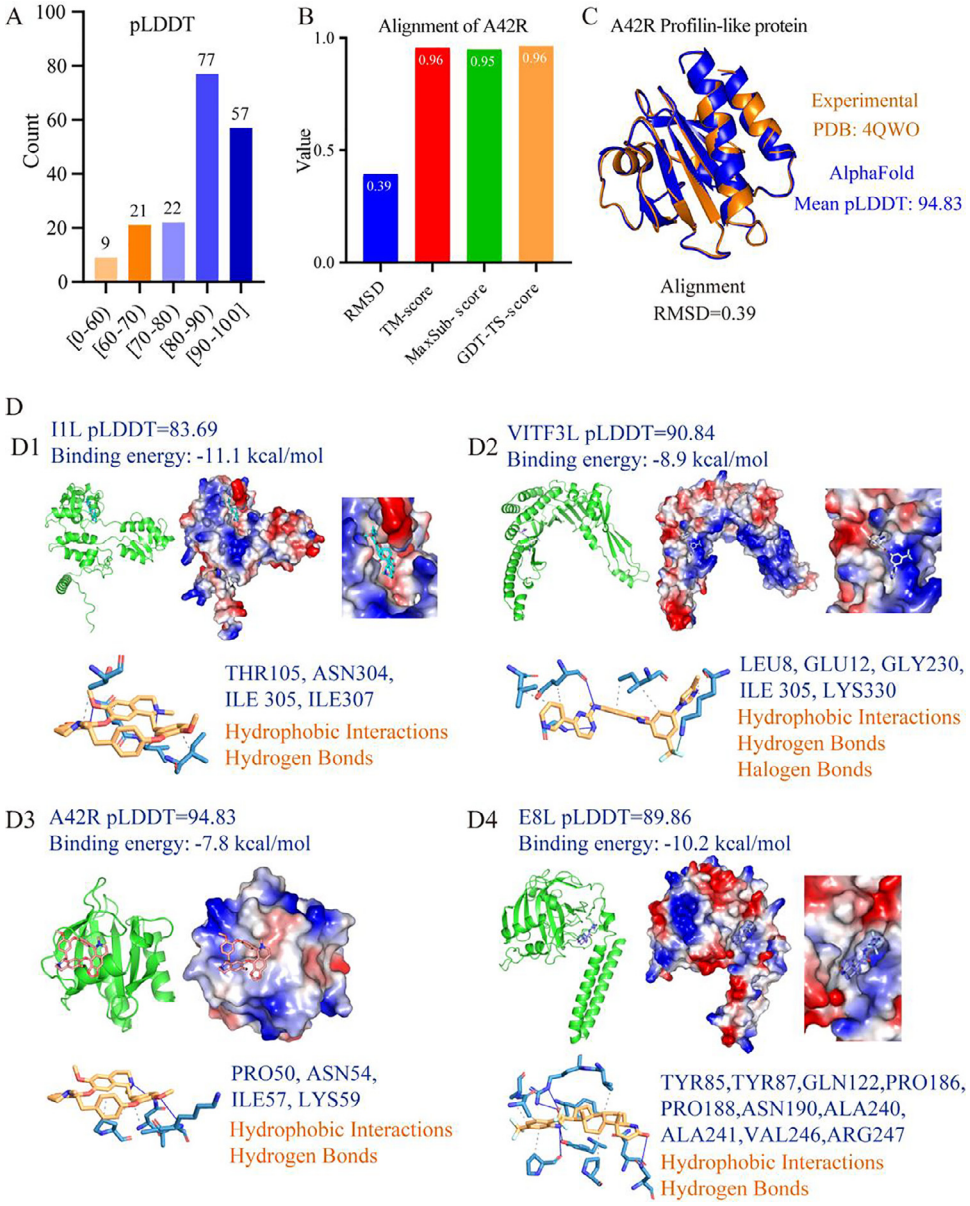

Fig. 1. Protein structural analysis and drug screening of the monkeypox virus. (A) The pLDDT values of all 186 monkeypox virus proteins. (B) Comparison between experimental structure (PDB: 4QWO) and AlphaFold2-predicted structure of A42R profiling-like protein. (C) The alignment of experimental structure and AlphaFold2-predicted structure of A42R profiling-like protein. (D) The interactions between Cepharanthine and four monkeypox virus proteins, including I1L (D1), VITF3L (D2), A42R (D3), and E8L (D4). The molecular structures of cepharanthine in different protein complexes are shown in different colors. The green "cartoon" model and the electrostatic surface present the protein structures. Red and blue indicate negative and positive charges on the electrostatic surface. The detailed interactions between amino acids (light blue) and cepharanthine (yellow) are under the four protein structures. (For interpretation of the references to color in this figure legend, the reader is referred to the web version of this article.)

break of the Monkeypox virus, which was first reported in the United Kingdom in May of 2022 and has since spread to more than 72 territories causing up to 14,533 cases according to the World Health Organization (WHO), as of the 20th of July 2022 (www.who.int/). In response to rising concerns over monkeypox, researchers are focused on acquiring structures of essential monkeypox proteins and have succeeded in producing crystal structures of the A42R Profilin-like protein (PDB: 4QWO), as well as simulating the structure of envelope protein F13, also known as C19L.[2] The structures of most of the monkeypox virus proteins remain unknown, knowledge of which would significantly enhance our understanding of the molecular mechanisms underlying critical viral processes such as viral entry and replication. AlphaFold2 is a powerful open-source computational approach developed to help predict protein structures,[3] which has been used successfully in acquiring accurate protein structures of the human and SARS- CoV-2 proteomes.[4-6]

Here, we used AlphaFold2 to predict the protein structures of the reference monkeypox virus proteome (Uniprot ID: UP101269[7]), yielding a total of 186 highly accurate protein structures (Supplemental Table S1). The mean predicted Local Distance Difference Test (pLDDT) values of 156 of the 186 proteins are above the threshold of 70, which suggests that the predicted structures for these proteins are highly accurate (Fig. 1A). Furthermore, among these proteins, 77 protein structures had mean pLDDT values of between 80 and 90, while 57 protein structures showed mean

Table 1
Virtual screening of potential drugs targeting the ten proteins. Related to Table S3.

Proteins	Drugs	Values	Proteins	Drugs	Values
B4R	ZINC164528615	−11.3	G9R	Trypan Blue	−9.4
	Trypan Blue	−11.2		ZINC3934128	−8.7
	ZINC208774715	−11.1		ZINC40164432	−8.7
	Ixabepilone	−10.9		ZINC14879959	−8.6
	ZINC40165257	−10.8		Irinotecan	−8.5
	Differin	−10.7		ZINC8220175	−8.5
	ZINC43195321	−10.6		ZINC14879961	−8.4
	Vumon	−10.5		Indacaterol-8-O-Glucuronide	−8.4
P28	Yaz	−9.7	D10L	Lumacaftor	−9.3
	Ergotamine	−9.2		ZINC3934128	−9.1
	Xaliproden	−9		Dihydroergotamine	−9
	Indocyanine Green	−9		Trypan Blue	−9
	Trypan Blue	−9		Dihydroergotoxine	−8.9
	Bisoctrizole	−8.9		Gliquidone	−8.8
	Orobronze	−8.9		Lestaurtinib	−8.8
	ZINC1530886	−8.8		ZINC253632968	−8.7
I1L	Cepharanthine	−11.1	E4R	Glycyrrhizinate Dipotassium	−9.7
	Trypan Blue	−11.1		Trypan Blue	−9.7
	ZINC3934128	−10.2		Nilotinib	−9.6
	ZINC14880001	−10.2		Naldemedine	−9.6
	Avodart	−10.1		Lifitegrast	−9.5
	ZINC3917540	−9.9		ZINC936069565	−9.5
	Lumacaftor	−9.9		ZINC14880001	−9.4
	Nilotinib	−9.7		ZINC43195321	−9.4
PRO132	Antrafenine	−11.4	VITF3L	Trypan Blue	−9.6
	Dihydroergotamine	−11		ZINC164528615	−9.1
	ZINC43195321	−11		Midostaurin	−9
	Cabozantinib	−11		Nilotinib	−8.9
	Trypan Blue	−11		Cepharanthine	−8.9
	Lorazepam Glucuronide	−10.9		ZINC253633751	−8.9
	ZINC8234383	−10.8		Avodart	−8.8
	Lomitapide	−10.8		ZINC14880001	−8.8
E8L	Trypan Blue	−11.4	A42R	Tipranavir	−7.9
	Dihydroergotoxine	−10.9		Trypan Blue	−7.9
	Naldemedine	−10.9		ZINC936069565	−7.9
	ZINC14880001	−10.6		Cepharanthine	−7.8
	Irinotecan	−10.3		Daclatasvir	−7.8
	Cepharanthine	−10.2		Dihydroergotamine	−7.7
	Fluspirilene	−10.1		Penfluridol	−7.7
	Dihydroergotamine	−10.1		Dihydroergotoxine	−7.7

pLDDT values above 90. To further evaluate the predicted protein structures, we compared the AlphaFold-predicted structure with the experimental crystal structure (PDB: 4QWO) of A42R Profilin-like protein. The resulting Template Modelling (TM), Global Distance Test (GDT)-TS, and the maximal subset (MaxSub) scores between two protein structures are above 0.95 (Fig. 1B). The aligned structure between two proteins has a root means square deviation (RMSD) value of 0.39 (Figs. 1B and 1C), suggesting that the two protein structures are highly similar (Figs. 1B and 1C). Taken together the above suggests that the predicted structures can be considered to be highly accurate.

Previously approved drugs for smallpox, tecovirimat and brincidofovir have been shown to be effective against the monkeypox virus, both in vitro and in animals[8]; however, given the global emergency, it is necessary to identify alternative drugs that could be used to fight the outbreak. Thus, we endeavored to uncover potential drugs to treat monkeypox based on accurate prediction of the monkeypox protein structures and 5903 approved drugs from the Zinc database[9] (Supplemental Table S2). We first selected ten target proteins based on their high pLDDT values, essential functions, and potential pharmacophores. The selected proteins were B4R, A42R, PRO132, VITF3L, E8L, I1L, D10L, P28, and G9R. We subsequently calculated the binding energies of all ten proteins with the 5903 drugs (Supplemental Table S3). The top best docking drugs targeting the ten proteins showed low binding energies (Table 1, S3, and FigureS1-S10), suggesting they might have strong interactions.

Trypan Blue and Cepharanthine display significant binding affinities to all ten target proteins (Supplemental Table S3). Trypan Blue interacts with the proteins by forming hydrogen bonds, salt bridges and hydrophobic and pi-cation interactions (supplemental materials). Cepharanthine shows high binding affinities to I1L (Fig. 1D1), VITF3L (Fig. 1 D2), A42R (Fig. 1 D3), and E8L (Fig. 1D4) through hydrophobic interactions and hydrogen bond formation. We have generated an extensive drug dataset consisting of 43,800 protein-drug paired data for the monkeypox virus, which could contribute to discovering the potential drugs for fighting monkeypox. Combatting the outbreak would require rapid research in the following: 1. Development of suitable pseudovirus and animal models of the current subtype of monkeypox virus; 2. Clarification of the mechanism of infection, reproduction, and transmission of monkeypox virus; 3. Identify and validate potential drugs that can be used to treat the viral infection.

In conclusion, here we acquired 186 highly accurate protein structures of the monkeypox virus reference proteome using AlphaFold2, which provided the most comprehensive database of monkeypox virus protein structures worldwide. Moreover, we have screened the potential drugs for binding the ten crucial proteins of the monkeypox virus, including B4R, A42R, PRO132, VITF3L, E8L, I1L, D10L, P28, and G9R, and generated a drug dataset containing total 43,800 protein-drug paired data, which could be helpful for drug discovery to the monkeypox virus.

Authors' contributions

Q.Y. and S.Y. conceived and designed the study. Q.Y. and X.S. analyzed and interpreted the data. Q.Y., A.A.S.S, and S.Y. wrote the first draft. Z.W. provided the softwares.

Data availability

The detailed methods are described in supplemental Methods. The protein structural files predicted by AlphaFold2 and the interaction analysis results between drugs and proteins were available on Github (https://github.com/lg10is1/monkeypox-virus-protein-structures). The RStudio code used in this study to perform statistical analysis and visualize data are available upon request.

Declaration of Competing Interest

The authors declare that they have no known competing financial interests or personal relationships that could have appeared to influence the work reported in this paper.

Acknowledgments

This work was supported by Shanghai Municipal Science and Technology Major Project (2017SHZDZX01), Natural Science Foundation of China (32070679, U1804284, 81871055), the National Key R&D Program of China (2019YFA0905400, 2017YFC0908105, 2021YFC2702103), Taishan Scholar Program of Shandong Province (tsqn201812153) and Natural Science Foundation of Shandong Province (ZR2019YQ14). The computations in this paper were run on the Siyuan cluster supported by the Center for High-Performance Computing at Shanghai Jiao Tong University.

Supplementary materials

Supplementary material associated with this article can be found, in the online version, at doi:10.1016/j.jinf.2022.08.006.

References

1. Awan U.A., et al. Monkeypox: a new threat at our doorstep!. *J Infect* 2022;**85**:e47–8. doi:10.1016/j.jinf.2022.05.027.
2. Li D., Liu Y., Li K., Zhang L.. Targeting F13 from monkeypox virus and variola virus by tecovirimat: molecular simulation analysis. *J Infect* 2022. doi:10.1016/j.jinf.2022.07.001.
3. Jumper J., et al. Highly accurate protein structure prediction with AlphaFold. *Nature* 2021;**596**:583–9. doi:10.1038/s41586-021-03819-2.
4. Tunyasuvunakool K., et al. Highly accurate protein structure prediction for the human proteome. *Nature* 2021;**596**:590–6. doi:10.1038/s41586-021-03828-1.
5. Yang Q., et al. Structural comparison and drug screening of spike proteins of ten SARS-CoV-2 variants. *Research* 2022;**2022**:9781758. doi:10.34133/2022/9781758.
6. Yang Q., Syed A.A.S., Fahira A., Shi Y.. Structural analysis of the SARS-CoV-2 omicron variant proteins. *Research* 2021;**2021**:9769586. doi:10.34133/2021/9769586.
7. Shchelkunov S.N., et al. Human monkeypox and smallpox viruses: genomic comparison. *FEBS Lett* 2001;**509**:66–70. doi:10.1016/s0014-5793(01)03144-1.
8. Delaune D., Iseni F.. Drug development against smallpox: present and future. *Antimicrob Agents Chemother* 2020;**64**. doi:10.1128/aac.01683-19.
9. Sterling T., Irwin J.J.. ZINC 15–ligand discovery for everyone. *J Chem Inf Model* 2015;**55**:2324–37. doi:10.1021/acs.jcim.5b00559.

Qiangzhen Yang, Disong Xia, Ali Alamdar Shah Syed, Zhuo Wang
Bio-X Institutes, Key Laboratory for the Genetics of Developmental and Neuropsychiatric Disorders (Ministry of Education), Shanghai Jiao Tong University, 1954 Huashan Road, Shanghai 200030, China

Yongyong Shi*
Bio-X Institutes, Key Laboratory for the Genetics of Developmental and Neuropsychiatric Disorders (Ministry of Education), Shanghai Jiao Tong University, 1954 Huashan Road, Shanghai 200030, China
Biomedical Sciences Institute of Qingdao University (Qingdao Branch of SJTU Bio-X Institutes), Qingdao University, Qingdao 266003, China
Shanghai Key Laboratory of Psychotic Disorders, Shanghai Mental Health Center, Shanghai Jiao Tong University School of Medicine, Shanghai 200030, China
Shanghai Key Laboratory of Sleep Disordered Breathing, Shanghai Jiao Tong University Affiliated Sixth People's Hospital, Shanghai, China
The First Affiliated Hospital of Zhengzhou University, Zhengzhou 450052, China
Department of Psychiatry, First Teaching Hospital of Xinjiang Medical University, Urumqi 830046, China

*Corresponding author.
E-mail address: shiyongyong@gmail.com (Y. Shi)

Accepted 5 August 2022
Available online 11 August 2022

https://doi.org/10.1016/j.jinf.2022.08.006

Peculiar Variations of the Electrostatic Potential of Spike Protein N-terminal Domain Associated with the Emergence of Successive SARS-CoV-2 Omicron Lineages

Dear Editor,

Zeng and collaborators (1) have recently discussed the potential of the porcine tyrosine-protein kinase receptor UFO (AXL) to interact with the N-terminal domain (NTD) of the spike (S) protein of some SARS-CoV-2 Variants of Concern (VOC). Omicron (BA.1.1.529) is the last VOC that, after its first detection in South Africa in the late 2021, has spread worldwide and has generated several subvariants of which those belonging to the BA.2 lineage (BA.2.12.1, BA.4 and BA.5) are now the most prevalent in several countries (www.who.int). Omicron subvariants markedly differ in resistance to antibody neutralization, that has been largely attributed to changes in the mutational landscape of RBD region of the Spike (S) protein (2) Little comparative attention is currently reserved to the mutational landscape of the S protein NTD although this domain also carries a distinctive set of mutations which markedly distinguish BA.1 (and BA.3) from the subvariants of the BA.2 lineage (BA.2.12.1,and BA4/5). In addition, BA.4 and BA.5 carry a HV69-70 deletion that is absent in the BA.2 and BA.2.12.1 subvariants.

We have recently shown that the mutational landscape of both RBD and NTD largely determines their net surface charge, i.e. an indirect estimate of the dominant charge of the surface electrostatic potential (EP) (3,4) . Changes in these potentials can modify the kinetics/strength of receptors recognition, or other suggested NTD functions, hence influencing the biological properties of SARS-CoV-2. in particular its transmissibility and infectivity(4-7). In all the pre-Omicron VOC, the EP of both RBD and NTD is dominantly positive, a finding that has been interpreted to favour their binding to negatively charged surfaces of the ACE2 (RBD) or the less characterized receptor(s) of NTD (4-7: see also below). Interestingly, the first emerged Omicron VOC (BA.1.1.529), while maintaining the usual positive net charge of the RBD region, showed a negative net charge of the NTD region, differently from all other previous VOC(4).

We have therefore considered to be of interest reporting here the net-charge values of all Omicron subvariants. Surprisingly,

Table 1
Predicted net charge (electrostatic potential) of the Spike RBD and NTD (folded state) of SARS-CoV-2 VOC, compared with previous main VOC[1]

SARS-CoV-2 VOC	Pango Lineage	EP-RBD	EP-NTD
Wuhan	B.1	2.15	1.30
Alpha	B.1.1.7	3.18	1.69
Delta	B.1.617.2	4.15	1.28
Omicron	BA.1.1.529	5.22	-1.10
Omicron	BA.3	5.22	0.02
Omicron	BA.2	5.18	0.80
Omicron	BA.2.12.1	5.18	0.80
Omicron	BA.4	5.19	1.39
Omicron	BA.5	5.19	1.39

[1] Calculated as described in Ref.4.

these EP-NTD values differed in the different subvariants. As shown in Table 1, only the first appeared Omicron strain had a dominantly negative EP. All others had a neutral (BA.3) or slightly positive (BA.2 and BA.2.12.1) or frankly positive (BA.4/5) value. Interestingly, the EP value of these last two subvariants falls in the range of all pre-Omicron VOC, being equal to that of the Delta variant. In contrast, no appreciable changes were observed in the high positive value of the RBD-EP of all Omicron subvariants (Table 1) demonstrating that variations in the electrostatic potentials of the NTD regions occur independently on those of the RBD region.

We notice that the negativity of the BA.1 Omicron variant is probably contributed to or just determined by its unique EPE insertion at the position 214 of NTD sequence, meaning the double acquisition of the negatively charged (at physiologic pH) glutamic acid. Thus, the trend toward positivity of all other Omicron subvariants could be mostly due to the loss of the EPE insertion. In-silico mutagenesis of the Glu residues of the EPE insertions with Ala moves the net charge toward neutrality. The same effect can be seen by replacing Asp142 with Ala. Interestingly, Asp142 is shared by all the BA subvariants and by Delta. Also in this case, replacement with Ala increases the positivity of the domain net charge.

We previously (4) suggested that the negative EP value of BA.1 NTD might have hindered the NTD recognition by known or postulated,NTD- receptors, including gangliosides and, particularly, the AXL receptor which is mostly expressed in lung cells (5-7). In fact, the net charge of the AXL domain that is putatively involved in the interaction with NTD (as reported in the PDB structure 2C5D) is negative at around -5.5 according to our calculations. The electrostatic potential of AXL has been displayed and the most negative portion of its surface appears to coincide with the predicted interface with NTD (1). If so, the EP-NTD reversion to positivity of the BA.2 subvariants, in particular BA.4/5 could actually imply the rescue of NTD receptor recognition function that was lost or decreased in the progenitor Omicron BA.1n this line, it is of some interest that these EP-NTD variations appear to parallel the increased resistance of the BA.2 lineage subvariants to neutralization by antibodies as well as their increase in the experimental pathogenicity reported by Kimura and collaborators, as compared to BA1 lineage (8). In particular, the gradient of fusogenicity, a marker of SARS-CoV-2 pathogenicity, of these subvariants (BA.1 toBA.2 to BA-4/5 in increasing order) coarsely parallel the gradient 0f EP-NTD trend to positivity from BA.1 to BA4/5. . In addition, evasion of innate immunity appears to be markedly higher in BA.5 than in BA.1 and BA.2 (9,10).

We are aware of the rather speculative nature of our data interpretation above. Nonetheless, the here reported, peculiar variations of the electrostatic potential of the S-protein NTD region of the Omicron lineages may be virologically relevant, thus worthy being carefully investigated.

Declaration of Competing Interest

The authors declare that they have no known competing financial interests or personal relationships that could have appeared to influence the work reported in this paper.

REFERENCES

1. Zeng C., Ye Z., Fu L., Ye Y.. Prediction analysis of porcine AXL protein as a potential receptor for SARS-CoV-2. *J. Infect.* 2022;**84**:579–613.
2. Yamasoba D, Kosugi Y, Kimura I, Fujita S, Uriu K, Ito J, et al. Neutralisation sensitivity of SARS-CoV-2 omicron subvariants to therapeutic monoclonal antibodies. *Lancet Infect Dis* 2022;**22**:942–3.
3. Pascarella S, Ciccozzi M, Zella D, Bianchi M, Benedetti F, Benvenuto D, et al. SARS-CoV-2 B. 1.617 Indian variants: Are electrostatic potential changes responsible for a higher transmission rate? *J Med Virol* 2021;**93**:6551–6.
4. Pascarella S, Ciccozzi M, Bianchi M, Benvenuto D, Cauda R, Cassone A.. The value of electrostatic potentials of the spike receptor binding and N-terminal domains in addressing transmissibility and infectivity of SARS-CoV-2 variants of concern. *J. Infect* 2022;**84**:e62–3.
5. Zhang Q, Xiang R, Huo S, Zhou Y, Jiang S, Wangand Q et al. Molecular mechanism of interaction between SARS-CoV-2 and host cells and interventional therapy Signal Transduction and Targeted Therapy 2021; 6:233
6. Fantini J, Noura Y, Fodil A, Chahiniana H.. Structural dynamics of SARS–CoV-2 variants: A health monitoring strategyfor anticipating Covid-19 outbreaks. *J.Infect* 2021;**83**:197–206.
7. Fantini J, Yahi N, Colson P, Chahinian H, La Scola B, Raoult D.. The puzzling mutational landscape of the SARS-2-variant Omicron. *J Med Virol* 2022;**94**:2019–25.
8. Wang S., Qiu Z., Hou Y., Deng X, Xu W, Zengh T, et al. AXL is a candidate receptor for SARS-CoV-2 that promotes infection of pulmonary and bronchial epithelial cells. *Cell Res* 2021;**31**:126–40.
9. Kimura I, Yamasoba DT, Tamura TN, O-da Y, Mitoma S. et al. Virological characteristics of the novel SARS-CoV-2 Omicron variants 2 including BA.2.12.1, BA.4 and BA.5 3 BioRxiv, 2022, preprint doi: https://doi.org/10.1101/2022.05.26.493539; this version posted May 26, 2022
10. Reusch A, Thorne LG, Whelan MVX, Mesner D, Ragazzini R, et al. Enhanced innate immune suppression by SARS-CoV-2 Omicron subvariants 2 BA.4 and BA.5. *bioRxiv* 2022 preprint doi.

Stefano Pascarella
Department of Biochemical Sciences "A Rossi Fanelli", Sapienza Università di Roma, Rome, Italy

Massimo Ciccozzi, Domenico Benvenuto
Medical Statistic and Molecular Epidemiology Unit, University of Biomedical Campus, Rome, Italy

Alessandra Borsetti
National HIV/AIDS Research Center (CNAIDS); Istituto Superiore di Sanità (ISS), Rome, Italy

Roberto Cauda
Department of Healthcare Surveillance and Bioethics, Catholic University of Sacred Heart, Rome, Italy

Antonio Cassone*
Center of Genomics, Genetics and Biology, Siena, Italy

*Corresponding author: Prof Antonio Cassone, Center of Genomics, Genetics and Biology, Universita degli Studi di Siena, Siena, Italy
E-mail address: a.cassone@pologgb.com (A. Cassone)

Accepted 22 July 2022
Available online 29 July 2022

https://doi.org/10.1016/j.jinf.2022.07.018